SUPERCONDUCTORS IN ALTERNATING FIELDS

by

R.M.F.Linford M.A.(Oxon).

(Being a thesis submitted, in partial fulfillment of the requirements for the degree of Doctor of Philosophy, at the University of Warwick)

School of Engineering Science
University of Warwick
August 1968.

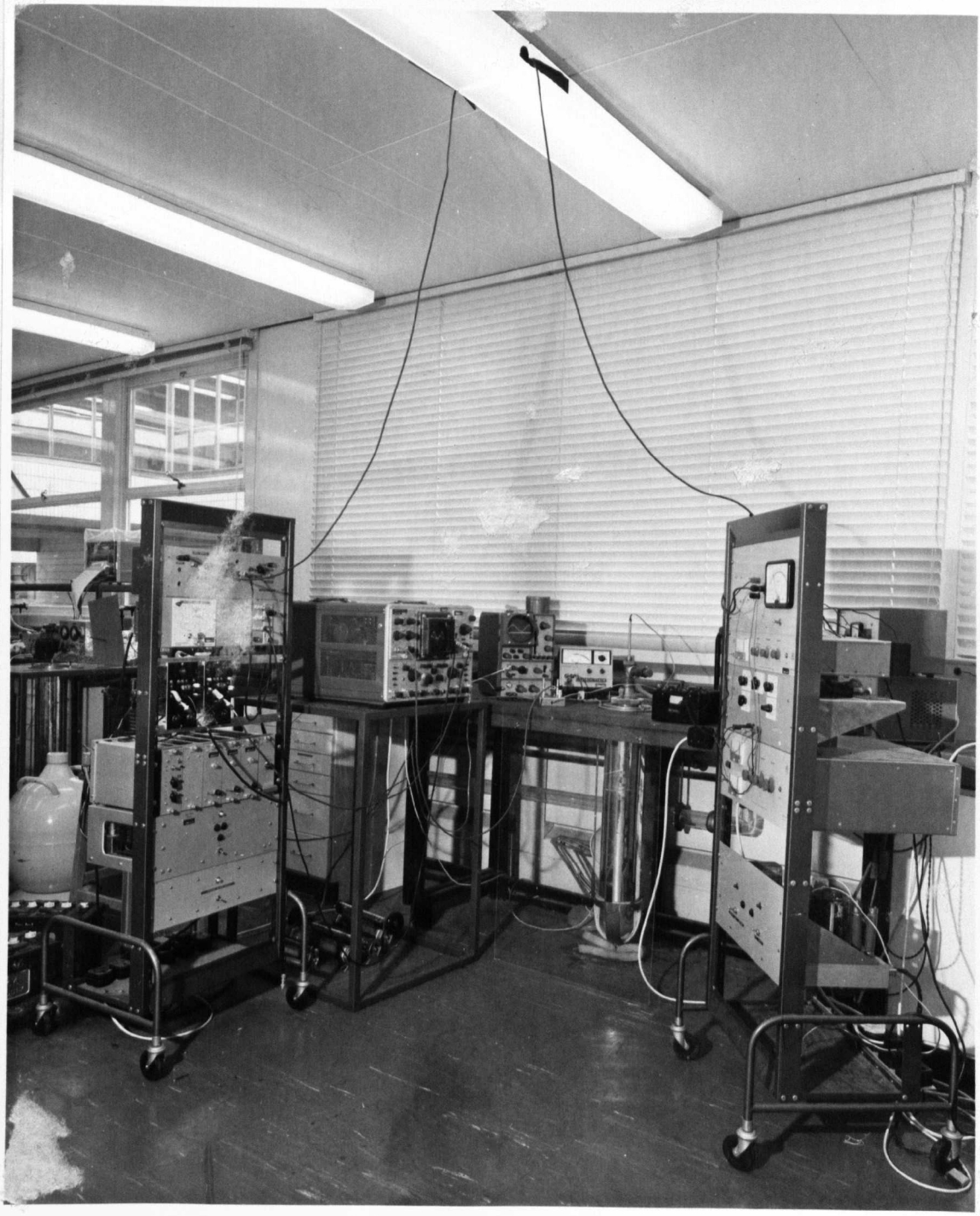

Preface

In the course of the work presented in this thesis I have been assisted by many people, but the conception and completion of the experiments has been my own responsibility. No part of this thesis has been presented to any other institution at any time.

Several laboratories have generously provided samples for my work and I am grateful to Drs.K.Bowen (Oxford University, Metallurgy Department), R.Hancox (Culham Laboratory), D.Jones (Birmingham University, Centre for Materials Science) and Messrs.A.Barber (IMI), R.J.Slaughter and E.C.Rogers (both BICC Research Organisation) to this end. Dr.Jones has also made available the Scanning Electron Microscope, and Professor Kurti (Oxford University, Clarendon Laboratory) kindly loaned the electric flowmeter.

Acknowledgement is also made to the Science Research Council who financed the later part of the work.

Any experimental project of this nature would have been impossible without the help of skilled technical staff and H.W.Woodgate and R.Hodierne have excelled in the manufacture of equipment and preparation of samples.

I have also benefited from the many discussions with my colleagues Messrs.J.E.Goodfellow, R.J.A.Seebold and P. Brankin. Throughout the work, and especially during the preparation of the manuscript of the thesis, the guiding hand and encouraging word of my supervisor, Dr.R.G.Rhodes, has been invaluable.

The list of long sufferers must include Mrs.Jean Norman who made an ordered typescript from my hieroglyphics.

However, at the head of the list stand my wife and family who have suffered the "thesis backlash" during the last three years. To them this document is dedicated, especially to Harriet, whose birth was in direct competition to submission.

Abstract

After a general introduction to the fundamentals of superconductivity, the concept of the critical state is introduced and its application to alternating field conditions discussed. A comprehensive review of the a.c.measurements in the literature and the relevance to the predictions of the theories is then given. Details of the comprehensive experimental facilities constructed are described, including the development of a sophisticated technique for the measurement of a.c.losses. The equipment is essentially a sensitive wattmeter, with a small analogue computer used to operate on the voltages, from pickup-coils wound directly on the samples.

The experiments reported start with work undertaken to investigate the dissipation in applied fields, below the critical field. The part played by surface irregularities is explored and the general field dependence of the losses explained on a simple model. A large section is then devoted to the response of type II superconductors to large fields. Results are given on high-K materials and on both reversible and hysteretic niobium samples. The predictions of the critical state model are found to hold, if suitable modifications are made to account for the field region below H_{c1} and the surface currents. In particular, the applied field H_m can be replaced by $(H_m - \Delta H/2)$, where ΔH is the overall shielding effect of the surface currents. The value of these currents has been determined from the pickup-coil voltage waveforms and the interpretation of these waveshapes has also been advanced to determine the critical current density.

A decrease in the surface currents, with roughening of the sample surface, is described, and their variation with bulk properties discussed. A correlation between the critical current density and the surface currents has been discovered, and examined on the basis of "surface barrier" pinning.

Contents

	Frontispiece	i
	Preface	ii
	Abstract	iv
	Contents	v
1.0.	Introduction	1
2.0.	General properties of superconductors	3
	2.1. Fundamentals of superconductivity	3
	2.1.1. Microscopic theory of superconductivity	7
	2.1.2. Phenomenological theories of superconductivity	8
	2.1.3. Magnetic behaviour of ideal superconductors	15
	2.2 The Critical State	20
	2.2.1. Pinning phenomena	25
	2.2.2. Surface currents	28
	2.3. The critical state model and a.c. dissipation	31
	2.3.1. The Bean-London model	32
	2.4. Survey of the alternating field measurements in the literature	40
	2.4.1. Techniques for measurement of a.c. losses	41
	2.4.2. Dissipation in the Meissner State	42
	2.4.3. Dissipation in the mixed state	46
	2.4.4. Dissipation in a.c.coils	50
	2.4.5. The a.c.superconducting-normal transition	50
	2.5. The aims of the present work	52
3.0.	The Experimental Techniques	54
	3.1. The Cryogenics	54
	3.2. Measurement of a.c.losses	55
	3.2.1. Calorimetric experiments	56
	3.2.2. Theory of the electrical technique for the measurement of a.c.losses	58
	3.2.3. The apparatus	60
	3.2.4. Compensation procedure	65
	3.2.5. Assessment of the technique	67
	3.3. Measurement of critical currents	68
	3.3.1. The apparatus	69
	3.3.2. Exploratory measurements	70

3.4. Magnetisation measurements 72

3.5. Measurement of surface currents 76

4.0. The Experiments 78
4.1. Dissipation in the Meissner state 78
4.1.1. Experiments on high purity lead 78
4.1.2. Experiments on niobium samples 85
4.1.3. Discussion of surface losses 92

4.2. Dissipation in the mixed state - high-K materials 94
4.2.1. Niobium-zirconium and niobium titanium 95
4.2.2. Discussion 101

4.3. Dissipation in the mixed state - cylindrical niobium samples 104
4.3.1. Polycrystalline samples 105
4.3.2. Heat-treated polycrystalline samples 111
4.3.3. Single-crystal samples 116
4.3.4. Discussion 121

4.4. Dissipation in the mixed state - niobium strips 124
4.4.1. Kawecki/Hancox strip 125
4.4.2. Strips of varying thickness 132
4.4.3. Discussion of strip measurement 139

4.5. Surface currents 141
4.5.1. Discussion 145

5.0. Conclusions 147

Appendix A Calculation of the critical current of a conductor 152

Appendix B Publications by the author 153

References vii

1.0. Introduction

The dreams of the Leiden scientists, over a half a century ago, have still yet to be completely fulfilled. The discovery of superconductivity and its resistanceless state led to immediate speculation of massive, lossless currents being employed in engineering devices and producing magnetic fields. These hopes were soon shattered by the discovery that the magnetic fields which would quench superconductivity, the critical fields, were only a few hundred Oersteds for the materials then known. Even when Niobium was found to have a critical field of several kilo-Oersteds, interest in possible applications was not revived. Then in 1961, Kunzler's team at the Bell Telephone Laboratories discovered the intermetallic compound Nb_3Sn which is now known to be superconducting in fields in excess of 200 k.Oe., at $4.2^{\circ}K$. With these advances has come the development of both small, high-field and large scale superconducting magnets, in some cases giving 140 k.Oe, and they are now finding application in nuclear physics, d.c. machinery and many laboratory experiments.

Superconducting devices carrying steady currents are now firmly established in technology, but alternating current devices, on the other hand, have hardly left the physicists' bench. The delay in applying these attractive materials to power cables, generators, motors and transformers, with all the power and weight saving this would offer, has been due to the small but serious power dissipation in the superconductor, under alternating conditions. This "a.c. loss" has been the object of much

research during the last five years, some of which is reported here, and at the time of writing much serious thought is being devoted to possible a.c. devices.

The author first became interested in the subject in the laboratories of British Insulated Callendar's Cables, London, where an a.c. cable was being actively considered. Since transferring to the University of Warwick, his research activities have broadened, but a close link has been maintained with the need for information relevant to technology. New techniques of measurement have been developed, a wide range of experimental work completed and some fundamental thinking devoted to a.c. superconductivity in general.

For this thesis some elements of the theory of superconductivity, relevant to the understanding of the a.c. properties, are reviewed and the experimental techniques that have been used are described. The experimental results are displayed and general conclusions regarding the results, possible applications and future work are elaborated.

2.0. General properties of superconductors

To help in the understanding of the topics discussed in the latter part of this thesis we first include an introduction to the basic properties of superconductors. This is, of necessity, fairly concise and for a more detailed study we refer to the books by Lynton[1] and de Gennes[2] and the review articles by Livingstone and Schadler,[3] Dew Hughes,[4] Catterall[5] and others.[6-12]

We shall then introduce the concept of the critical state and discuss the experiments in the literature which attempt to account for the a.c. behaviour of superconductors in terms of this model. Finally the aims of the present work will be outlined.

2.1. Fundamentals of superconductivity

Two basic properties characterise superconductors, perfect conductivity and the exclusions of magnetic fields. It was this first property that led to the identification of this fascinating class of materials by Kammerlingh Onnes[13] when he did his first experiments and concluded the resistance of hismercury samples had "practically vanished" at 4.2°K. Various exhaustive measurements have since been made to determine whether the resistance completely disappears or just falls to a very low level. The present upper limit has been set at 10^{-23} Ohm-cm. by Quinn.[14]

The superconductive state is, of course, a phenomena of very low temperatures and, although some two dozen elements as well as over a thousand alloys and intermetallic

compounds together with a few semiconductors are known to exhibit superconducting behaviour , the maximum critical temperature is only about 20°K. (The critical temperature Tc is the temperature below which a material is superconducting. It is a characteristic of a particular material, although it is somewhat sensitive to structural defects, impurities, etc.)

The metallic elements known to be superconducting include several common metals such as lead, aluminium and mercury, but notably absent from this group are the noble metals copper, gold, silver and platinum, and the ferromagnetics iron, cobalt and nickel. It is possible that these elements are superconducting at temperatures below those at which the materials have been hitherto examined, but it is likely that the electron-phonon interaction, which is basic to superconductivity, is too weak in them. Among the elements, Niobium has by far the highest critical temperature, 9.2°K, and for this and other reasons to be discussed later, this metal has been the subject of many experiments from the point of view of possible applications.

Roberts [15] has listed many superconducting alloys and compounds, some of the most important of which are included in Table 2.1, together with their critical temperatures and upper critical fields (to which we shall refer later). Of these the Niobium alloys Nb-Ti and Nb-Zr and the compound Nb_3Sn are commonly used commercially for winding superconducting magnets. The search for higher critical temperatures has led into three phase systems and a Nb-Al-Ge alloy [16] has the highest known value to date with Tc=20.05°K.

Material	Critical Temperature T_c °K	Upper Critical Field (4.2°K) Hc_2(k.Oe.)	
Nb_3 Al	17.1	245)	
Nb_3 Sn	18.2	225)	Ref.21
V_3 Si	16.9	220)	
V_3 Ga	14.5	196)	
Nb25%Zr	10.8	80	
Nb33%Ti	9.3	135	

Table 2.1. Critical Temperatures and Upper Critical Fields (at 4.2°K) for some high field superconductors.

The response of an ideal superconductor to an applied magnetic field H is the second of its characteristic features and distinguishes it from a material having only perfect conductivity. Meissner and Ochsenfeld [17] found that, in addition to excluding a magnetic field applied after cooling below Tc, as indeed a perfect conductor would do, a superconductor will also expel the fluid if this is applied first and the material then is cooled through Tc. This is the so-called Meissner effect and is true only for magnetic fields below a certain threshold value, known as the critical field. For an ideal "soft" superconductor this is the thermodynamic critical field H_c and it varies with temperature T according to the approximate relation;

$$H_c(T) = H_c(0)\left[1-(T/T_c)^2\right]$$

where $H_c(0)$ is the value of H_c at T = 0.

If the concepts of reduced temperature $t = T/T_c$ and reduced critical field $h(t) = \frac{H_c(T)}{H_c(0)}$ are introduced, this last equation becomes

$$h(t) = (1-t^2) \qquad (2.1)$$

The exclusion and expulsion of magnetic flux is a diamagnetic feature as the average magnetic induction

$$B = \underline{H} + 4\pi \underline{m} = 0$$

where $\underline{m}$ is the magnetisation per unit volume of a sample, and thus the susceptibility

$$K = M/H = -1/4\pi$$

In fact the diamagnetism is not perfect as the magnetic field does not change discontinuously at the specimen surface but falls off over a thin surface layer, as we shall see later. The field gradients in this "penetration depth" are equivalent to circulating currents, having a distribution unique to a given specimen shape. These supercurrents are stable and the reversibility of the superconducting-to-normal transition has enabled Gorter [18] and others to apply thermodynamics to the problem. Keesom[19] had showed that the transition was of the second order with a jump in the specific heat at Tc, but with no discontinuity in the latent heat, in zero field. Gorter and Casimir[20] developed a complete model on thermodynamic arguments, on the following lines.

If gs(H) is the Gibbs free energy per unit volume of the superconducting phase, in an applied field H,

$$gs(H) = gs(0) - \int_0^H \underline{m}\, d\underline{H}$$

However, for a perfect diamagnetic

$$\underline{m} = -1/4\pi \underline{H} = -\frac{H}{4\pi}$$

so $$gs(H) = gs(0) + H^2/8\pi$$

or at the transition, where $H = H_c$ and the free energy of the normal state $gn(H_c) = gs(H_c)$,

$$gn(H_c) - gs(0) = H_c^2/8\pi \qquad (2.2)$$

From equation 2.2 it is apparent that the superconducting state is of lower energy, sometimes called the condensed state. Gorter and Casimir[22] also derived a reasonable fit to the experimental specific heat data with their two fluid model. They assumed that a fraction W of the electrons are in the superconducting state, W varying from 1 at 0°K to zero at Tc, and identified W as the order parameter. The best fit to the experimental results was obtained with

$$W(T) = 1-t^4.$$

2.1.1. Microscopic Theory of Superconductivity

The two-fluid model was the first attempt at a microscopic theory of superconductivity but the first successful model to account for all the properties of superconductors was not evolved until 20 years later. Bardeen, Cooper and Schrieffer[23] (BCS) developed a quantum-mechanical model.

As early as 1935 it was being suggested that there might be a gap in the energy spectrum of the excited states of quasi-particles. Daunt and Mendlessohn[24] presented specific heats in support of this idea. Confirmation of the existence of such a gap first came from Goodman's[25,26] thermal conductivity measurements which showed a 1/T dependence, and all the results of surface impedance, ultrasonic and tunnelling experiments lent support to this idea. In the years following the war, the rapid advances in nuclear physics made available a wide range of atomic isotopes and Serin[27] and others discovered a dependence of Tc on the isotopic mass of a given element. This

indicated that the motion of the ions must somehow be relevant to superconductivity and enabled Fröhlich[28] and Bardeen[29] to develop a theory, in which attractive forces between pairs of electrons arise from their interaction with lattice ions. These attractive forces lead to bound pairs of electrons, of equal and opposite momentum, and so the transfer of energy to the electron fluid requires the breaking of such a pair. The energy must thus exceed the binding energy of a pair and this lower limit in the energy transfer is responsible for the gap in the energy spectrum. The existence of this energy gap means that electron pairs can move up to a certain velocity without scattering. The number of paired electrons decreases as the temperature increases until at T = Tc all the electrons are fully normal in all respects (c.f. the order parameter in the two fluid model).

Bardeen and his colleagues[23] elaborated on these ideas and their predictions of such properties as the specific heats, electromagnetic properties, thermal conductivity, ultrasonic attenuation, nuclear spin relaxation, Knight shift and a variety of others, have received close experimental verification.

2.1.2. Phenomenological Theories of Superconductivity

In parallel with the progress on a microscopic theory have developed a series of phenomenological treatments.

F. and H. London[30] were the first to undertake such a study to account for the macroscopic characteristics of a superconductor. Their work resulted in the two

equations relating current density $\underline{J}$ to the electric and magnetic fields:

$$\text{curl } \Lambda \underline{J} = -\underline{H}/c \qquad 2.3(a)$$

$$\partial/\partial t (\Lambda \underline{J}) = \underline{E} \qquad 2.3(b)$$

where $\Lambda = \frac{m}{n_s e^2}$, n_s the density of superconducting electrons, m their mass and e the electronic charge. (In keeping with most of the literature on this subject Gaussian units are used here. $\underline{E}$ and $\underline{J}$ are in e.s.u. and $\underline{H}$ in e. m.u.)

For a semi-infinite slab in the y-z plane the solution of equation 2.3(b) gives

$$H_y = H_{app} \exp[-x/\lambda_L]$$

where $\lambda_L = (\frac{\Lambda c^2}{4\pi})^{\frac{1}{2}}$ and is a characteristic length known as the penetration depth. The existence of this form of penetration was confirmed by Schoenberg[31] and λ_L is typically 5×10^{-6} cms. for an elemental superconductor. It is also temperature dependent according to:

$$\lambda_L(t) = \lambda_L(0)[1 - t^4]^{-\frac{1}{2}}$$

Although the London equations 2.3(a) and (b) are only valid at low frequencies and the validity of their theory is limited by long range coherence effects, it provides a useful approximate description of the electromagnetic properties of a superconductor.

From the London equations it can be shown that the magnetic energy per unit volume of a specimen with dimensions smaller than λ_L is less than for a bulk sample. Thus it would be energetically favourable for finely divided superconducting-normal (s-n) regions to be formed in the latter. As this does not happen the energy per unit surface

of superconducting domain must be greater than $\lambda_L/2 \times H_c^2/8\pi$, in effect the London equations predict negative surface energy. Other weaknesses of the theory included the dependence of λ_L, on alloying and on the applied magnetic field, and the implication that the wavefunctions of the superconducting electrons stopped abruptly at the s-n boundary.

To account for these points Pippard[32] introduced the concept of range of coherence of the superconducting wavefunctions, allowing them to vary slowly over a finite length, ξ, the coherence length, which is many times longer than λ_L. (In pure metals $\xi \approx 10^{-4}$ cm, $\lambda_L = 10^{-5}$ cm.) (The coherence length has its equivalent in the BCS theory in the size of the wavefunction of a superconducting electron pair.) If the concept of the vector potential $\underline{A}$ is introduced, where $\underline{H}$ = curl $\underline{A}$ then the London equation 2.3(a) becomes

$$\underline{J} = -\frac{ne^2}{m}\,\underline{A}.$$

Pippard modified this, to allow for the effect of the mean free path on the penetration depth, to:

$$\underline{J} = -\frac{ne^2}{m}\,\frac{\xi(l)}{\xi_0}\,\underline{A}$$

where ξ_0 is the coherence length for a pure superconductor and $\xi(l)$ for a material with meanfree path l. The penetration depth is given by

$$\lambda = \lambda_L \sqrt{\xi_0/\xi(l)} \qquad \text{when } \xi(l) \ll \lambda$$

and as a rough approximation

$$1/\xi(l) = 1/\xi_0 + 1/l \qquad (2.4)$$

Thus with alloying l is decreased and when it is comparable with $\xi(l)$ this too is reduced, the scope of the disturbance is smaller and λ varies with the field.

The extension of a disturbance a distance ξ at a s-n boundary (i.e. the density of superconducting electrons n_s reaches the mean level at ξ from the boundary) means an increase in the free energy of the superconductor. This is equivalent to a positive surface energy and is often referred to as the configurational surface energy. The total surface energy α_{ns} is thus the sum of this configurational component and the negative London surface energy and may be expressed, approximately, as:

$$8\pi\alpha_{ns} = [\xi H_c^2 - \lambda H^2]$$

As we have noted, for pure metals, $\xi \approx 10\lambda$ so there are no values of H below H_c for which α_{ns} is negative, but for materials with a short mean free path and hence small ξ, α_{ns} may take up negative values. The field distribution and the variation of the density of the superconducting electrons, n_s, at a s-n boundary, are shown in Figure 2.1 for the two types of material.

An extension of the London-Pippard phenomenological theories was developed by Ginzburg and Landau[33], for temperatures close to the critical temperature. They introduced an order parameter ψ, such that $|\psi|^2 = n_s$, and ψ is interpreted as the effective wavefunction of the superconducting electrons. Their expression for the free energy in zero field is:

$$g_s(0) - g_n(0) = \alpha|\psi|^2 + \beta/2|\psi|^4$$

where α and β are functions of temperature. Minimizing the total free energy, they showed that the penetration depth λ is given by:

$$\lambda^2 = mc^2/4\pi e^{*2}|\psi_0|^2$$

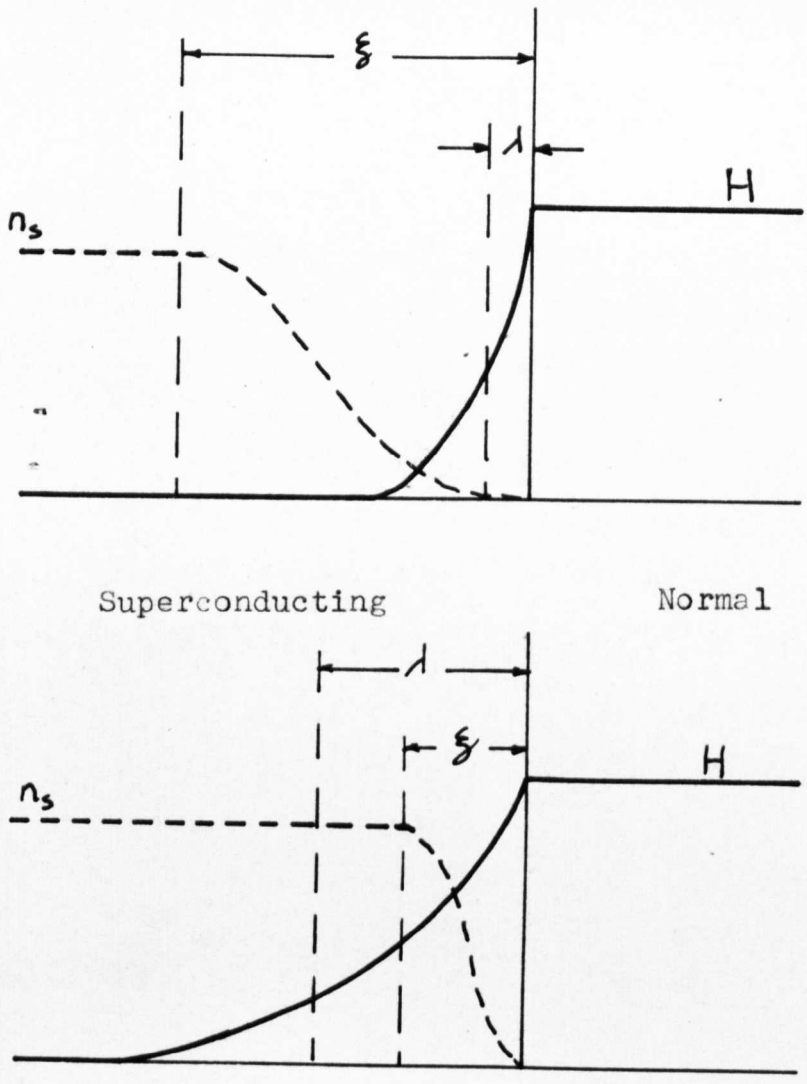

Figure 2.1 Variation of H and n_s across a superconducting-normal boundary for Type I and Type II superconductors.

where $|\psi_0|^2 = -\frac{\alpha}{\beta}$ and e^* is the charge on the superconducting electrons. If $e^* = e$ and $|\psi_0|^2 = n_s$ then $\lambda = \lambda_L$.

They also introduced a parameter κ where

$$\kappa^2 = \beta/2\pi\left[\frac{mc}{e^*\hbar}\right]^2 = \left[\frac{2e^{*2}}{\hbar^2 c^2}\right] H_c^2 \lambda^4.$$

κ is widely used to characterise superconducting materials and isknown as the Ginzburg-Landau parameter. It is related, approximately, to the penetration depth λ and the coherence length $\xi(l)$ by:

$$\kappa \approx \lambda/\xi(l)$$

The major significance of κ, however, is that, according to the Ginzburg-Landau theory, the surface energy of the s-n boundaries is positive, if κ is less than $1/\sqrt{2}$, but for all values of $\kappa > 1/\sqrt{2}$ this energy is negative. This enables us to be more explicit about the surface energy states predicted in the London-Pippard approach and, as a result, define two types of superconductor as, Type I $\kappa < 1/\sqrt{2}$, $\xi(l) > \lambda$, positive surface energy Meissner state until $H = H_c$.

Type II $\kappa > 1/\sqrt{2}$, $\xi(l) < \lambda$, negative surface energy, field penetration for $H > H_{c1}$ in the form of finely divided regions.

The penetration of the bulk of a type II superconductor, in the form of a series of superconducting-normal domains, to minimize the total free energy, is known as the mixed state. It commences at the lower critical field H_{c1}, the value of which is dependent on κ according to

$$H_{c1}/H_c = 1/\sqrt{2}\left[\ln\kappa + 0.08\right]$$

The value of H_{c1} is therefore always less than H_c and, for high κ materials, is often very small (H_{c1} for Nb25% is about 250 Oe compared with Hc $\approx$ 1,500 Oe.)

The Ginzburg-Landau equation has solutions between H_{c1} and an upper critical field H_{c2} defined by

$$H_{c2} = \kappa\sqrt{2}\, H_c$$

Values for H_{c2} vary widely, with κ, but for some hard materials $H_{c2} > 200$ k.Oe. Some of the highest values are shown in Table 2.1.

For fields greater than H_{c2}, a sample should be fully normal. This however assumes an infinite medium and neglects boundary effects. St.James and de Gennes[34] have shown that at a plane insulating-superconducting surface, in the field interval $H_{c2} < H < H_{c3}$, superconductivity is not entirely destroyed. The bulk of the material is normal but a superconducting sheath persists in surface regions parallel to the applied field. These surface effects are also apparent in some type I superconductors and for $0.42 < \kappa < 1/\sqrt{2}$ a sheath is observed for $H_c < H < H_{c3}$. For $\kappa < 0.42$, $H_{c3}\,(< H_c)$ is extremely difficult to measure, but nucleation measurements by Faber have been interpreted [2] to yield values for H_{c3}, and thus κ, for Al, In and Sn. For all materials, the nucleation field H_{c3} is given by

$$H_{c3} = 2.4\,\kappa H_c = 1.695\, H_{c2}$$

and the dimension of the sheath is of the order of ξ, the coherence length. The existence of this sheath has been the subject of much study in recent years and the ratio of H_{c3} to H_{c2} has been often verified.[35] The presence of a normal metal, in place of the insulator, is found to reduce H_{c3} and this too has been a subject of fundamental interest.

Three critical fields have therefore been introduced and key values of κ identified. The values of these fields, in reduced form $h_1 = \frac{H_{c1}}{H_c}$, $h2 = \frac{Hc2}{Hc}$ and $h_3 = \frac{Hc3}{Hc}$, are described in Fig. 2.2 as a function of κ.(36)

2.1.3. Magnetic behaviour of ideal superconductors

We shall now consider the reversible magnetisation curves of ideal type I and II superconductors. For all the curves we present it is assumed that there are no demagnetising effects arising from specimen shape.

Type I superconductors exhibit the Meissner state (B=0) until $H = H_c$, and above H_c the normal state is stable. The magnetisation curve is of the form shown in Figure 2.3(a) and, in the ideal case, is completely reversible.

Type II superconductors are also diamagnetic in applied fields less than H_{c1}, but for $H_{c1} < H < H_{c2}$ the bulk of the material is in the mixed state as predicted by the phenomenological theories. The structure of the mixed state has been the subject of much study. The major contribution has come from Abrikosov(37) who, in a remarkable and strangely unnoticed paper, predicted that the penetrating flux would be quantised. He found that the minimum energy condition was that each of the packets of flux should contain an equal amount of flux $\phi_0 = \frac{hc}{2e} = 2 \times 10^{-7}$ gauss-cm^2. The packets or tubes of flux have been variously called fluxoids, fluxons and vortices and are essentially a normal core approximately of radius ξ, surrounded by a supercurrent vortex over a region λ.(38) The relative distributions of

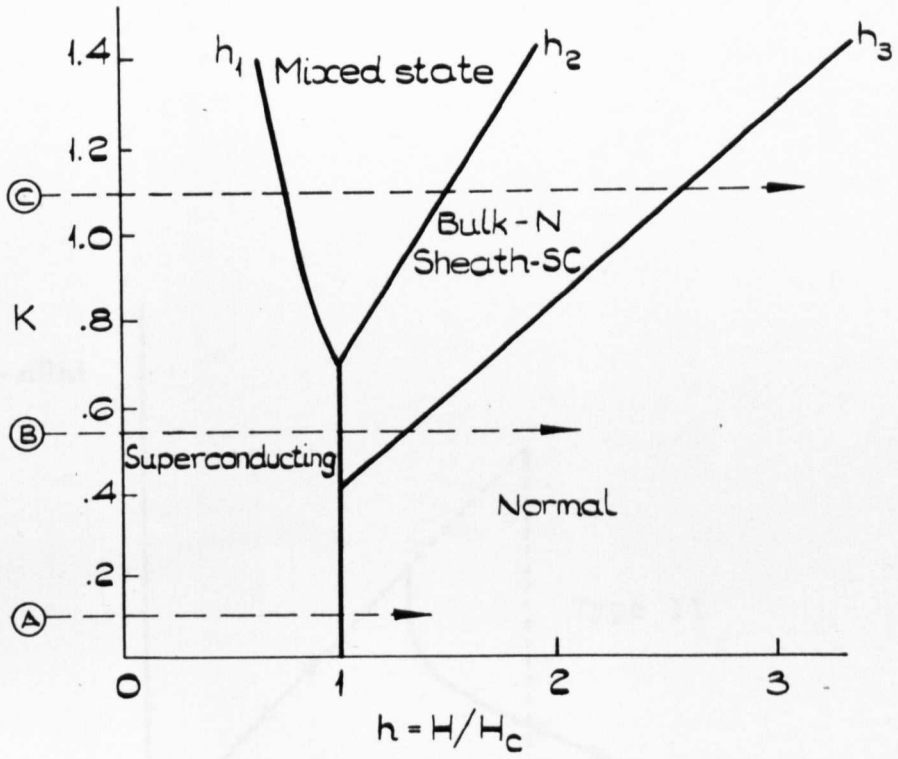

Figure 2.2 The variation of the reduced critical fields as a function of K.

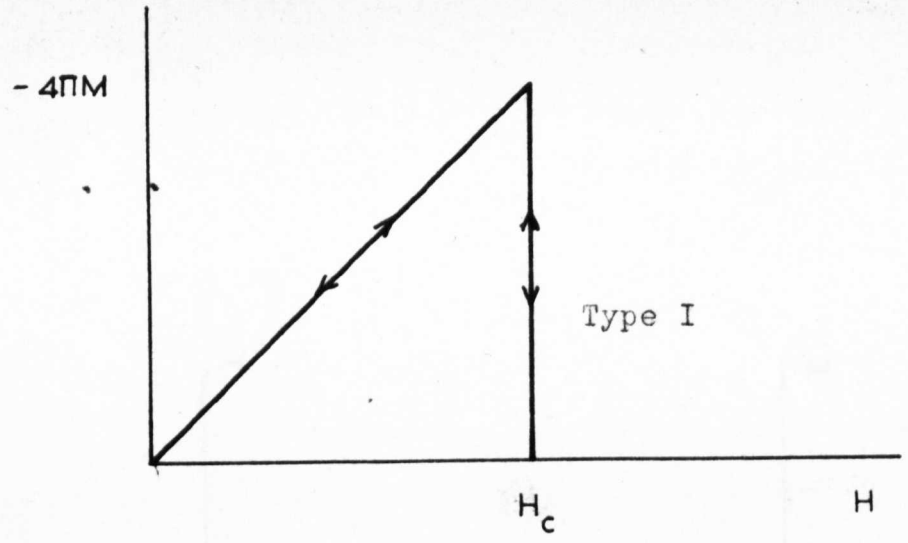

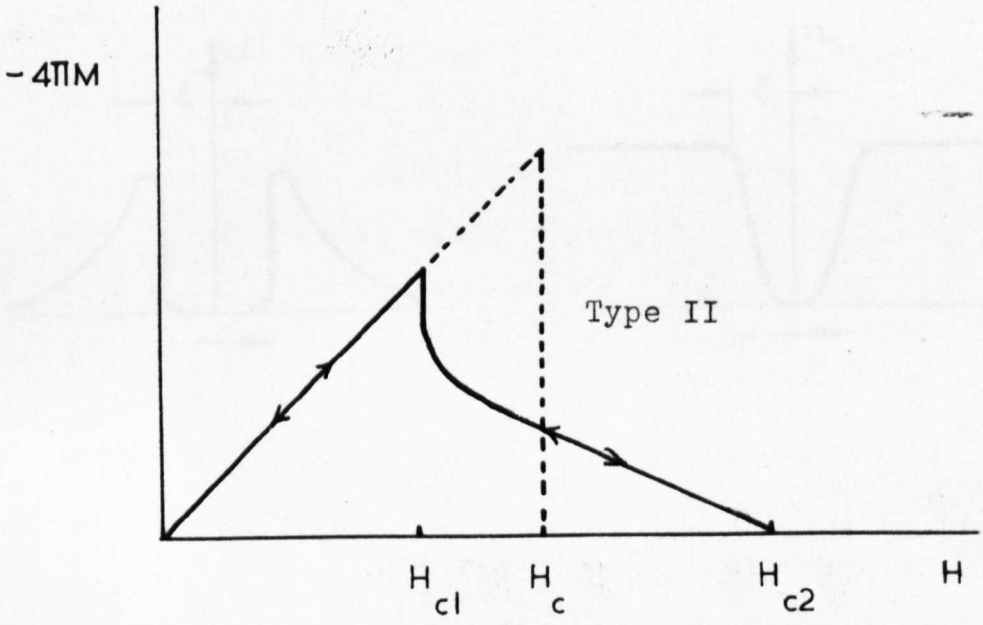

Figure 2.3 Ideal magnetization curves.

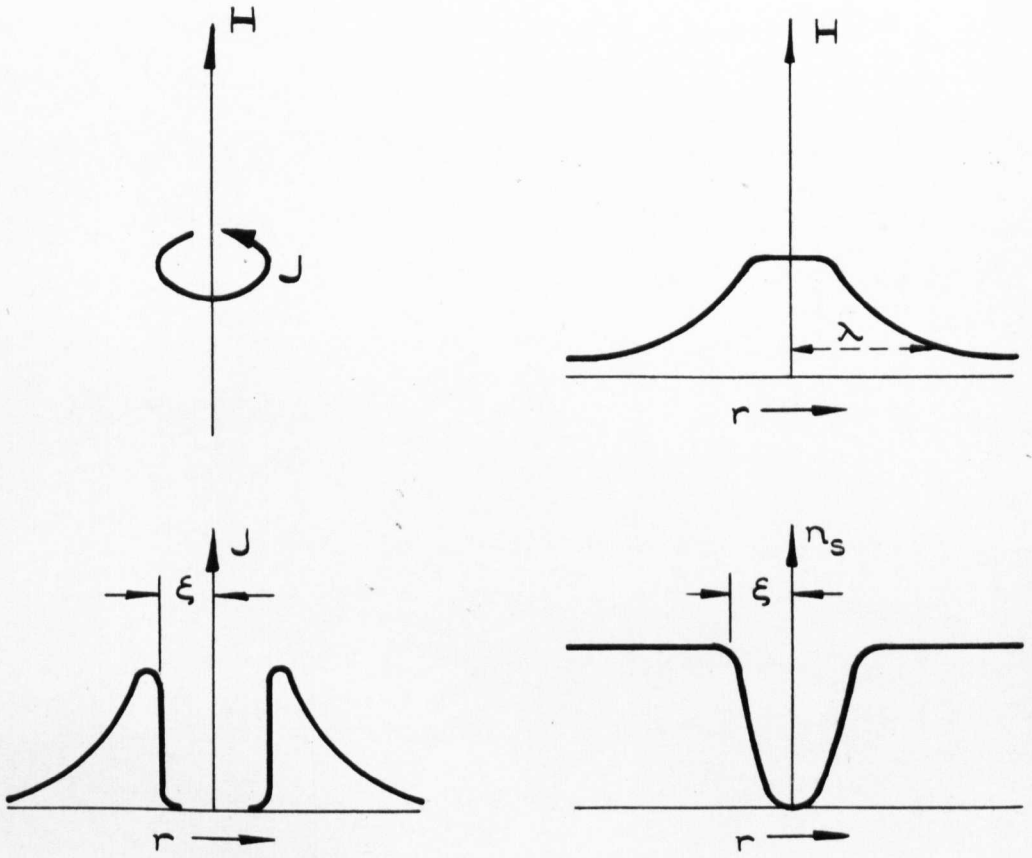

Figure 2.4 Structure of a fluxoid. The normal core of size ξ contains most of the flux, but the field and the circulating current extend over a distance λ .

the current, flux and superconducting electrons are illustrated in Fig.2.4. The quantisation of the flux has been experimentally verified by Deaver and Fairbank[39], amongst others.

Thus, in an ideal and defect-free material, flux is excluded at low fields but, when H exceeds H_{c1}, fluxoids are nucleated at the sample surface and are distributed uniformly throughout the cross-section. Their equilibrium positions are such that the mutual repulsions are balanced by the magnetic pressure of the applied field. Abrikosov[38] proposed that the fluxoids should take up positions in a square lattice but Matricon and Goodman[40] suggested a triangular array. This has now been confirmed experimentally[41] and the resultant reversible magnetisation curve is shown in Fig.2.3(b). As the field is increased from H_{c1} the separation of the fluxoids decreases and when this becomes comparable with ξ the normal cores overlap and there is no superconductivity. Therefore, as a rough approximation:

$$H_{c2} \simeq \phi_0/4\xi^2$$

The theory of the mixed state as developed through the Ginzburg-Landau equations by Abrikosov[37] and extended by Gorkov (the GLAG theory) has been very successful in predicting the magnetic properties of reversible type II superconductors. Goodman[42] proposed an alternative laminar model, with similar characteristics to the GLAG theory, but a detailed examination of experimental magnetisation curves near H_{c1} favours the latter.

2.2 The Critical State

It follows from Ampere's Law that

$$\frac{4\pi}{10} \cdot \underline{J} = \text{curl } \underline{H}$$

where $\underline{J}$ is the current density (in Amps - cm^{-2}), that if a current is to be carried in a superconductor there must be an un-uniform magnetic field. The uniform, triangular fluxoid lattice, inherent in the GLAG model for an ideal type II superconductor, is therefore unable to carry an appreciable current.

Real materials are known to sustain very large current densities. These can be understood in terms of the "pinning" of magnetic flux by microstructural variations, thus producing a field gradient. This idea was developed by Anderson[43] to explain the results of Kim et al.[44,45] on the movement of flux through superconductors under the influence of the Lorentz force. He showed that the "flux creep" could be explained, by assuming that bundles of fluxoids were thermally activated over free energy barriers arising from the pinning effect of inhomogeneities. The "pinning centres", or just "pins", were thought to include precipitates, dislocations, strains and other physical defects. It was found that, following a change in the applied field, flux creep occurs initially and then falls below a practicably observable level . When this occurs the field gradients, and thus the currents, are everywhere at their maximum value and as such are said to be in a "critical state"[46]. This is a quasi-equilibrium state between the magnetic forces on flux lines and the pinning forces. The current density then

becomes the critical current density J_c. Above certain values of an applied field and transport current the critical state breaks down, the fluxoids move against the viscous forces of the pinning centres and "flux flow" occurs.

According the ideas behind the critical state, when a field in excess of H_{c1}, is applied to a type II superconductor containing pinning centres, the flux penetrates only to a depth as determined by the strength of the pins. The circulating screening currents are everywhere equal to the critical value J_c and the depth of penetration Δ (for a semi-infite slab in the y-z plane) is given by

$$\Delta = H/\left(\frac{dB}{dx}\right)_c = \frac{10}{4\pi} \cdot \frac{H}{J_c}$$

where B is the internal field and J_c is assumed, for simplicity, to be independent of B. This assumption was made by Bean[47] in the first published attempt to account for the magnetisations of type II superconductors in terms of the critical state. He originally conceived the idea in terms of the Mendlessohn[48] sponge model in which the high field properties are derived from very fine filaments of superconducting material in a multiply connected mesh. However, it is essentially a phenomenological theory and is equally applicable to critical state ideas.

Bean was able to work out complete magnetisation loops, with the critical current density held constant, and results have been especially useful in the consideration of a.c. results. It will be considered more closely when the theory of a.c. behaviour is examined later.

Although the assumption of a field independent J_c is

useful it is rarely valid in practice and a variety of empirical relationships have been established for the variation of J_c with B. Kim[45] introduced the relation:

$$J_c(H) = \frac{\alpha}{B+B_o} \qquad (2.5)$$

where α and B_o are constants for a given material and $B_o \approx H_c$. In the limit $B \gg B_o$ and in the absence of a field discontinuity at the specimen surface (so H = B), $J_c(H) = \frac{\alpha}{H}$.

Fietz et al[49] found a better fit to their results with:

$$J_c(H) = a/b \exp(-B/b) + c$$

where a, b and c are constants.

Several attempts have been made to reproduce these expressions theoretically, by considering the force balance in the fluxoid lattice. Silcox and Rollins[50] calculated the forces on a single flux line due to neighbouring fluxoids to be:

$$F = -3\phi_o \left(\frac{H(B) - H_{c1}}{8\pi B} \right) \frac{dB}{dx}$$

where H(B) is the applied field in equilibrium with induction B, for a perfectly reversible sample. This, they assume, was balanced by a pinning force:

$$Fp = pf_p$$

with p as the number of pinning centres per flux line and f_p the pinning force of one centre on one line. If P is the overall density of fluxoids then $p = \frac{P}{n}$ where $n = B/\phi_o$ = density of flux lines. Then

$$Fp = \frac{P\phi f_p}{B} = F$$

Their results gave reasonable agreement with observed magnetisation curves but the interesting feature is that

$J_c(H) \propto \frac{dB}{dx} \propto 1/B$, so that $J_c(H).B$ = constant, as demanded by the approximate Kim expression. (Equation 2.5)

One criticism of this model is that, at high flux densities, the fluxoids are probably not flexible enough to embrace all the possible pinning centres and so the assumption np = P is not valid. Kasukochi et al[51] derived the relation

$$np^2 = 2N/\sqrt{3}$$

where N is the number of pins per unit cross section of the material. This gave $J_c \sqrt{B}$ = constant and the derived magnetisation curves were found to fit their experimental results.

Campbell[52] considering a general, curved flux line in a field gradient, concluded the force F to be:

$$\underline{F} = - \emptyset o/4\pi \,.\, \text{curl}\ \underline{H}(B)$$

(This can be expressed as $\underline{F} = \underline{J} \times \emptyset o$ and is analogous to the Lorentz force.) In two dimensions this reduces to Friedel's[53] result, obtained independently,

$$F = -\emptyset o/4\pi \,.\, \frac{dH(B)}{dx}$$

In the critical state the pinning force is then given by

$$Fp(B) = F = \frac{-\emptyset o}{4\pi} \,.\, \frac{dH(B)}{dx} = \frac{-\emptyset o}{4\pi} \,.\, \frac{dH(B)}{dB} \,.\, \frac{(dB)}{(dx)c}$$

Campbell et al[54] have considered both cases of weak and strong pinning and have derived magnetisation curves from their results. For weak pinning, when the induction is small, i.e. fp small but $P \gg n$, Fp is expected to be independent of B, and Jc to be constant. In the case $n > P$, when several flux lines are pinned per centre, they chose a form for the pinning force similar to that used by Silcox and Rollins[50] ie.

$$(dB/dx)_c = \alpha/2B$$

where $\alpha = \frac{8\pi\delta_{pm}}{l^2}$, l being the separation of the pins and m the gradient of the reversible B-H curve. As $\frac{1}{l^2} = P$ and $m_t \frac{H(B) - Hc1}{B}$, Campbell's expression[52] can be rewritten as:

$$\frac{P\phi_o f_p}{B} = -2\phi_o \frac{H(B) - Hc1}{8\pi B} \frac{dB}{dx}$$

which differs from Silcox and Rollins' result by a factor $\frac{2}{3}$.

The most recent attempt to account for the properties of strongly pinned samples has been that of Irie and Yamafuji[55] who derived a more flexible form for the pinning force. Making allowances for possible anisotropies of pins, they have concluded that the number of pins occupied by fluxoids, per unit volume, is $\frac{a'}{8\pi} B^{\gamma}$ where a' and γ are constants for a given sample. In a sample with few pinning centres $\gamma \sim 0$ corresponding to the Silcox-Rollins model; in a sample with many pinning centres $\gamma \sim 1$ and J_c is constant as in the Bean model. When $\gamma = \frac{1}{2}$, $J_c \propto 1/\sqrt{B}$ as determined by Yasukochi[51]. Irie and Yamafuji have calculated a value of γ from the peak in Yasukochi's magnetisation curves and find it to be 0.45. They also produced an excellent fit to the latter author's results.

To account for their a.c. measurements, Green and Hlawiczka[56] developed a mathematical analysis with a pinning force $F_p \propto H^n$, $n < 0$. This was an entirely arbitrary choice of function and the use of n = -3, to fit someof the results, is suspect.

The critical state model, in its various forms, has proved very useful in predicting the steady state magnetic behaviour of hysteretic type II superconductors. However,

there appears to be some limitations to its application in materials with low pinning, especially where surface currents are appreciable. Schweitzer[57] has recently claimed to have produced non-critical states by various means. Nevertheless the simple concepts of the model are widely used in the interpretation of experimental results.

2.2.1. Pinning phenomena

One of the basic concepts of Andersons flux-creep theory (43) was that microstructural variations cause minima in the free energy of the vortices and thus effectively pin the magnetic flux. In his original letter[43] he speculated on the form of these variations and since then a considerable amount of work has been published on the nature of the pinning centres.

Deformation has been found to increase the current-carrying capacity and magnetic hysteresis of superconductors (58-60). Narlikar[61] showed dislocation tangles to be effective in pinning. Later work by Narlikar[62] led him to conclude that this tangled structure effectively reduced the mean free path and increased the value of the Ginzburg-Landau parameter κ. For $\kappa \gg 1$ the line energy of a vortex can be written[2]

$$E_\ell = \left(\frac{\phi_0}{4\pi\lambda}\right)^2 \ln\left(\frac{\lambda}{\xi}\right)$$

which means that

$$E_\ell \propto \ell \ln\left(\frac{\text{constant}}{\ell}\right)$$

To a first approximation E_l is proportional to ℓ and so the dislocation tangles are essentially regions of low line energy. This mechanism also shows that a given defect will

have a greater effect in low-K materials (high ℓ) than in high-K materials of already short mean free path. van Gurp has confirmed this in experiments on niobium and vanadium[63] foils.

Narlikar[62] also discovered that there was a strong interaction between cores of the vortices and dislocations in a non-uniform distribution. This has been calculated by Webb[64] and is accounted for by the variation in the elastic moduli between the normal core and the superconducting matrix. Recent work by Williams [65] and van Gurp[63] has also shown that the interaction is greatest when the fluxoids are parallel to the dislocations.

Interstitial impurities, larger than the host ions are especially effective as pinning centres[66], presumably because of the distortion and resultant strain in the lattice.

Second phase precipitation is a prime cause of hysteresis and has been extensively studied by Livingstone[67]. It is however not entirely clear how precipitates actually pin fluxoids. It has been shown[67], for the Pb-Sn system that the optimum size of precipitate is less than 0.2 μ, which is still much larger than the coherence length ξ, but this may be due to an increase in the total precipitate-matrix surface area. Sutton and Baker[68] found a maximum in Jc when the precipitate size, in their aged Nb-Ti alloys, was of the order ξ. Levy, Kim and Kraft[69] have discovered a linear variation in Jc with the precipitate surface area per unit volume, for their eutectics, and both they and Livingstone find that normal precipitates pin better than those which are superconducting. Hanak and Enstrom[70] detected a

similar relation between J_c and grain boundary area in Nb_3Sn.

The most recent work of Campbell[71] has shown that the pinning forces in their Pb-Bi alloys are directly proportional to the surface area of the precipitates and he has concluded that it is this boundary between the superconducting matrix and the normal bismuth-rich particles, that pins the fluxoids. Campbell[71] shows theoretically that the bulk of a large precipitate will not pin vortices but that there will be interaction of both the vortex core and the circulating currents with the precipitate boundary. Using an approach similar to the "image force" calculations of Bean and Livingstone[72] he derived an expression for the critical current density:

$$Jc(H) = \frac{S_v M(rev)}{\lambda} \left(\frac{\phi_o}{B}\right)^{\frac{1}{2}}$$

where S_v is the total phase boundary per unit volume perpendicular to the driving force, and $M_{(rev)}$ is the reversible magnetisation at a field H. This result finds good agreement with the experimentally determined results.

This approach can also be used to analyse surface currents in the mixed state and will be discussed in the next section.

2.2.2. Surface Currents

We have seen that when a type II superconductor is in an applied field H, less than H_{c1}, it obeys the Meissner relation. The bulk of the material is completely shielded by circulating currents flowing in a thin surface layer of thickness λ. These currents are, in theory, completely reversible. Hysteresis is sometimes observed but this will be considered later.

Above H_{c2} St.James and de Gennes' solution of the Ginzburg-Landau equations predicts surface superconductivity for $H_{c2} < H < H_{c3}$. These currents are not quantised and flow in a sheath of thickness comparable to the coherence length ξ. Abrikosov,[73] Park[74] and Yamafuji[75] have all calculated the critical value of these currents and the results of Bellau,[76] Swartz and Hart[77] and many other authors, are in qualitative agreement with their predictions. In this field interval the bulk of the superconductor isnormal and the internal field differs from the applied field by the value of the sheath currents.

These two regions of surface superconductivity are well documented. Between H_{c1} and H_{c2} the bulk of a type II superconductor is in the mixed state, with the fluxoids distributed according to the arrangement and strength of the pinning centres. In recent years various authors[77-82] have suggested that surface currents flow throughout the mixed state, and contribute to magnetic hysteresis. Fink[83] and Park[84] extended the St.James-de Gennes calculations and predicted that the surface sheath should exist in this field interval.

The reduction of hysteresis on plating with a normal

metal supported this idea at first.[78] However the magnitude of the currents involved were often much larger than predicted by the solutions of the Ginzburg-Landau equations. Gradually the idea of another form of surface current evolved.[77,83]

Bean and Livingstone[72] had calculated that a fluxoid near the surface of a specimen would be acted upon by its "image" in the surface. They used these ideas to show that the field of first penetration $H_s > H_{c1}$ and their approach was confirmed by experiments.[84,85] (de Gennes[86] and Fink[87] have calculated that H_s may be as large as H_c). This"surface barrier" concept has been enlarged by Campbell[71] to account for the existence of surface currents in high-K materials, in terms of pinned fluxoids. He used this idea to explain the low-field hysteresis in otherwise reversible specimens and, as discussed earlier, the pinning of fluxoids by precipitates.

An alternative surface pinning model has been proposed by Hart and Swartz,[88] in terms of "flux spots" (i.e. the normal cores of the vortices) pinned at points of low free energy. These minima they associated with points where the fluxoids are perpendicular to the local surface. Roughening of the surface, which would increase the number of such sites, should therefore increase the surface currents. Transport current measurements [76,88,89] have lent support to their ideas. In contrast, a few experiments, [89,90] in which the surface currents were field induced, show the currents to decrease with roughening. This is the trend expected from the Bean-Livingstone ideas.

Hart and Swartz[88] have suggested the apparent discrepancy is due to the fact that in their transport current measurements, fluxoids are nucleated at the corners of the slabs used. In field induced measurements on cylindrical samples the number of nucleation points is probably the dominant factor.

In the experiments that we shall consider the surface currents will always be field induced. The sheath currents considered by Fink and Park and the pinned currents of Campbell - Bean - Livingstone are probably most significant. Experiments in which samples were plated with normal metals show that hysteresis is almost completely removed in some low-K materials but to a much lesser extent in high-K samples. This is probably due to the relative values of λ and ξ which represent the respective surface layers of the two types of currents. In low-K materials $\xi \sim \lambda$ and both will be affected by surface plating, while in high-K samples $\lambda \gg \xi$ and only the sheath currents are reduced.

Evidence that the surface currents are influenced by bulk pinning properties, has come from the work of Love[82] on Nb-Zr. The field dependence of the surface currents was markedly similar to that of the bulk currents. Campbell[91] in his latest work has added more evidence to this idea.

The part played by surface currents, in magnetic hysteresis and a.c. losses is only just becoming clear. In a later section we shall discuss experiments relevant to this point.

2.3 The critical state model and a.c. dissipation

The basic concept of the critical state is that the flux lines are in a quasi-equilibrium state under the influence of the pinning and Lorentz forces. If, therefore, the flux distribution changes when the externally applied field is altered, the fluxoid motion will be resisted and energy will be dissipated in the process. If a complete magnetisation curve is plotted this energy loss manifests itself as an irreversibility, i.e. hysteresis, and in the course of a low frequency cycle there will be power dissipation. The reasonable success of the various versions of the critical state model has encouraged several authors to apply it to alternating field conditions to predict the losses during a complete cycle.

Each calculation makes its own approximations but there are several assumptions implicit in all forms of the a.c.-critical state model. These are:-

(a) that the dynamic and static critical current densities are the same,

(b) that the response of the current-field distribution to a change in the applied field is instantaneous,

(c) that the temperature of the sample does not rise under the influence of the dissipation ,

(d) that there are no flux jumps in the course of the cycle ,

(e) that the sample is homogeneous.

Hart[92] has considered (a) and (b) and concluded that if the slope of the electric field, E, vs. current density, J, curve, at the point of operation,

$$\frac{\ln E}{\ln J} \gg 1$$

then the assumptions are valid. He calculated that the condition was reasonably well satisfied by Nb-Zr and excellently by Nb_3Sn.

The temperature rise mentioned in (c) has been predicted by Bean, assuming J_c and the thermal conductivity K to be constant;

$$T_{max} - T_{bath} = \frac{\omega H_m^4}{K J_c^2} \left(\frac{10^{-5}}{3(4\pi)}\right)^4$$

this applies only in the low field limit. Flux jumps and inhomogenities can be detected by observation.

We shall refer to these assumptions when considering our own experiments. In the next section the various a.c. loss calculations based on the critical state model will be discussed.

2.3.1. The Bean-London model

As we have seen earlier, Bean[47] developed a model for hysteresis in type II superconductors on the basis of the Mendlessohn sponge model[48]. The treatment is, however, equally valid in terms of the critical state and is worth investigating in detail.

Several assumptions are basic to this model:

(a) The current density is everywhere either at its critical value, J_c, or zero.

(b) J_c is independent of the applied field H.

(c) The sample isin the mixed state throughout the complete field cycle.

(d) There is no field discontinuity at the surface, due to surface currents.

For the purpose of this review we shall consider a sample radius r in longitudinal field H.

Ampere's law, curl H = $\frac{4\pi J_c}{10}$, and the assumptions made above, result in a constant field gradient, dH/dr. The current and field distributions, in increasing and decreasing fields are shown in Figure 2.5. The depth of penetration is defined as $\Delta = \frac{10H}{4\pi J_c}$ and a field Hp is chosen as the value of H when Δ = r, i.e. the whole sample is penetrated. Thus:

$$Hp = \frac{4\pi J_c r}{10} \qquad (2.6)$$

If the magnetic field applied to the cylinder is cycled between Hm and -Hm, the field distributions are dependent on the relative values of Hm and Hp. This is illustrated in Figure 2.6 where field distributions are displayed at various parts of a half-cycle for (a) $Hm < Hp$ (b) $Hp < Hm < 2Hp$ (c) $Hm > 2Hp$. In every case, as the field is decreased from Hm, the circulating currents reverse, from the surface inwards. At zero applied field the trapped flux B_r is as illustrated in the second figure of each set. For fields greater than 2Hp, B_r is independant of Hm, and $B_r = Hp/2$. (There is an error here in Bean's paper[47]).

The entire hysteresis loop for the cylinder can be calculated[47]:

$$B = \frac{HHm}{Hp} \pm \frac{(H^2 - Hm^2}{2Hp} \pm \frac{(Hm^3 + HHm^2 - H^2Hm + H^3/3}{4Hp^2}$$

for $H_m < Hp$, with the positive signs applying between $-H_m$ and $+H_m$ and the negative signs from +Hm to $-H_m$. The energy loss per unit volume during the cycle is then:

$$W_v = 1/4\pi \oint HdB$$

and for $H_m < Hp$ (H in Oersteds, J_c in Amps-cm^{-2})

$$W_v = \frac{5Hm^3}{6\pi^2 r J_c} \times 10^{-7} \text{ Joules-cm.}^{-3} \qquad (2.7a)$$

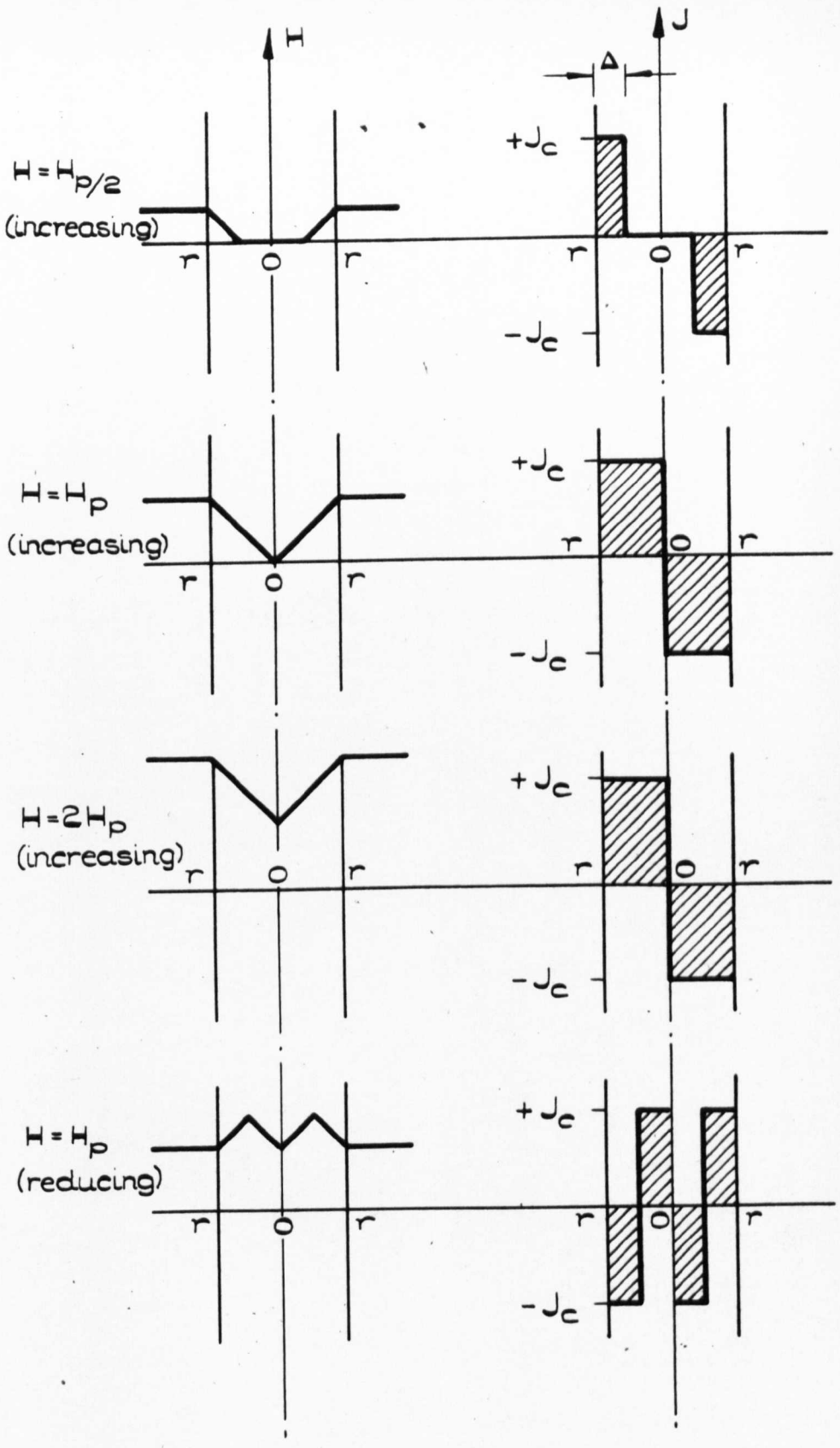

Figure 2.5 Magnetic field and circulating supercurrent distribution, in a cylinder radius r, as the applied field is increased to $2H_p$, then reduced.

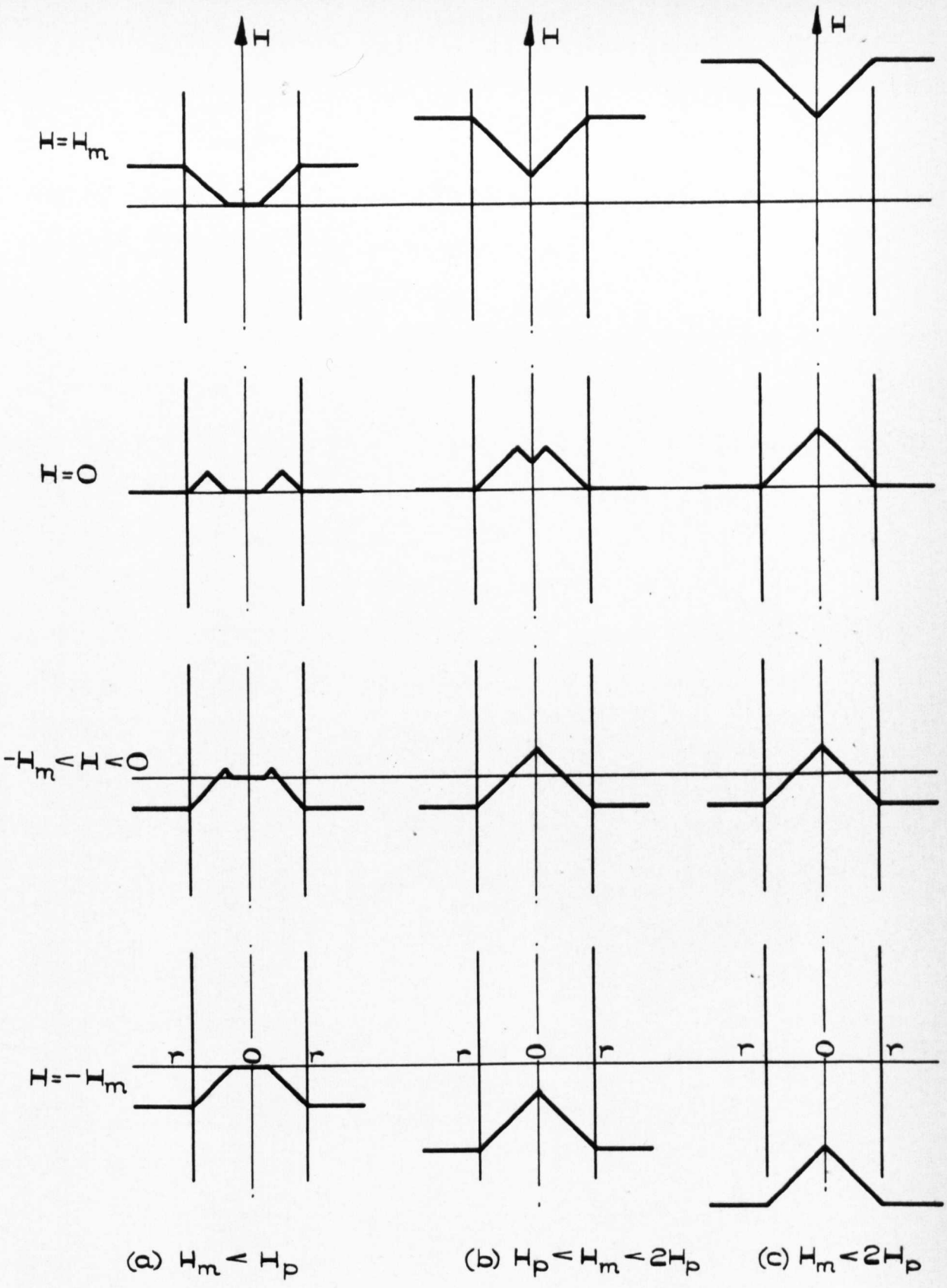

Figure 2.6 Magnetic field distribution in a cylinder radius r as the field is decreased from $+H_m$ to $-H_m$, for three values of H_m.

while for $H_m \gg H_p$,

$$W_v = \frac{2J_c r\, H_m}{15} \times 10^{-7} \text{ Joules-cm.}^{-3} \qquad (2.7b)$$

Equations (2.7a) and (2.7b) can also be expressed as surface losses and the corresponding equations are:

$(H_m < H_p)$ $W_s = 4.22 \times 10^{-9} (H_m^3/J_c)$ Joules-cm.$^{-2}$ (2.7c)

$(H_m \gg H_p)$ $W_s = 6.67 \times 10^{-8} (H_m J_c) r^2$ Joules-cm.$^{-2}$ (2.7d)

Similar calculations, assuming J_c to be constant, have been made by London[93] and Hart[92]. Hancox[94] has elaborated on a range of conductor geometries and combinations of impressed currents and fields.

The critical current density J_c has not been found to be independent of the applied field except over a limited field range in a few very hysteretic superconductors. In low fields, J_c often varies very quickly with H and in higher fields the Kim relation $J_c(H) = \frac{\alpha}{H+B_o}$ applies. If this latter expression for $J_c(H)$ is approximated to $J_c(H) \propto 1/H$ then from equation (2.7c), for $H_m < H_p$, $W \propto H_m^4$. Any other form for $J_c(H)$ will similarly impress itself on the loss equations. Hancox[94] actually used the Kim expression in a loss calculation and found:

$$W \propto \frac{(H_m)^3 (H_m+B_o)}{\alpha} = \frac{(H_m)^3}{J_c(H_m)} \qquad (2.8)$$

Voigt[95] assumed a general form for $J_c(H)$ and derived an expression:

$$W = P \frac{(H_m^3)}{J_c(H_m)} + \frac{Q\, H_m^4}{J_c(H_m)} \cdot \frac{d}{dH} (J_c(H_m)) + \ldots\ldots$$

where P and Q are constants. In the limit of $H_m \ll J_c(H_m) \Big/ \frac{d}{dH}[J_c(H_m)]$ this reduces to Hancox's expression (Equation 2.8).

According to the model of Irie and Yamafuji[55] for hysteresis, referred to earlier, the expression for the

power loss, in low fields is given by:

$$W_v = (0.054 \pm .002)(2-\gamma) H_m^{(4-\gamma)} / H_a^{(2-\gamma)} \qquad (2.9)$$

where γ and H_a are constants obtained for the primary magnetisation loop for a particular material. When $\gamma = 1$ equation 2.9 reduces to Bean's expression (2.7a) and with $\gamma = 0$ to the Kim limit (2.8).

Green and Hlawiczka[56] derived a proportionality between W and $H^{(3-n)}$ with n a negative number. Once again, with n = o and n = -1 their result is similar to equations 2.7a and 2.8 respectively. If values of $n < -1$ are chosen the dissipation is predicted to vary with a high power of the applied field. Some such high powers are observed experimentally but there is no physical justification for such a choice of n.

A further modification to the Bean-London expressions is required to account for the surface currents below H_c, and in the mixed state. Bean himself[96] undertook a simple calculation to cover both regions, in one expression:

$$W_s = \frac{5}{12\pi^2} \frac{Hm^3}{J_{cT}} \quad (dB/dH) \qquad (2.10)$$

where J_{cT} is the total critical current density, including the surface currents and dB/dH is the slope of the reversible B-H curve. Three regions of response to a.c.fields are defined by (2.10), i.e.

(a) near H_{c1}, $dB/dH \to \infty$ so there will be very large losses,

(b) below H_{c1}, dB/dH = 0 so zero loss is predicted,

(c) in high fields when $dB/dH \sim 1$ the original formula (2.7c) is closely obeyed.

Ullmaier[97] considered the influence of surface currents above the mixed state assuming the effective applied field to be $H_m = \frac{1}{2}(2Hm - \Delta H)$ where ΔH is the screening effect of the surface currents. The value of ΔH varies with the applied field [82-98] but for small values of Hm:

$$W_s = 5/6(4\pi)^2 (2H_m - \Delta H)^3 . 10^{-7} \text{ Joules-cm}^{-2}$$

For $2Hm < \Delta H$ there will be no dissipation according to this expression. If ΔH is due to a sheath current this will be true[99] but should the surface currents be pinned then some dissipation is expected.

As a fair proportion of the a.c.measurements reported in the literature have been made in applied alternating fields with $Hm \sim H_{c1}$ and with no steady bias field, the region $H_{c1} > H > -H_{c1}$ is of special interest. When a field greater than H_{c1} has been applied to a type II superconductor and then reduced below H_{c1} the internal flux distribution is somewhat uncertain. In semi-reversible materials the magnetisation curves in this region often have diamagnetic behaviour but there is some trapped flux which remains constant until $-H_{c1}$ is reached. In other more irreversible samples it has been found that flux moves across the surface even in this region below H_{c1}. No satisfactory theory has been developed for this behaviour and so a.c. loss calculations can only be made using simplifying assumptions. Such a study has been carried out by Easson[100]. This author assumed that the flux in a sample at H_{c1} is fully trapped between $H_{c1} > H > -H_{c1}$. The hysteresis loop which corresponds to this model is shown in Fig.2.7 where ϕ, the total flux

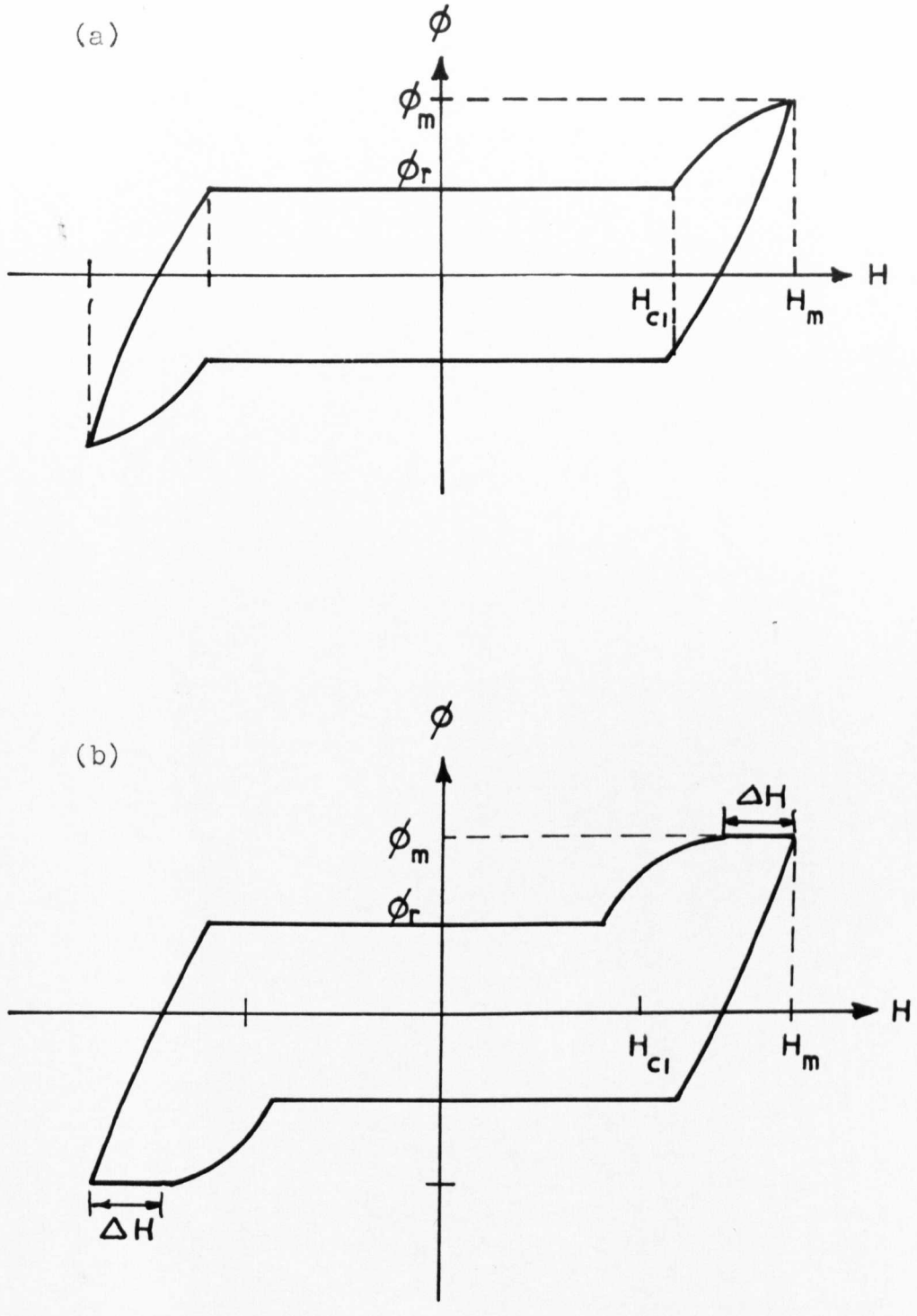

Figure 2.7. Hysteresis loops predicted by Easson's[100] model, allowing for H_{cl}.
(a) no surface currents
(b) with surface currents.

in a sample, is plotted against the applied field H.

Easson's expressions for the dissipation are

$$W_s = 0 \quad \text{for } Hm \leq Hc1 \qquad (2.11a)$$

$$W_s = \frac{5}{12\pi^2 J_c} (Hm-Hc1)^2 (H_m + 0.5Hc1) \times 10^{-7} \text{ Joules-cm.}^{-2} \qquad (2.11b)$$

To account for the variation of J_c with H they approximated the Kim expression (2.5) to $J_c(H) \propto \frac{1}{(H-H_{c1})}$ and (2.11b) became

$$W_s = 5/12\pi^2 J_c (H_m-H_{c1})^2 \left[\sqrt{2}H_{c1} + 1.026(H_m-H_{c1})\right] \qquad (2.12)$$

2.4. Survey of alternating field measurements in the literature

The aim of this section is to review the experiments on the a.c. properties of superconductors, reported in the literature, and to relate the results to the critical state theories.

The discovery of the type II superconductors and their large critical fields immediately led Fagan[101] and McFee[102] to speculate on potential engineering applications. As the majority of the designs involved the carrying of alternating currents by the superconductive windings, Jones and Schenk[103] set out to study the a.c. behaviour of these materials. The results of their work, in which appreciable power losses were measured, initiated a flurry of other experiments which can now be assessed in terms of modern theories. A good deal of conflicting information was published, due, in part, to unrealistic experimental conditions.

The a.c.loss phenomena is the main topic considered but some attention will also be given to critical currents and other a.c.properties.

2.4.1. Techniques for the measurement of a.c.losses

Among the techniques used to measure the dissipation in an alternating cycle are included:

(a) Boil-off calorimeters, in which the power dissipation was determined from the rate of helium evaporation.[103-111,121]

(b) Adiabatic calorimeters where a small temperature rise was recorded[112-115]

(c) Hysteresis loop measurements [116-120]

(d) Wattmeter measurements [116,122,123]

(e) Current - voltage measurements [105,122,124-6]

(f) Q-measurements on L-C circuits [130,131]

Owing to its simplicity the boil-off technique has been, by far, the most popular technique, but it is limited in sensitivity and in the information provided. Adiabatic calorimeters extend the sensitivity range but still integrate the dissipation over the whole cycle. The other four techniques all require more sophisticated equipment but are much more informative on the field distributions throughout the cycle. The wattmeter measurements are perhaps the most useful especially when linked with observation of the voltage waveforms. It is this technique that we adopted for our experiments.

Not only have the methods of measurement been varied but a wide range of sample geometries and electromagnetic conditions have been employed. These can be summarised as:

(a) Transport currents in wires and strips[104-110,115,124-6]

(b) Applied fields on cylinders and slabs (112,114,116-20,126-9)

(c) Transport currents and impressed fields (103,113,121-3)

The first two geometries can often be analysed in terms of the critical state model, although transport current measurements are difficult to interpret. Moreover, long lengths of wire are required to produce measureable power levels. Strip measurements are bedevilled by field concentration at the edges and by the methods used to cut them to shape (133).

Multilayer coil experiments are complicated by complex field distributions in the winding and temperature variations due to the heating effects of the current. (113,122) For these reasons experiments, in which alternating fields are applied to thin slabs and cylinders, have been found the most useful in providing results for comparison with theory.

The critical state considerations define three major field intervals for the response of superconductors to alternating fields: (a) $0 < H < H_{c1}(H_c)$ (b) $H_{c1} < H < H_p$ (c) $H_p < H < H_{c2}$. In a considerable section of the literature these boundary limits are ignored.

In considering the results of this reported work the experiments can be roughly classified into (a) and (b) plus (c).

2.4.2. Dissipation in the Meissner state $0 < H < H_{c1}(H_c)$.

The ideal magnetisation curve for a type I superconductor below H_c, and for a type II below H_{c1}, is completely reversible according to theory. The circulating currents

induced by an applied alternating field, or indeed alternating transport currents with low self-field, would be expected to flow without resistance within the penetration depth . Evidence to the contrary however has come from Buchold and Molenda's experiments on lead and niobium(112). Using a sensitive adiabatic calorimeter, they measured dissipations of between 10^{-10} and 10^{-8} Joules-cm.$^{-2}$ in peak alternating fields of less than 500 Oersteds for lead (H_c = 550 Oe.) and less than 1000 Oe. for niobium (H_{c1} = 1,400 Oe.). The measured losses were found to depend linearly on the frequency and on a high power of the amplitude of the applied field, i.e. $W \propto H_m^n$ (values of n between 2.5 and 7.0 were recorded). Similar experiments by Rhodes et al(105) on drawn wires produced values for the dissipation as high as 10^{-5} Joules cm.$^{-2}$ just below the appropriate critical fields for Pb and Nb. Bogner and Heinzel(124) also measured a.c.losses in niobium wires, in low fields. There was very poor agreement between the various authors' results on similar materials, even when the different metallurgical histories of their samples was considered. Large variations recorded for nominally identical samples measured in the same laboratory were even found.(112)

One feature, however, that was common to all the reported work at the time, was the hysteretic nature of the losses, implied by the linear frequency dependence. This led Buchold(117) to develop a hysteresis model in which small multiply-connected regions occur at the surface. He variously identified these regions with voids, impurities, local resistive regions and, most important, irregularities

in the surface profile. His model predicted that

$$W_s \propto H_m^2 \, \delta(H_m)$$

where $\delta(H_m)$ isthe depth of penetration of the hysteretic flux. The variation of $\delta(H_m)$ with the maximum applied field Hm will depend on thephysical and metallurgical properties of the surface. These are factors which are very difficult to express mathematically, but it is to be expected that high powers of Hm will be involved for a particular surface. This would account qualitively at least for some of the very steep $H_m - W_s$ curves observed experimentally and also for the wide range of results produced.

The contribution of the surface irregularities towards the a.c. losses is best understood in terms of premature penetration by the magnetic field due to small scale demagnetising effects. If local areas of the surface experience fields greater than the critical field, before the overall field exceeds this value, some of these irregularities will be multiply connected and hysteresis will result. Any surface treatment that removes such peaks and hollows would therefore be expected to reduce the losses. Evidence that this happens has been presented by Buchold[119] when he reduced the dissipation in an annealed niobium sample, by a factor 10, by lapping the sample surface. Rocher and Septfonds[114] observed a similar trend on their high purity niobium specimens after electropolishing. Mechanized polishing of Eassons cold worked Niobium strips also reduced the losses[132]. Rocher's work[114] has also shown that the more reversible samples exhibit higher losses probably because of increased mobility of the magnetic flux once it has penetrated.

Even when the specimen surface is polished there is often a measurable dissipation.[114] Buchold,[120] once again, has developed a theory, the basis of which is that the penetration depth λ is field dependent. Since the penetration depth depends on the mean free path l and, when $l \sim \xi$, λ varies with H, he has suggested that this variation could be expressed as:

$$\lambda = \lambda_0 + aH^2 + bH^4 + \cdots$$

In a sample containing defects and impurities the magnetic flux, within this depth, would be pinned. From these ideas he derived a value for W_s

$$W_s = \tfrac{8}{3} K_0 (\lambda_0 H_m^2 + a H_m^4 + b H_m^6 \cdots)$$

where K_0 represents the physical properties of the surface layers. While many of the ideas behind these equations are approximate their chief value is in establishing the high power relation between W_s and H_m.

A further experimentally determined feature of the surface dissipation, in this field interval, is the increase in the losses when a sample is cooled in a steady applied field. Buchold[112] found that cooling fields of the order of the earths magnetic field trebled the losses while Rocher[114] found the increase to be tenfold. It seems likely that the cooling field is trapped in the surface layers and modifies the value of λ, and then the dissipation. The level of the losses at which these factors are important is, however, only about 10^{-10} Joules cm.$^{-2}$ in polished materials and, not only is this difficult to measure, but it is certainly negligible for engineering applications. It is of interest to see how well one must polish a surface to

reduce the losses to a reasonable level and this is one of the topics on which we shall report later.

2.4.3. Dissipation in the mixed state ($H_{c1}<H_m<H_{c2}$)

Measurements of a.c. losses with peak fields greater than H_{c1} have been made predominantly on four materials: elemental niobium and the high field superconductors Nb_3Sn, Nb-Zr and Pb-Bi eutectic. The majority of the experiments were performed in large applied fields such that for part of the cycle $H>H_{c1}$. In a few of the reported experiments steady bias fields were used, so that the samples were in the mixed state throughout the whole cycle.

The element niobium has been very popular with workers in this field because of its large lower critical field, H_{c1}, and ease of preparation. However as values of H_m less than 2,500 Oe. were usual in their experiments and $H_{c1}\sim 1400$ Oe. the Bean-London version of the critical state model was hardly applicable. Furthermore, surface effects which produced large dissipations in the Meissner state undoubtedly influenced the results in the upper field region. This last factor has been demonstrated by Easson[132] when he greatly modified the shape of the dissipation-field curves, above H_{c1}, by polishing the sample surface. If low-field losses are reduced in this way some attempt can be made to use the modified critical state equations(2.11). Easson[100] has tried this for his own results on niobium strip and achieved a moderate fit. Surface currents above H_{c1} have not even been considered by most authors.

The effect of the bulk properties of the materials has also often been ignored. Rogers and Linford[107] demonstrated the increase in dissipation on successive heat treatments, presumably due to a decrease in $J_c(H)$ as pinning centres were annealed out. Otherwise, the effect of the static magnetisation and metallurgical conditions on a.c. losses have usually been left unexplored.

The critical state ideas have been far more successful in predicting the a.c. behaviour of the high field superconductors. The lower critical fields of these materials are usually less than 500 Oe. so that diamagnetic effects contribute little to the overall results. Figgins and Shepherd[110] found that measurable losses first occured in their lead-bismith wires when the self-field of the transport current exceeded H_{c1}. Above this field value the results were in rough agreement with Bean's predictions.[47] Kamper [128] also found that dissipation commenced at about 300 Oe. ($\approx H_{c1}$) in the Pb-Bi eutectic.

The first reported results on Nb_3Sn suggested very low losses[127]. Then careful experiments by Hart and Swartz,[111] on this material, showed that the losses were much as expected from the Bean-London ideas. They measured a power dependence, of the losses as a function of the applied field H_m, of approximately three, indicating a constant critical current.

By far the most widely studied materials have been alloys in the niobium-zirconium system. There has also been some measure of agreement between different authors as we demonstrate in Figure 2.8. Here several sets of results, all taken on commercial Nb 25% Zr 0.010 in. wires, are plotted. Also

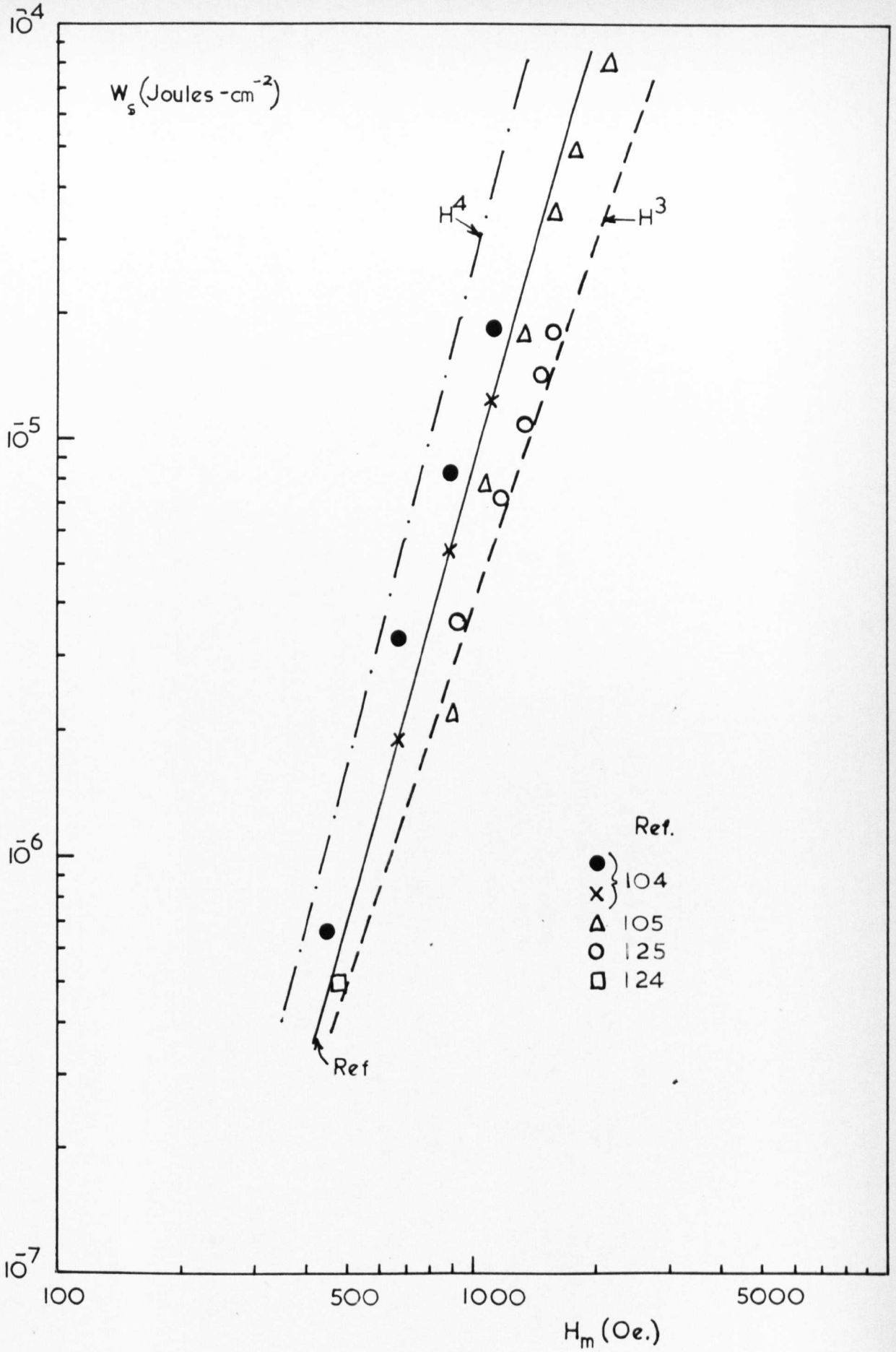

Figure 2.8 Comparison of various dissipation measurements on Nb25%Zr wires.

drawn, in the diagram, are lines of slope 3, corresponding to the Bean limit (J_c constant), and slope 4, corresponding to the Kim expression ($J_c \propto 1/H$). The majority of the lines have slopes between these two values. A detailed calculation from Irie's theory[53] (equation 2.9) using values of H_a and γ obtained from magnetisation curves due to Yasukochi[51] gives the solid line drawn, of slope 3.55. It can be seen that points taken from Pech's results[104] on a similar wire (sample 2), from the same manufacturer, fit the line extremely well. A good fit can also be obtained for Pech's sample 1 using data from Fietz's [49] results, again on similar wires. Taylor[134] matched his own results with equation 2.8 using $\alpha = 1.34 \times 10^6$ kGA-cm^{-2} and $B_o = 0.55$ kG. Damman et al[125] found a power dependence of 4.0 for a Nb-Ti alloy.

The effect of surface currents in the mixed state on a.c. results in large fields is probably small compared with that of H_{c1}. If bias fields are used however, these factors are more apparent. Ullmaier[97] has demonstrated this neatly by eliminating the discrepancy between Heinzel's results[126] and Voigt's calculations,[95] by inserting a surface current term in the loss calculation.

To summarise, the critical state model appears to be very successful in accounting for the a.c. losses in current-carrying wires of hysteretic, high-k superconductors. There is a lack of information of the effect of alternating applied fields on both low - and high - k materials and the part played by H_{c1} and surface currents is in need of thorough investigation.

2.4.4. Dissipation in a.c. coils

However interesting short sample measurements may be, should superconducting materials be used in a.c. engineering devices, it is likely that a.c. coils will be required. Analysis of results on coils is made difficult by complex field distributions and temperature variations. They are therefore of little use for comparison with theory so we shall only summarise the reported work. Nearly all the results in the literature are for Nb-Zr coils.

The first a.c. loss measurements, of Jones and Schenk[103] were made on multilayer coils. The losses were found to depend on $Hm^2 \times f$, where f was the frequency of the applied field, but, as London[93] pointed out this is tantamount to an $H_m^4 \times f$ dependence, in keeping with the critical state. Although Jones and Schenk apparently observed no heating effects, Grenier and Elschner[113] actually measured temperature variations due to the dissipation. Pech and Fournet[122] studied the thermal condition of their coils and were successful in analysing these mathematically. The same authors[121] produced a model for the field distribution and the resultant losses. With a combination of their magnetic and thermal calculations they have been able to predict the behaviour of a given coil within a factor of two.[122]

2.4.5. The a.c. superconducting - normal transition

Two alternative mechanisms are available to drive a superconductor normal in alternating conditions, i.e. the "quench" may be either thermal or magnetic.

In thermally insulated coils the temperature can exceed

the critical temperature due to the a.c.dissipation[113] and the critical current has been observed to increase sharply as the temperature of the helium bath is reduced through the lambda-point[135] (superfluid helium gives better heat exchange between the coils and the helium bath). The critical current decrease with increasing frequency[124] and Thomas[136] has evolved the empirical relation $I_c \propto f^{-n}$ with $n = \frac{1}{4}$ for niobium coils and n = 1/2.8 for Nb 25% Zr. On the other hand there is some evidence of a correlation between the value of the applied field and the quench in some well-cooled coils[123].

Single conductors are less likely to undergo a thermal quench but heating effects are still important. Rogers[137] has shown that lead can be driven normal by a peak field $H_m = H_c$ but, being a good thermal conductor, it returns to the superconducting state as the field drops in a later part of the cycle. Niobium, on the other hand, once normal, remains so until the field or current is completely removed.

The critical state model predicts that a type II superconductor will carry transport currents until the full cross-section is utilised. When this point is reached the superconductivity should be quenched. In the Bean limit (J_c constant) the critical current, expressed as a surface current density (ψ_c A-cm^{-1}), should be directly proportional to the thickness, d, of a strip or the radius, r, of a wire. In the Kim limit ($J_c(H) \propto 1/H$) $\psi_c \propto d$ or r (see Appendix A).

Results taken by the author on cold rolled niobium strip[138] showed a square root dependence of ψ_c on strip thickness and a linear variation was found for as-drawn wires.[139] Other reported results[140,141] are difficult to explain on

this model. As the sample dimensions are increased the critical current has been observed to be frequency dependent [108,138,140] and the transition to occur at a constant level of dissipation.[142]

The whole question of the two types of quench and the effect of the presence of a direct current has been thoroughly aired in correspondence between Rogers[143] and Hlawiczka.[144] More recently Finzi[145][146] has evolved a model for a thermal-magnetic quench which fits closely to his results on Nb-Zr wires.

2.5. The aims of the present work

During the period of this study considerable advances have been made in the understanding of the a.c.properties of superconductors, which have modified our outlook. This, however, has not altered the original aims of the author, to measure a.c.losses under controlled conditions and interpret the results in the light of modern theory.

An attempt was to be made to develop a technique for measurement of a.c.losses which eliminated many of the features open to criticism in much of the reported work. It was deemed very important that the specimen shape should be conductive to easy metallurgical and surface preparation. (These two factors have often been overlooked in much of the literature.) Ease of mathematical analysis was also desirable. A further demand made of the technique was that it should provide results easily, in quantity and with good accuracy and sensitivity.

It also seemed essential that, apart from the dissipation,

measurements should be made of the steady-state magnetisation curve and the critical current density, on the same samples. In the magnetisation measurements the requirements of the equipment were that it should provide complete magnetisation curves quickly, at the expense of sensitivity. The critical current measurements had to give information on the current densities without necessarily postulating a $J_c(H)$ - H model, as required when using the standard four point probe techniques.

Although the overall objective was to assess the usefulness of the critical state concept in predicting the a.c. behaviour of superconductors, certain aspects were of special interest. These included the role of the surface currents, their dependence on surface condition and the influence of H_{c1}. In addition the effects of specimen size and metallurgical state were to be considered. Finally it was hoped that information useful to the applications engineer would emerge.

In the following chapters, the development of our experimental techniques, our results and their significance, will be described.

3.0 The Experimental Techniques

In this chapter we shall first describe the general cryogenic background to the work and the facilities we have assembled. Details of the techniques for measurement of a.c.losses, magnetisation curves and critical current densities will then be given.

3.1 The Cryogenics

Silvered glass dewars were used throughout the work except for the magnetisation measurements, which were made in 7.5 cm. Oxford Instrument Co.metal cryostat. A variety of inner helium dewars were used each with the upper six inches made of a single layer of glass, to reduce diffusion of helium gas into the vacuum interspace. The support ring system for the dewars was designed so that all the cryostats and fittings were interchangeable. A helium gas recovery system was installed with the novel feature of plastic piping and glued joints. This was found to greatly reduce the cost of the installation and the time of assembly. The majority of the experiments were performed in free boiling liquid helium but pumping facilities were provided for the production of lower temperatures. A single-stage 250 $l.\text{-}min^{-1}$ rotary pump was used on a 1" line and control of the vacuum was with 1" and ½" valves and an Edwards Cartesian Manostat, in parallel. The temperature was read on a Wallace and Tiernan 10" dial-gauge calibrated directly in ^{o}K. The sensitivity was approximately $0.001^{o}K$ and the reading was accurate within 1%. With this arrangement a temperature of about $1.5^{o}K$ was obtainable and the control was within $\pm$ $0.005^{o}K$ at $3.0^{o}K$.

The limitation on the control was the small reference volume in the cartesian manostat. Much more stable conditions could have been obtained with an increased volume.

3.2 Measurement of a.c.losses

To meet the requirements listed in Section 2.5 a cylindrical sample was chosen for most of the work. The typical sample was 3 cm.long and of 5 mm.diameter. The demagnetisation coefficient was therefore small and rounding the ends of the sample hardly affected the result. Mathematical analysis was also straight forward and surface and metallurgical treatment was facilitated.

Longitudinal alternating fields were used and were provided by a liquid nitrogen cooled, copper solenoid, supported round the tail of a special helium dewar. In its final form the coil had 20 layers of 24swg enammelled copper wire on a tufnol former 5½ cm.diameter x 8 cm.long. The field calibration, obtained with a precision wound search-coil, was 336 Oe.-Amp.$^{-1}$ It was uniform to 1% over the central 1.5 cm. and the maximum peak field obtained, without undue heating, was in the region of 3,000 Oe.

For measurements at variable frequencies the coil was driven by a Servomex L.F.Signal Generator and a Derritron 100 watt power amplifier via a matching transformer. When large 50 Hz fields were required the mains supply was used via an isolating transformer and two controlling Variac autotransformers. With both modes of supply the coil was series-turned with a variable capacitor bank. This had the advantage of ensuring a sinusordal field and increasing the maximum field available.

3.2.1. Calorimetric experiments

Previous a.c.loss measurements made by the author had incorporated the helium boil-off technique.[107,108] Therefore, in the initial experiments this method of measurement was adopted. A small nylon calorimeter, with nylon boil-off tube, was made to fit inside the field solenoid. The gas flow-rate was measured with an electrical flowmeter of the type developed by Brown and Krδenberger.[147] The apparatus is represented diagrammatically in Figure 3.1. The gas flowed down a thin walled nickel tube which was electrically heated at the centre. Two closely matched platinum resistance coils monitored the temperature distribution along the tube and changes were detected with the bridge circuit shown. The passage of the gas caused the temperatures to be asymmetric and theoutput reading from the bridge was a direct measure of the dissipation within the calorimeter. A chart recorder was used on this output so as to establish the attainment of thermal equilibria. The flowmeter itself was borrowed from the Clarendon Laboratory, Oxford and the control circuit added.

From the outset difficulties were experienced with the calorimetric apparatus. They can be summarised as:-

(a) Lack of sensitivity due to high heat in-leak,

(b) long thermal time constants,

(c) thermal vibrations,

(d) a variety of other minor instabilities due to back pressures, temperature variations and environmental changes.

In addition to these,field inhomogeneities and demagnetising effects introduced large errors on the final results.

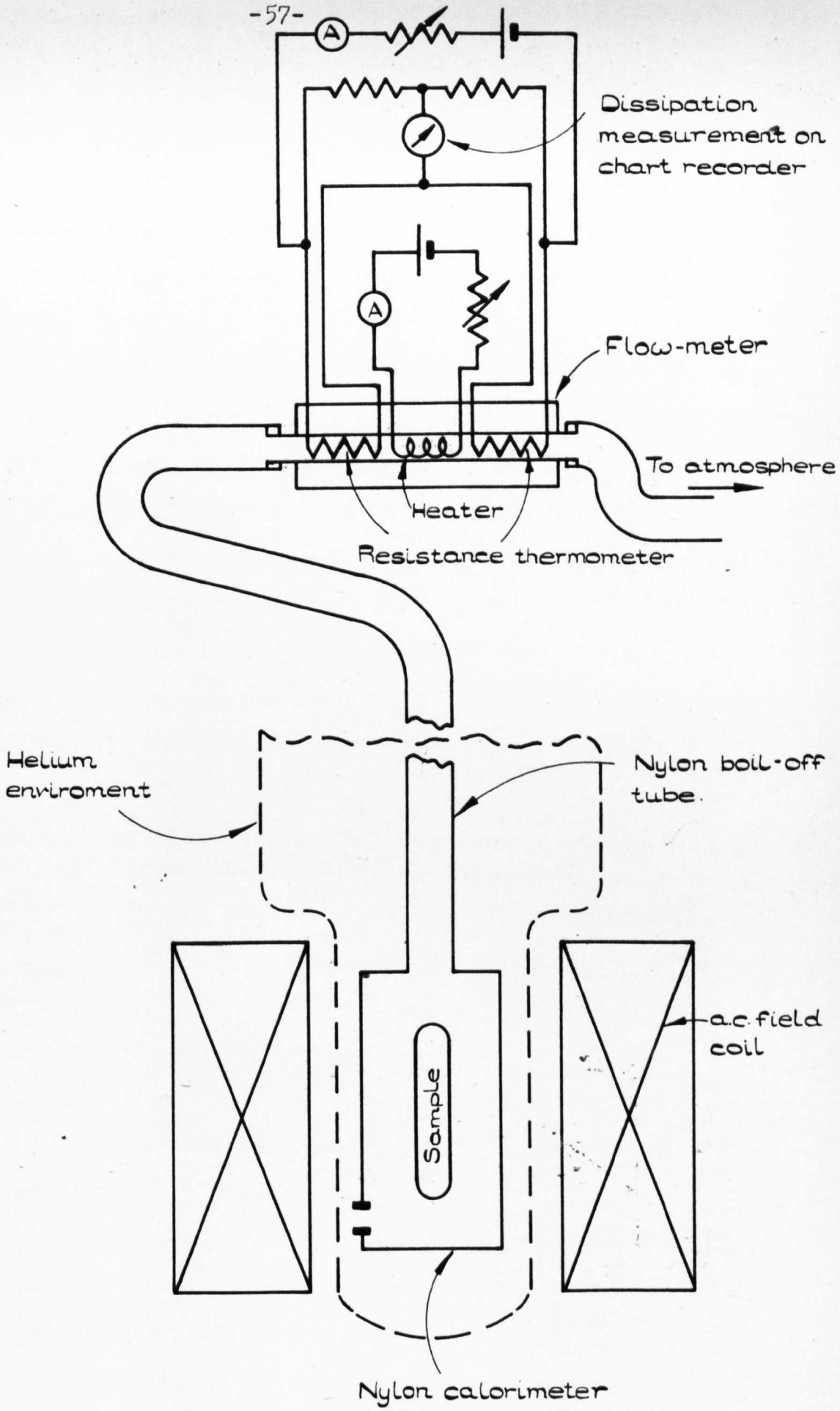

Figure 3.1 Diagram of the calorimetric apparatus.

It was, therefore, decided to abandon the experiment. (A colleague of the author has subsequently succeeded in eliminating some of the experimental weaknesses and put the apparatus to limited use. A similar flowmeter has been used by Lorch.[148])

A new technique for dissipation measurements was then developed. The hysteresis in an alternating cycle was derived from the voltages induced in small pick-up coils wound directly on the central portion of the sample surface. This method had been used by Buchold[117] and was being developed along similar lines by Easson and Hlawiczka,[116] when this work commenced. With this technique thermal factors are virtually eliminated; and effects and field variations beyond the length of the pickup coil likewise do not affect the result.

3.2.2. Theory of the electrical technique for the measurement of a.c.losses

When a magnetic sample is subject to a changing magnetic field H(t) the increase in the magnetic energy of the sample per unit volume, dW_r, is related to the increase in the average flux density $\overline{dB}$ by

$$dW_v = \frac{1}{4\pi} H(t)\overline{dB} \qquad (3.1)$$

(c.g.s.units are used throughout and so W_v is in ergs-cm^{-3}, H in Oersteds, B in Gauss).

But the average flux density B(t) is defined as $\frac{\phi(t)}{A}$ where $\phi(t)$ (Gauss-cm^2) is the total flux within the sample and A is its cross sectional area. Therefore

$$dW_v = \frac{1}{4\pi} H(t) \frac{d\phi(t)}{A} \qquad (3.2a)$$

or the increase in energy per unit sample length

$$dW_L = \frac{1}{4\pi} H(t).d\phi(t) \qquad (3.2b)$$

or for unit surface area of a cylinder radius r

$$dW_A = \frac{1}{8\pi^2 r} H(t)\, d\phi(t) \qquad (3.2c)$$

Thus the total energy dissipated in one complete alternating cycle

$$W_A = \frac{1}{8\pi^2 r} \oint_{cycle} H(t)\, d\phi(t). \qquad (3.3a)$$

or, $$W_A = \frac{1}{8\pi^2 r} \oint_{cycle} H(t)\, \frac{d\phi}{dt}(t).\, dt. \qquad (3.3b)$$

Equations (3.3a) and (3.3b) form the basis of two methods for the measurement of the a.c.dissipation. If an n-turn pick-up coil is suitably wound on a sample and unwanted stray voltages are compensated for, the output voltage from the coil

$$V(t) = -n \frac{d\phi(t)}{dt} \times 10^{-8} \text{ volts} \qquad (3.4)$$

If this signal is integrated electronically the resultant voltage $V'(t) = \int V(t)\, dt = n\, \phi(t) \times 10^{-8}$

When $V'(t)$ is displayed on the Y plates of an oscilloscope, and the X plates are driven by a signal proportional to the applied field $H(t)$, the area of the hysteresis loop is proportional to $\oint_{cycle} H(t)\, d\phi(t)$. According to equation (3.3a), therefore, values of the dissipation W_A can be determined from CRO photographs. This is, however, a tedious and expensive procedure and, although some results quoted later were taken in this way, the majority were obtained by a more sophisticated approach.

Combining equations (3.3b) and (3.4) leads to:

$$W_A = \frac{10^8}{8\pi^2 r\, n} \oint_{cycle} H(t).\, v(t)\, dt. \text{ ergs-cm}^{-2}$$

and the power dissipated at a frequency f

$$P_A = f \times W_A = \frac{10f}{8\pi^2 r\, n} \oint_{cycle} H(t).V(t)dt. \text{ watts-cm}^{-2}$$

As $f = 1/\int_{cycle} dt$ this last equation can be rewritten as

$$P_A = \frac{10}{8\pi^2 r\, n} \quad \frac{H(t)V(t)dt}{dt} \quad \text{watts-cm}^{-2}$$

The term in the bracket represents the time average of the product H(t). V(t) and if this is expressed as a voltage V_{av} = K x {time average of H(t).V(t) } where K is a constant of the electronics, then

$$W_A = \frac{10}{8\pi^2 r\, nfK} \times V_{av} \quad \text{Joules-cm}^{-2} \qquad (3.5)$$

Equation (3.5) represents the basis of our technique.

3.2.3. The apparatus

The voltage pick-up coils were wound directly on the sample surface using 50 turns of 46 swg enamelled copper wire, held in place by a solution of "Evostick" in benzene. The completed specimen is shown in Fig.3.2. A few experiments were performed on strip samples and the coil arrangements were as shown in Fig.3.3. The cut ends of the samples were insulated with melinex tape.

A diagram of the perspex sample holder, is given in Fig. 3.4. The sample was held parallel to the applied field by small end caps. Above the sample but still within the applied field was a 20 turn compensation coil. The leads of this and the pick-up coil were tightly twisted and solder connections made well outside the field region. From the soldering pins ran a twin screened lead, up the centre of the stainless steel support tube and through a vacuum tight seal. At the

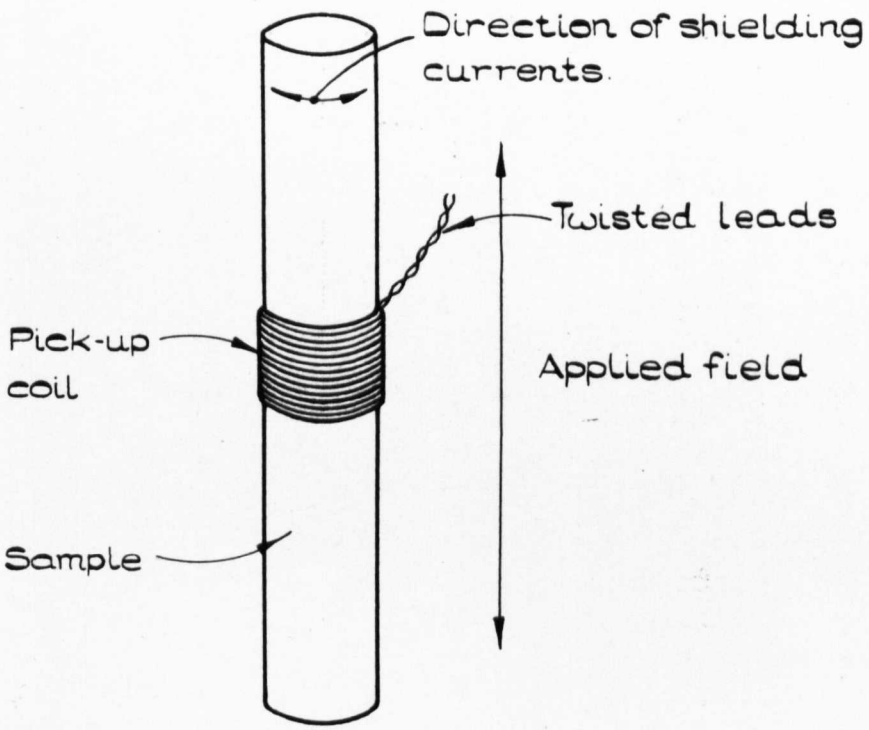

Figure 3.2.
Sample geometry for dissipation measurements on cylindrical samples.

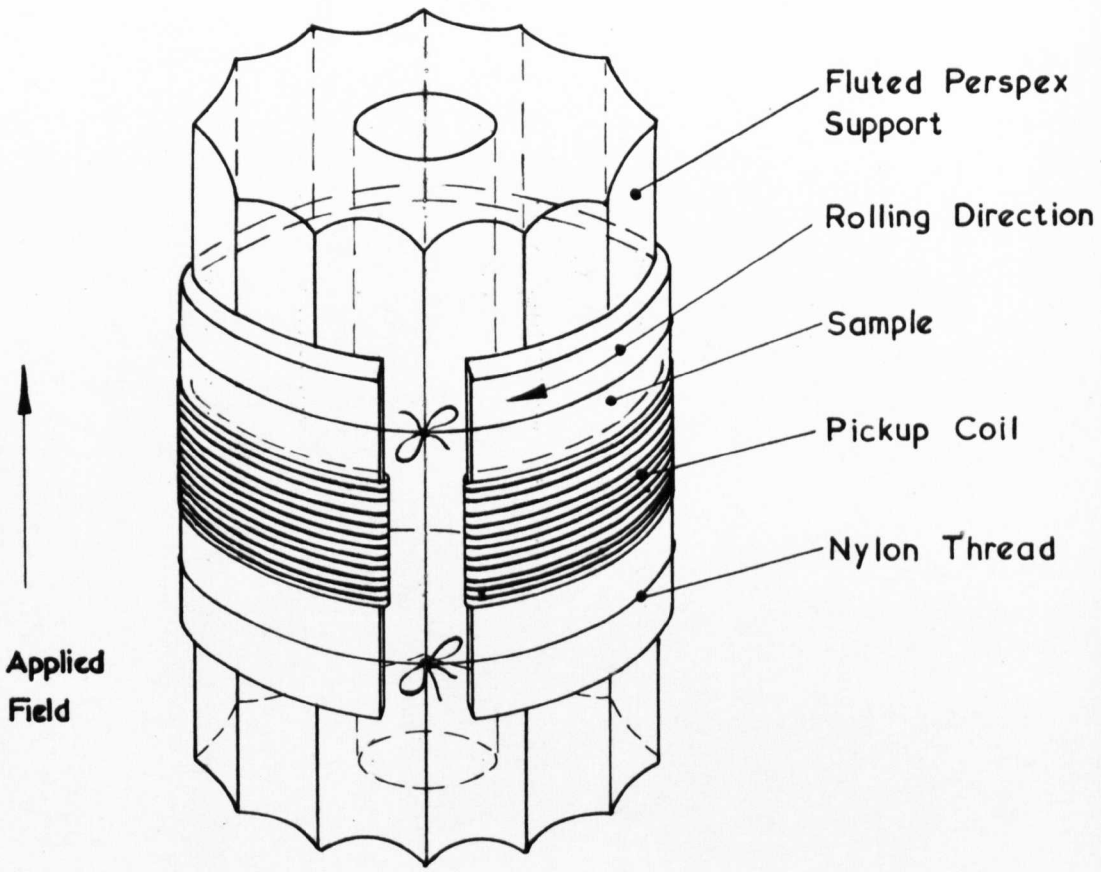

Figure 3.3 Mounting of strip samples for a.c. dissipation measurements

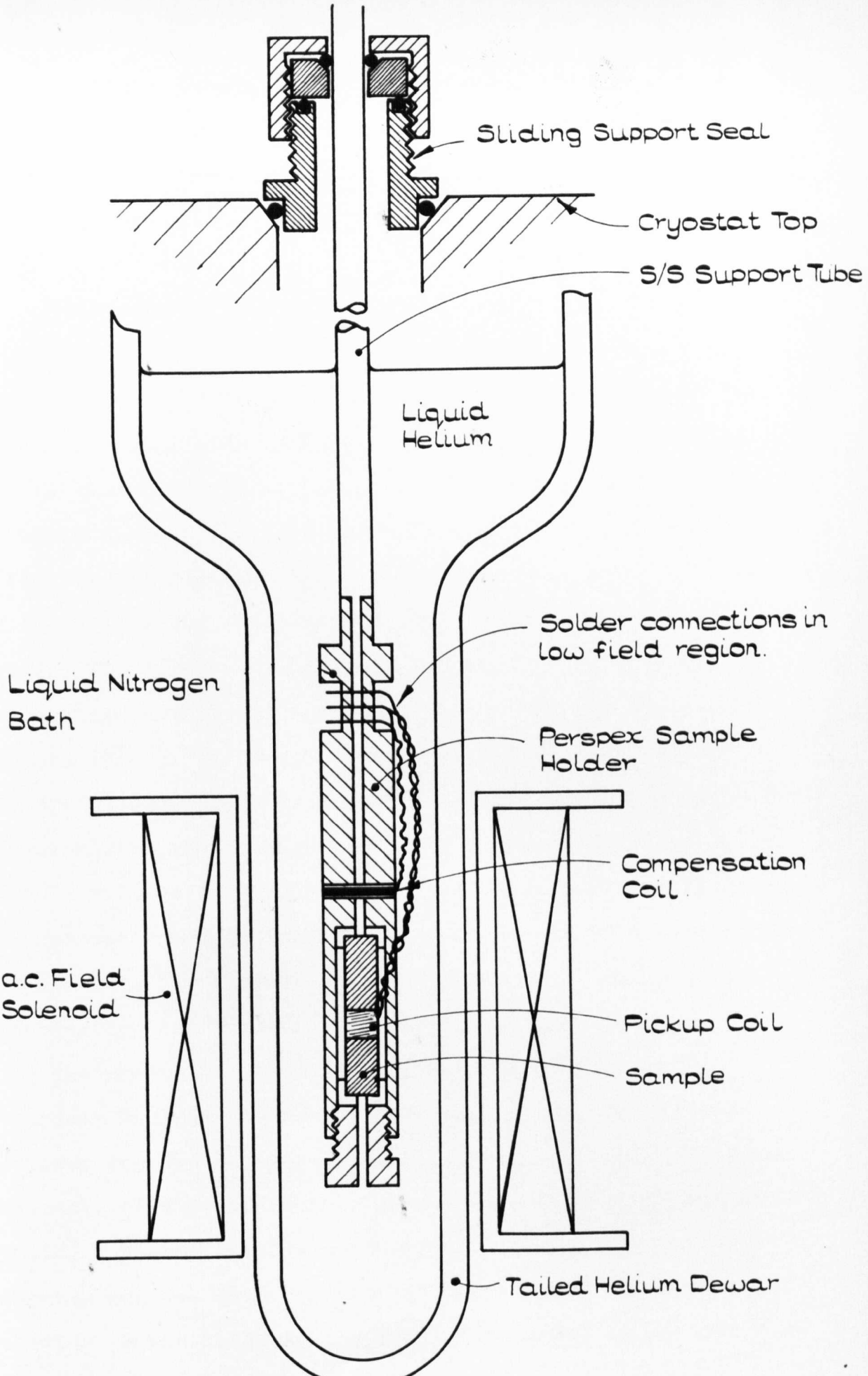

Figure 3.4 Sample holder and the experimental arrangement for the measurement of the dissipation in an alternating field cycle.

end of a short length of the wire, beyond the end of the probe was a diecast alloy box containing the compensation circuit and the connections to the preamplifier. Considerable care was taken with screening which was earthed at one point only.

The probe was supported in the cryostat by a sliding seal (Fig.3.4) so that the sample could be centred in the magnetic field. The whole assembly was designed to be leak tight, to facilitate variable temperature measurements.

A block diagram of the electrical connections in the external circuit is shown in Fig.3.5. In addition to the required signal voltages the pick-up coil voltage inevitably included unwanted components proportional to the applied field. These latter voltages which were often many times larger than signal voltages were removed by the compensation circuit (Fig.3.5). To do this a voltage was derived from a second "compensation" coil in the applied field. When suitably phase-shifted and attenuated it was subtracted from the pick-up coil voltage, in the differential preamplifier. Typical uncompensated and compensated wave forms are shown in figure 3.7 a and b, for a niobium sample. (We shall discuss the compensation procedure more fully in the next section.)

The preamplifier used in these experiments was a Textronix 2A61 CRO beam-amplifier which, with the filters suitably set had a noise level of about 5 micro-volts (peak-to-peak). The switched gain ranged to 2×10^5. A Princeton Applied Research CR4 Low Noise Preamplifier was acquired recently and was used for some of the results. A series resistor in the field-coil circuit (described in section 3.2)

provided a field dependent voltage. This was passed through a decade amplifier and fed into the multiplier circuits. To derive the time average of the product of the signal voltage and the field voltage a small analogue computer was assembled (Fig.3.6).

The phase of the field signal was adjusted with the network associated with operational amplifier A_1. Both signals were raised to the 100 volt level of the rest of the system by A_2 and A_3. The multiplier consisted of standard Solatron analogue computer modules. The Quarter Squares Multiplier (TR 1361) required, X, Y and -Y signals to derive a product XY and amplifier A_4 (AA1054) was used to invert the field signal. Amplifiers A_5 and A_6 (also AA 1054) completed the network. The output signal was averaged in a Hewlett Packard null-voltmeter. This meter reading, when multiplied by the constants of equation 3.5, was a direct measure of the dissipation. The waveforms at A, B, C and D were constantly monitored to detect saturation of the amplifiers and typical waveforms at A, B and D are shown in Figure 3.7 a, b and c respectively. The last of these waveforms represents the dissipation, which is time averaged on the output meter.

3.2.4 Compensation Procedure

Since the sinusoidal field component in the pickup coil waveform was often a hundred times, or more, the strength of the signal component, compensation was essential. This was achieved by subtracting an appropriate sinusoidal voltage from the pickup coil signal, in the differential pre-amplifier. The compensation circuit illustrated in figure 3.5 was used

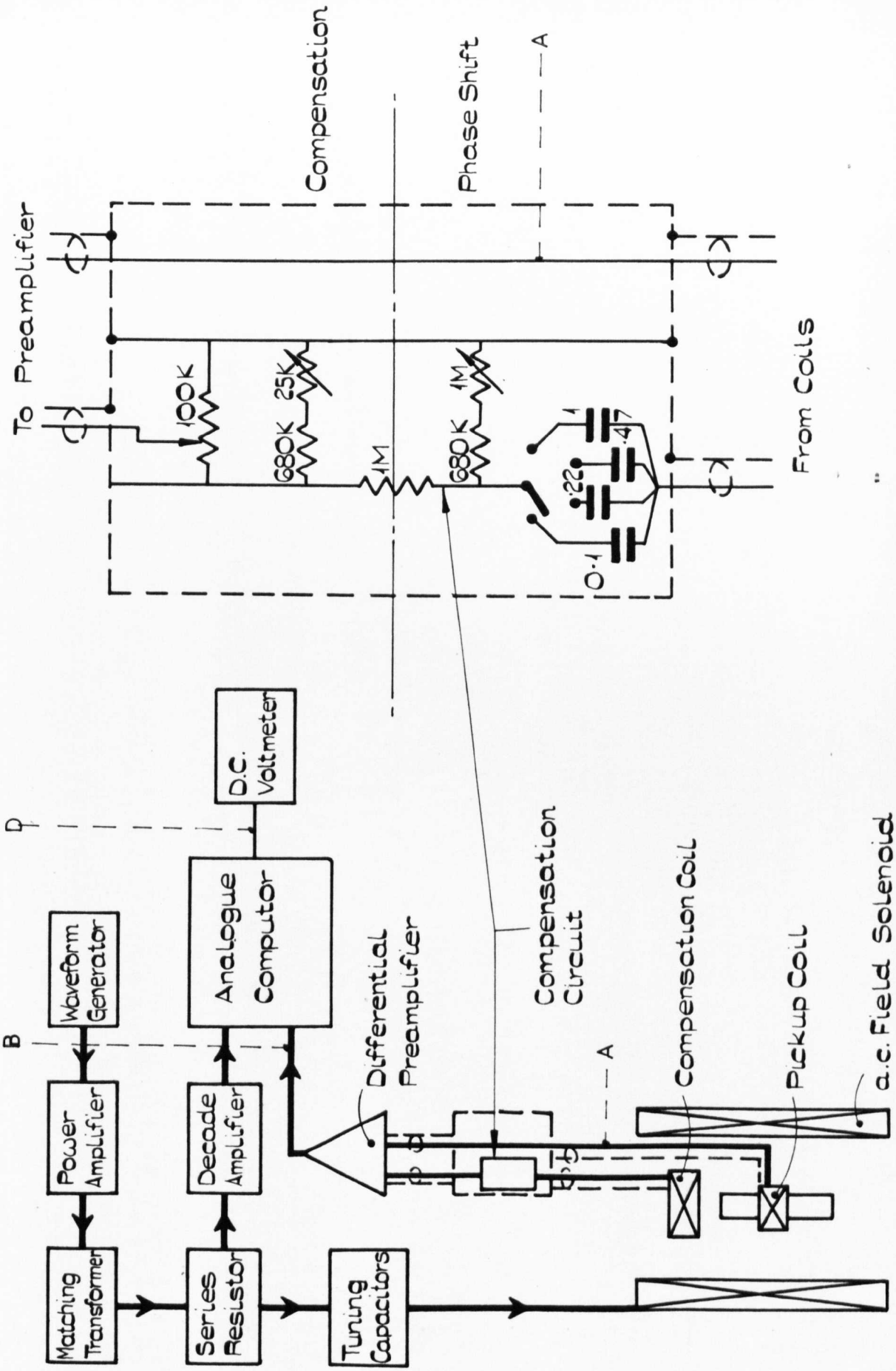

Fig.3.5 Details of the external and compensation circuits for measurement of the dissipation in an alternating field cycle.

Figure 3.6
Diagram of the components of the analogue computor used in the dissipation measurements.

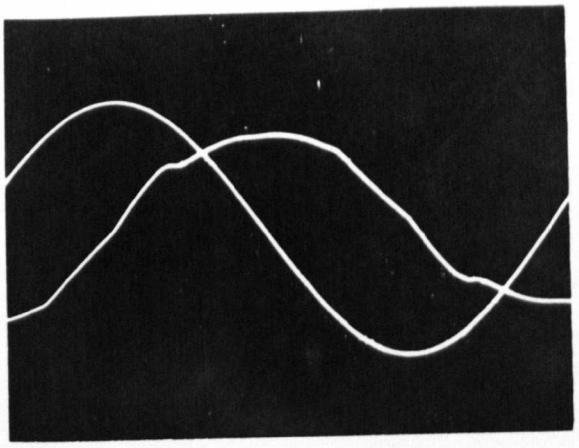

a

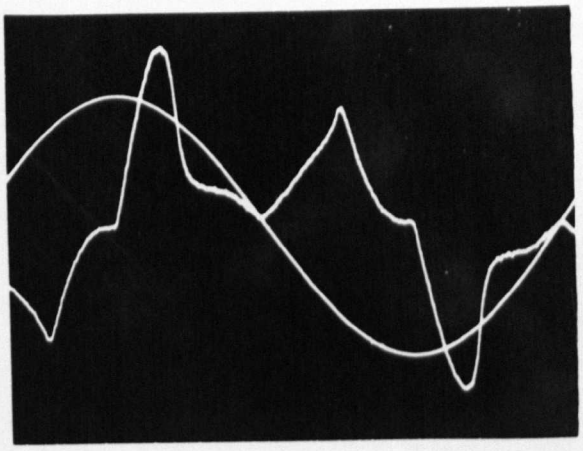

b

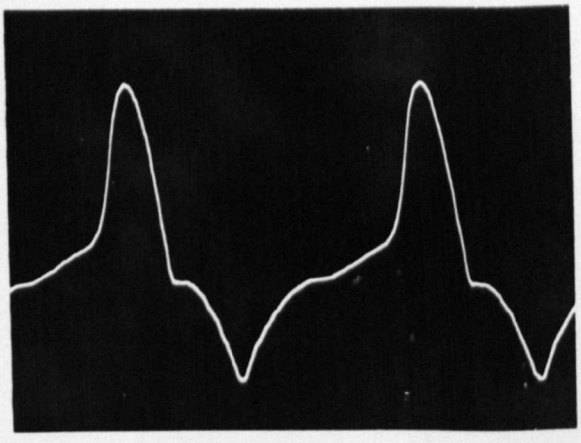

c

Figure 3.7 Voltage waveforms, A to D in figs.3.5 and 3.6, during a.c.loss measurement on niobium with H_m = 1500 Oe. (a) Uncompensated pickup-coil (A) (1mV/div) and field signal (C) (b) Compensated pickup-coil (B) (0.1mV/div) and field signal (C). (c) Computer output (D).

to make the necessary adjustments in phase and amplitude. Phase adjustments were found to be particularly crucial as, in the extreme case, a shift of as little as 0.1% introduced a 20% error into the final result.

A careful setting up procedure was therefore necessary as follows. Rough compensation was first achieved by adjusting the values in the compensation circuit to eliminate sinusoidal components in the compensated waveform, observed on an oscilloscope. Then in a low field, such that there was no observed penetration of the sample, the total pickup-coil voltage, now exclusively the sinusoidal dH/dt component, was multiplied by the field signal in the multiplying circuits. With the output meter switched to a sensitive range, the computer phase shift circuits (see figure 3.6) were set to give zero reading on the scale.

Fine adjustment of the compensation circuit was then made with respect to the field signal. With a sample that exhibited no field penetration whatsoever, in low fields, the potentiometers on the compensation box were set to give zero reading on the meter when the compensated and field signals were fed to the multiplier. In the case of a material that was dissipative in low fields a similar procedure was adopted in the smallest possible field compatible with the sensitivity of the equipment. However, on occasions, as the field was increased a negative loss reading was recorded due to over-compensation initially and in this case small phase adjustments were made until the negative reading disappeared. As a check on the adjustment Easson's[116] procedure was sometimes used. He inspected the flat portions of the dø/dt waveform in large

fields and varied the phase and amplitude until they lay on the zero line. We found, however, that this was not as sensitive as our approach for the dissipative materials.

3.2.5. Assessment of the technique

The overall sensitivity of the measurement is governed by the noise in the preamplifier, the size of the sample and the number of turns wound on the pickup-coil. In our experiments the maximum sensitivity was 10^{-9} Joules-cm^{-2} but under normal conditions 10^{-8} Joules-cm^{-2} was used as the onset of measurable dissipation.

Over most of the range an accuracy of better than 5% was estimated. The accuracy deteriorated at the lower limit of sensitivity but, as results were usually taken which varied over four orders of magnitude, the errors were not serious. When measuring large dissipations in very low fields the compensation procedure sometimes led to a scatter in the results and this was a basic weakness of the technique which we believe to be difficult to improve upon.

To summarise, the equipment was capable of providing accurate measurements of the dissipation in an alternating field, for a wide range of field amplitudes and frequencies, and at temperatures between 2.0 and 4.2°K. In addition to good sensitivity the equipment yielded loss results quickly and directly. The form of the samples led to versatility of preparation. Examination of the waveforms also provided information on the mode of field penetration and on both surface and bulk critical currents.

3.3. Measurement of critical currents

As most theoretical expressions for the dissipation in the mixed state involve the critical current density $J_c(H)$, measurements of this quantity were undertaken. Determination of $J_c(H)$ by direct transport current techniques was not considered practical for the large samples being used. Alternating field techniques for obtaining $J_c(H)$ were therefore adopted and three different methods were investigated as follows.

If a steady field H' is applied to a sample and then a modulating field $H_m \sin 2\pi ft$ is added, such that $H' \gg h_m$, then in the field interval $(H'-h_m) < H < (H'+h_m)$, it can be assumed that $J_c(H)$ is constant, in most cases. Having made this assumption the field penetration can be analysed on the Bean model of the critical state, and the value of $J_c(H')$ obtained. There are three possible approaches which are discussed below.

(a) Wave analysis. Bean[47] has shown that if the voltage waveform, from an n-turn pickup-coil wound on a cylindrical sample radius r, is analysed, the amplitude of the third harmonic

$$V_3 = \frac{4h_m^2 fnr}{J_c(H')} \times 10^{-8} \text{ volts}$$

Therefore, from a measurement of V_3 a value for $J_c(H')$ can be derived. This technique has been successfully used by Bean et al.[149] and Love.[82]

(b) Dissipation measurements. As $J_c(H')$ is assumed to be constant throughout the alternating cycle the calculation for the a.c. losses is valid. We have shown (equation 2.7b) that

$$W_s = 4.22 \times 10^{-9} \, (h_m^3/J_c(H')) \text{ Joules-cm}^{-2}.$$

Any technique that determines W_s can therefore be used to derive values of $J_c(H')$.

The presence of large surface currents might be expected to invalidate equation 2.7b and Easson[150] has suggested a modification to allow for these, viz:

$$W_s = 4.22 \times 10^{-9} (h_m - \Delta H/2)^2 (hm + \Delta H)/J_c(H')$$

where ΔH is the field change shielded by the surface currents. Surface currents similarly affect wave analysis measurements. Fourier analysis of the voltage waveform will yield an expression for J_c and ΔH, but in complex form.

(c) Triangular fields. If the sinusoidal modulating field is replaced by a triangular field then dH/dt is constant, between peaks, and analysis of the pickup-coil voltage waveforms is simplified. Ullmaier[98] has shown that the voltage at time t is proportional to $h_m^2/J_c(H') \left[t - \frac{\Delta H}{4h_m f} \right]$. Direct measurements of the voltages and time intervals can therefore yield values of J_c and ΔH.

3.3.1. The apparatus.

To make any of the three types of measurement the same field coils were required. In our experiments the large steady fields were provided by an Oxford Instrument 3cm, 30kOe. superconducting solenoid. The modulating coil was the subject of some experiment before a superconducting coil was preferred to one wound with normal copper wire. In its final form it consisted of 8 layers of insulated, copper-clad NbZr wire on a tufnol former and was driven by a signal generator and power amplifier. It was calibrated, in situ, with a precision wound search coil. Because of the linkage with the main solenoid the calibration was frequency dependent and varied between 418 Oe/Amp at 50 Hz and 294 OE/Amp at 1,000 Hz. The probe, preamplifier

and the compensation circuit were as described earlier and the loss measurements were taken as before. A Bruel and Kjoër Wave Analyser was used for the harmonic analysis.

3.3.2. Exploratory measurements.

To evaluate the relative merits of the three techniques some preliminary measurements were made on the critical current density of an aged lead-bismith eutectic sample. This was in the form of a short hollow cylinder machined from an "as cast" ingot and aged at room temperature for more than a month. The usual pickup-coil was wound on the outer surface and similar cylinders were used as guard-rings at each end. For comparison with the alternating field measurements a direct measure of the critical current was made by slowly sweeping the steady field until magnetic flux penetrated the centre of the cylinder. This was detected by amplifying the pickup-coil voltage on a Keithley 148 Nanovoltmeter and observing the output on an X-Y recorder.(151)

In figure 3.8 the solid line represents the results of these last measurements, and the circles and crosses indicate the harmonic and triangular field tests respectively. The various results were taken over a period of timeand the superconducting properties of this alloy are known to change with ageing. However the general trend in our results of reduced critical current in the older samples is consistent with published work.(152) When this is taken into account the agreement between the results from each of the techniques is reasonable.

Loss measurements were made on a second lead-bismith eutectic ring, using the hysteresis loop method, and a

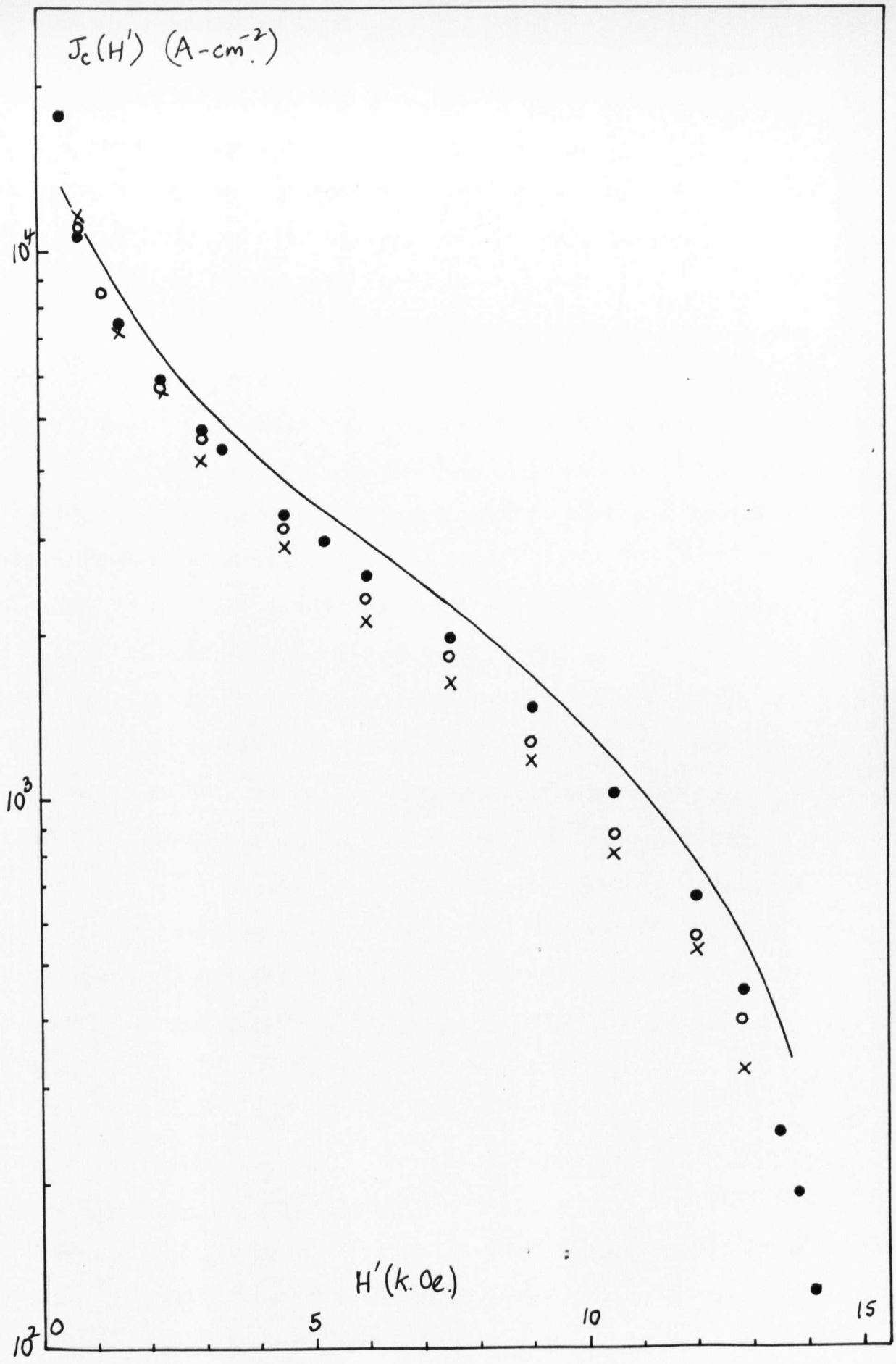

Figure 3.8. Measurements of the critical current density in ageing lead-bismith eutectic —— 31 days (swept field) • 35 days (harmonic anal.) o 90 days (harmonic anal.) × 90 days (Δgular fields.)

combination of steady and modulating fields. With $H' = 7.5$KOe., W_s was found to be directly proportional to $h_m^{3.0}$ for values of h_m up to 200 Oe. Also with $h_m = 120$ Oe. $W_s \propto 1/J_c(H')$ for a wide range of $J_c(H')$ values determined from the swept field measurements.

It seemed therefore that each of the three alternating field techniques was possible as a method of determining $J_c(H')$. It was realised however that the chosen test material was ideal in many respects as the surface currents were very small, the critical current varied gradually with H' and the Ginzburg-Landau parameter K was large.

The final choice was for the loss measurement approach. Once the present equipment had been assembled, this measurement was simple to take and its validity could be constantly checked by plotting W_s against h_m^3. The triangular field measurements were rejected because of the complications involved in producing large triangular fields, needed for measuring high critical current densities, and the inaccuracies introduced when taking readings from an oscilloscope screen. Wave analysis measurements had their attractions but an analyser was only available on short loan and further capital outlay was not merited.

3.4. Magnetisation measurements

One of the major weaknesses of much of the experiments on the alternating properties of superconductors, reported in the literature, has been the absence of reliable magnetisation data. Rarely have the results been related to values of critical

field obtained on the same sample. To avoid this situation in our work a vibrating sample magnetometer was assembled to plot complete magnetisation curves. The design was essentially a modification of the equipment used by Foner[153] with features suggested by Mr.I.Williams of the National Physical Laboratory.

The cylindrical samples were located in a longitudinal magnetic field between a matched pair of pickup-coils and vibrated along the common axis. A diagrammatic arrangement of the various components is shown in figure 3.9. Each of the coils consisted of 5,000 turns of 50 swg enamelled copper wire wound on the perspex former.

The tufnol sample holder was vibrated by a small vibrator outside the cryostat acting on the thin-walled stainless-steel support tube. Excitation of the vibrator was achieved with a Pye-Ling 3VA power amplifier and an oscillator (Servomex LF141). A range of frequencies was available but the mechanical resonances of the system and filter characteristics of the electronics led to a choice of 70Hz. The amplitude of vibration was less than 1 mm.

Adjustment was provided so that a specimen could be placed symmetrically between the coils. This position was determined as the condition for minimum output signal when the coils were connected in series. This setting-up procedure was extremely critical and both Mr.Williams and ourselves have found that incorrect positioning produces anomalous curves.

In operation the pickup-coils were connected in series opposition, the amplitude of the voltage output being directly proportional to the magnetisation of the sample.

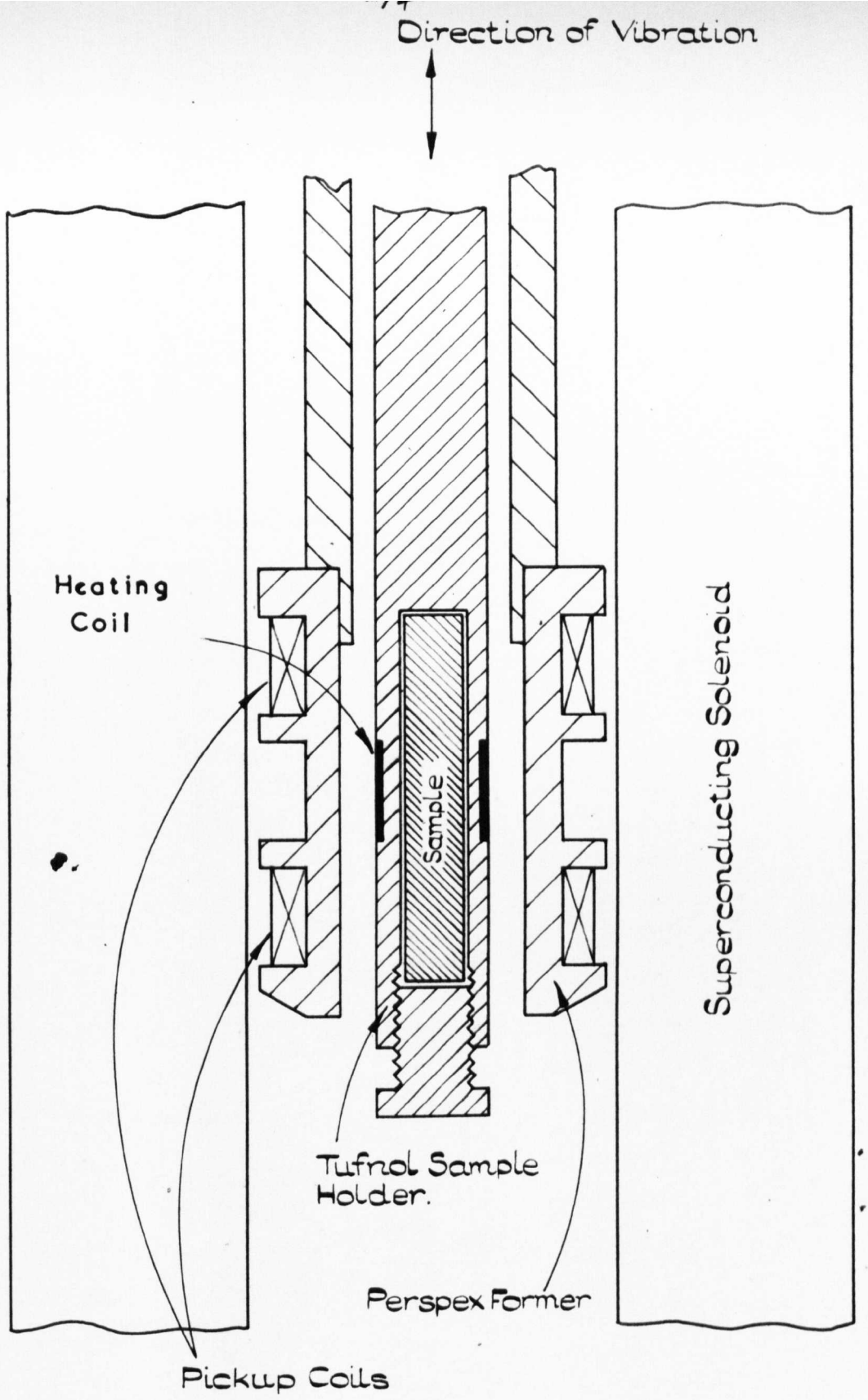

Fig. 3.9 Details of Vibration Magnetometer.

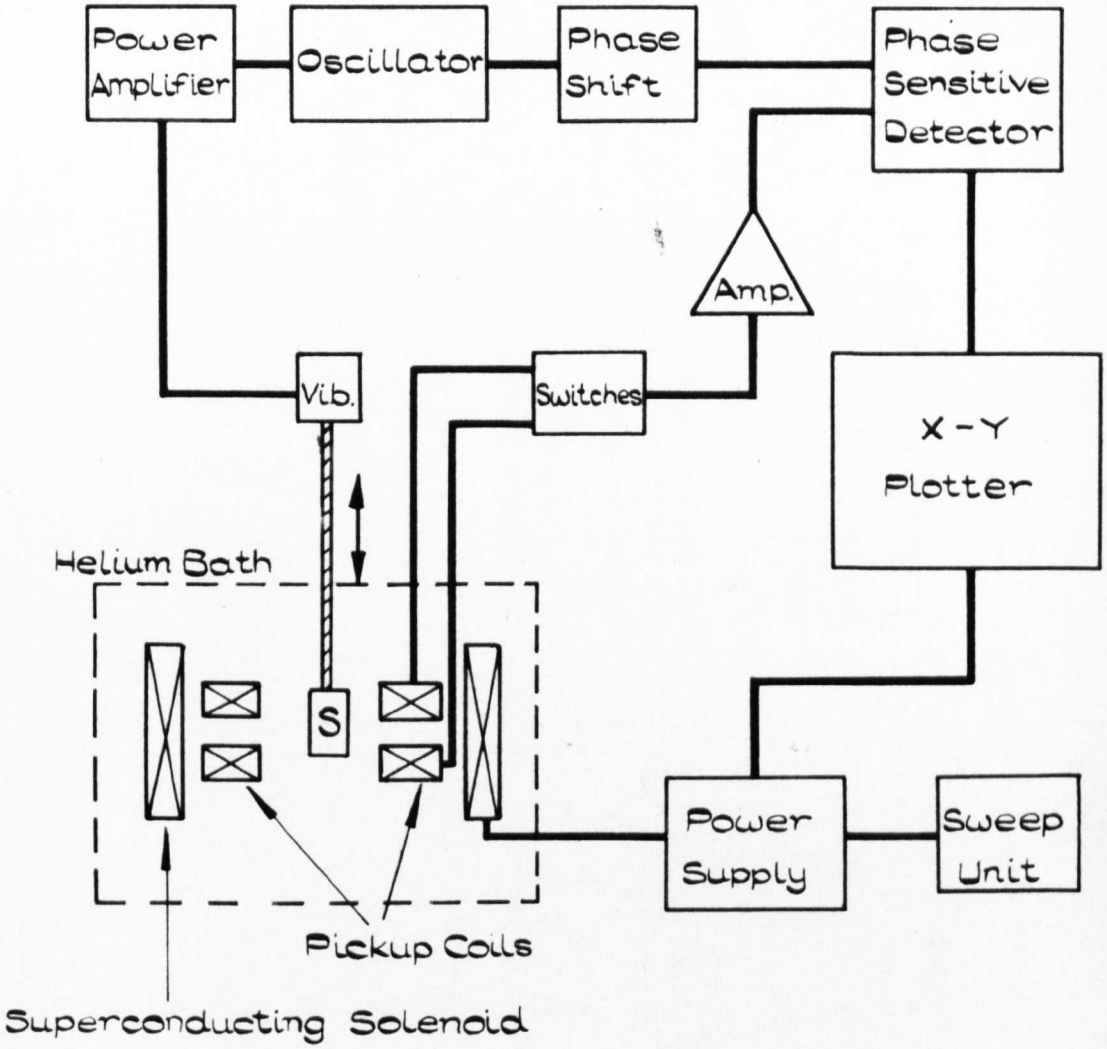

Fig. 3.10 Block Diagram of the Vibrating Sample Magnetometer.

The external circuit is illustrated in figure 3.10. After amplification the signal was fed to a phase sensitive detector (PSD) (Brookdeal Electronics PSD/Meter Unit). Reference for the PSD was provided by the phase shift unit on the oscillator. The resultant d.c. signal was displayed on a Moseley 7000A X-Y Recorder, the other axis of which was driven from the superconducting solenoid power supply.

The applied field could be swept in either direction over a range of sweep rates up to field strengths of 30 k Oe. A plot of a complete magnetisation cycle could be obtained in a few minutes. A heater, wound from 40 swg resistance wire, was provided on the sample holder to drive the sample normal when required. The resolution of the equipment, when used with our standard 5 mm. samples, was about 1 Gauss.

3.5. Measurement of surface currents

One of the great advantages of alternating magnetic field measurements, with a pickup-coil wound directly on the sample, is that direct observation of the voltage waveform can provide much information on the mode of flux penetration. In particular the values of the surface currents can be determined.

If an alternating applied field, greater than H_{c1}, is applied to a superconducting material, as the field passes through the peak value the surface currents will first be reduced to zero and then reversed. The result is that the bulk of the material is shielded against the field change for a field interval ΔH. This shielding manifests itself as zero voltage on the pickup-coil waveform for a time interval Δt

given by $\Delta H = H_m(1-\cos 2\pi f\Delta t)$, following the time at which $H = H_m$. Measurement of this time Δt, therefore, yields a value for ΔH.

Such measurements were made in the course of the loss experiments, with a large alternating field, and also in the critical current measurements when a modulating field was used. Also, in the course of the latter experiments, ΔH was determined from the value of h_m at which a signal-voltage appeared, in the presence of the steady field H'. Agreement between the results of the various approaches was excellent, especially in view of the error involved in measurements of time intervals on a CRO.

4.0 The experiments

Measurements of the dissipation in alternating magnetic fields have been made on a wide range of materials. The losses occurring below H_c and H_{c1} in low-K materials have been investigated and the effects of frequency, field amplitude and temperature considered. The dissipation in the mixed state has been measured for reversible and hysteretic, high-and low-K materials and the predictions from critical state model compared with the results. Surface currents have also been investigated, particularly on niobium. All the work has been related to the critical currents and the magnetisation curves.

4.1. Dissipation in the Meissner State

A.C.losses were measured below the appropriate critical field on lead and niobium samples, using the multiplier technique described previously. In addition to a variety of surface treatments both frequency and temperature effects were investigated.

4.1.1. Experiments on high purity lead

High purity lead of better than 99.999% purity, from the Johnson Matthey Co.Ltd., was used. The samples were spark-machined to size before the final surface treatment and were left at room temperature for some days before being measured.

Details of the surface preparations given to the samples are given below.

Sample Identification	Treatment
LC 1	coarse spark-machined (range 3)
LC 3	fine spark-machined (range 7)
LC 2	spk.-mch(7) then chem.polish

The surface treatments included spark-machining, using a Metals Research Servomet Mark II machine, and chemical polishing with a solution of 80% acetic acid and 20% hydrogen peroxide. Examination of the surfaces was undertaken on a Cambridge Instruments 'Stereoscan' scanning electron microscope and the micrographs are shown in figure 4.1. Plate (a) shows that the coarse spark-machining produced an extremely uneven surface a magnified feature of which is shown in plate (b). The finer range 7 of the spark-machine resulted in a much smoother surface but under the 2,700 x magnification (plate (c)) undulations are observed. The final chemical polish, shown in plate (d), leaves a flat surface with small-scale roughness on a scale much less than 0.1 microns.

The results of the loss measurements, taken at 4.2°K, on the three samples are shown in figure 4.2 as a function of the amplitude of the applied field H_m. Several observations are apparent from these results, i.e.

(a) All the curves show a sharp increase in the dissipation when H_m exceeds the critical field H_c, as determined by our magnetisation measurements.

(b) A considerable reduction in the dissipation, W_s, below H_c was produced by successive smoothings of the surface profile. The curves are coincident at or very near to H_c.

(c) The lines drawn in figure 4.2 represent the mean values of results taken on the three samples at 90Hz. Measurements

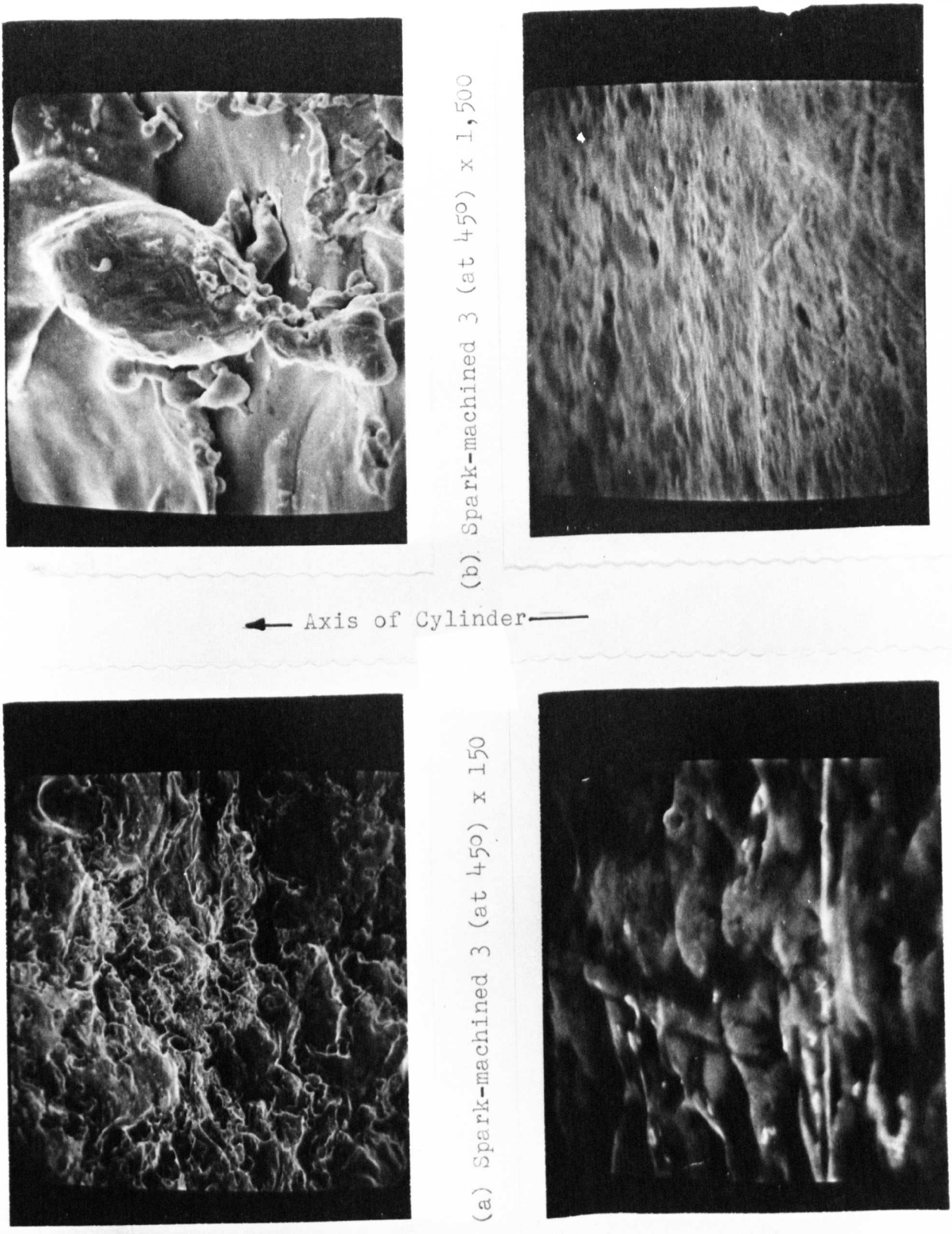

Fig.4.1. Scanning Electron Micrographs of Lead Surfaces

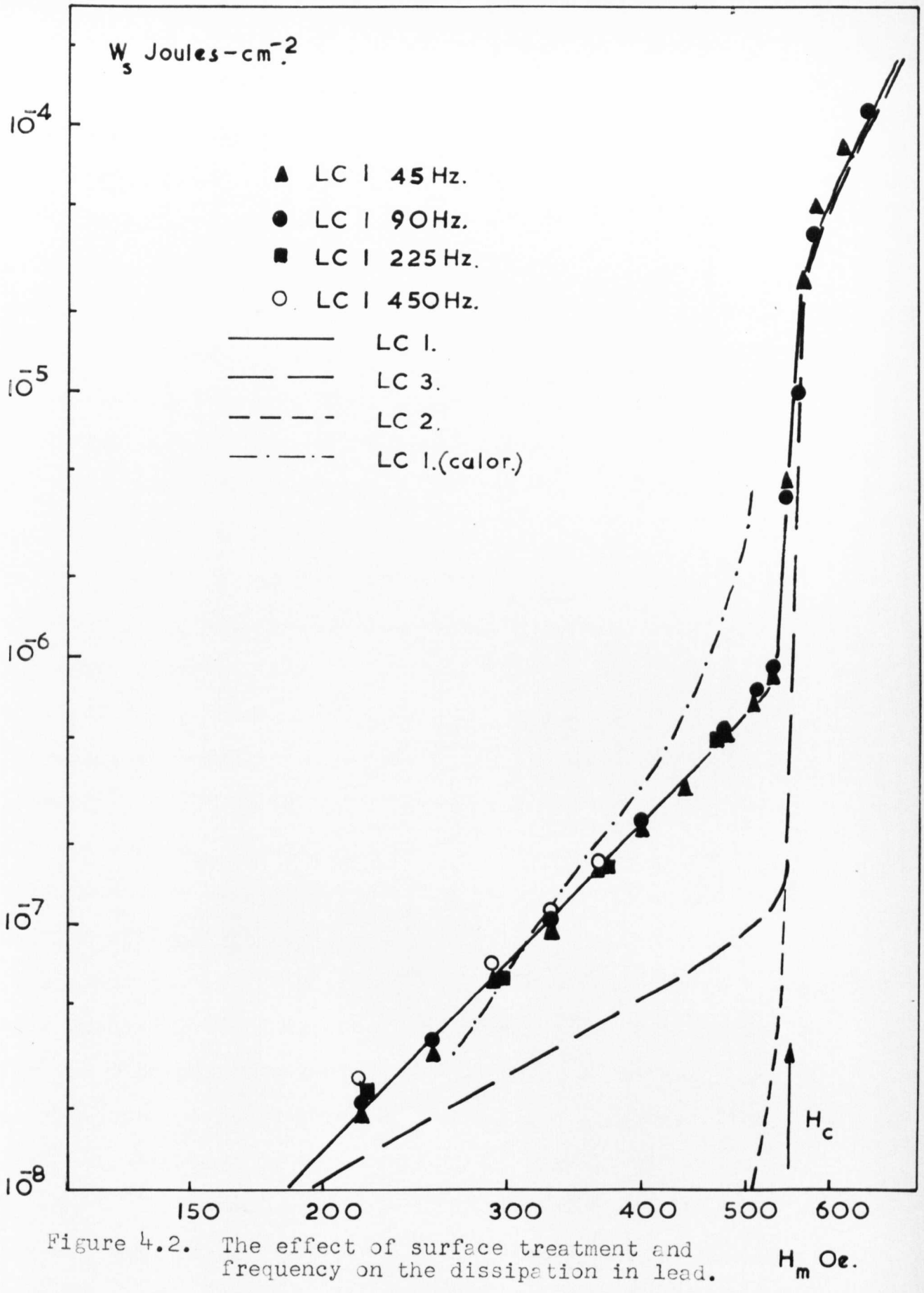

Figure 4.2. The effect of surface treatment and frequency on the dissipation in lead.

taken at other frequencies on LC 1 are shown as points about the 90Hz line. The loss per cycle was apparently independent of frequency between 45 and 450 Hz.

(d) Results taken on LC1 using the calorimetric technique are also plotted for comparison. While there is approximate agreement between the results of the two techniques the variation of W_s with H_m is quite different. We believe this demonstrates one of the weaknesses of the calorimetric technique, as we surmise that demagnetising effects at the sample ends give rise to the increase in dissipation below H_c.

The independence of W_s on frequency is indicative of the hysteretic nature of the dissipation, as resolved by other authors[114,117]. As all the samples came from the same starting material, received identical preliminary treatments and were allowed to age, we believe that the metallurgical state of their surface and near-surface layers to be similar. Therefore the variation in dissipation between the samples is probably a function of the surface profile only. Certainly a surface of the type illustrated in figures 4(a) and 4(b) will have very large demagnetising coefficients locally, at surface irregularities, and penetration of the field will take place at applied fields less than H_c. This is in agreement with Buchold's ideas for rough surfaces[117]. His expression for the dissipation was proportional to $H_m^2 \delta(H_m)$ where $\delta(H_m)$ is the depth of penetration of the surface irregularities. $\delta(H_m)$ is expected to be a function of high powers of H_m so $W_s \rightarrow H_m^{(2+n)}$ is predicted. The plots for LC 1 and LC 3 in Fig.4.2 show (2+n) to be 4.0 and 2.4 respectively. This reduction in n from 2 to 0.4, between the two spark-machined

finishes is consistent with a reduction in the local demagnetising coefficient.

Further evidence of the part played by local demagnetising effects is the variation of dissipation with sample temperature. Experiments were performed at temperatures below $4.2^{o}K$ by pumping on the helium bath, as described in section 3.1. The results are shown in Fig.4.3 for LC 3 where they are plotted against the reduced field Hm/Hc(t). H_c for each temperature was calculated assuming $H_c(4.2) = 550$ Oe. and $H_c(t) = H_c(0)(1-t^2)$ (see equation 2.1). The continuous line represents the results taken at $4.2^{o}K$ (from Fig.4.2) and all results were at 90Hz.

All the results taken at the four different temperatures lie very close to a common line. That Hm/Hc is therefore the important parameter, is indicative of the relevance of demagnetising effects to the a.c.losses.

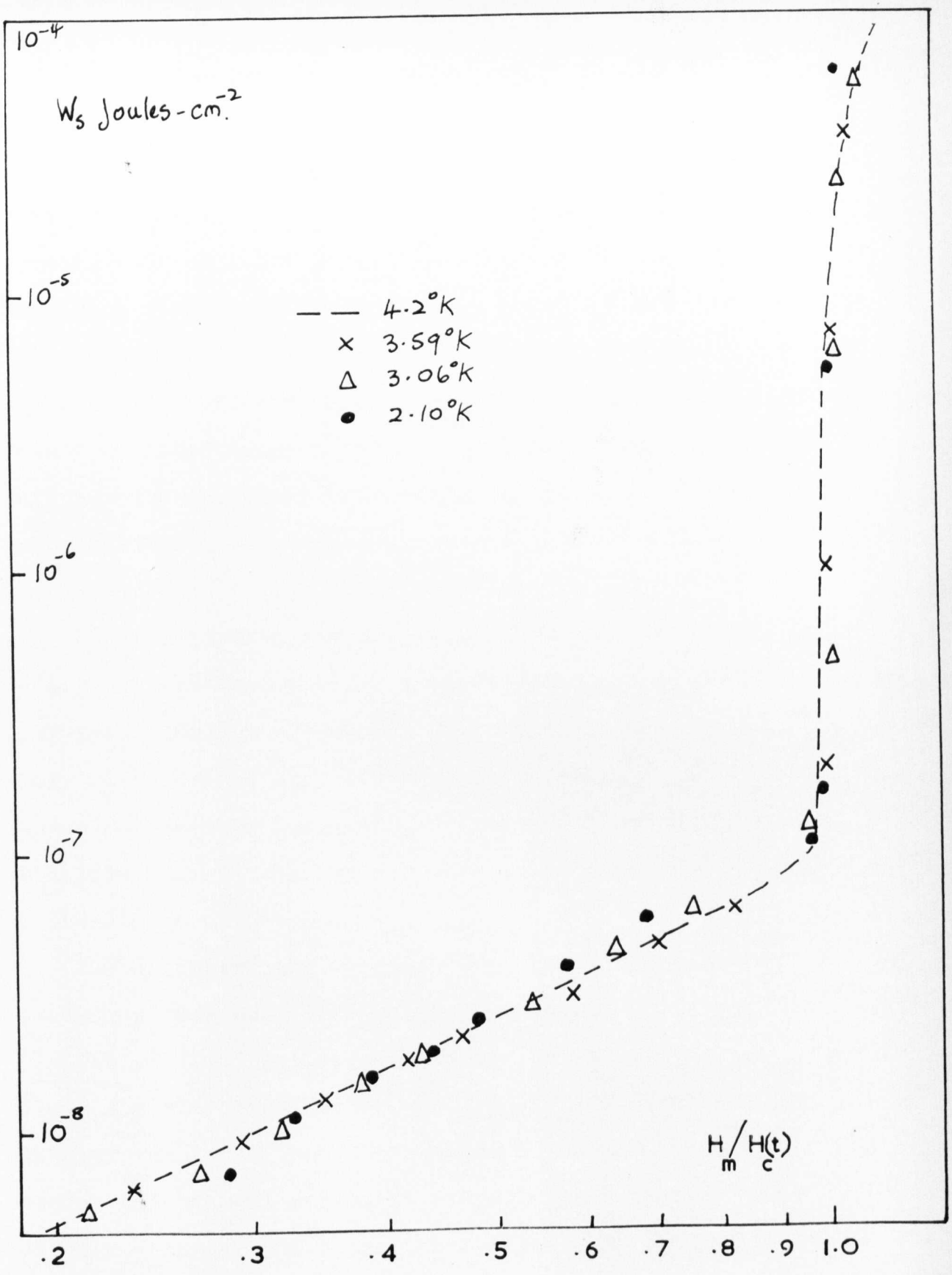

Figure 4.3. Dissipation measurements on a lead sample (LC3) over a range of temperatures.

4.1.2. Experiments on niobium samples.

As lead is a type I superconductor regions of normal material are formed, once the critical field H_c has been exceeded locally, andparts of the surface layer are essentially in the intermediate state. The resultant dissipation is therefore a function of the normal state resistivity. Type II superconductors, on the other hand, break down into the mixed state in fields above the lower critical field H_{c1}. Thus once field penetration has occurred at surface irregularities the resultant dissipation should depend on the superconducting parameters of the near surface layers. Rocher's measurements[114] have shown evidence of this.

To explore this feature dissipation measurements were made on cylindrical niobium samples 3 cm. long by 5 mm. in diameter. One set of samples came from cold-worked niobium rods, of 99.84% purity, supplied by Murex Ltd. A second set were electron-beam zone-refined from the first batch of materials and all the samples were in single-crystal form, of no particular orientation.

The detailsof the samples, and the various surface treatments they received are given in table 4.2 below.

The chemical polish was a solution of 75% HNO_3 and 25% HF and the electropolishing was done in a 90%H_2SO_4, 10% HF mixture. In the latter experiments a platinum beaker was used as the cathode with a current density of about 3A-cm^{-2}. During mechanical polishing, the samples were spun on a lathe while 200 and 600 grit paper and then 6-micron and 1-micron diamond cloths were applied. When the spark-machine was used samples were finished on the finest range 7.

Sample Identification		Surface Treatment
Polycrystalline		
NBC 2		as received
NBC 24		fine spark-machined (7)
NBC 19		chemically polished
NBC 18		1 micron mechanically pol.
NBC 16		1 micron mech.pol./elec.pol.
Single Crystal		
NBC 14	A	spk-mch 7/elec.polished
NBC 15	A	spk-mch 7/mech.pol./elec.pol.
NBC 23	B	as grown
NBC 22	B	fine spark-machined (7)
NBC 22(a)	B	spk-mch 7/mech.pol.
NBC 22(b)	B	spk-mch 7/mech.pol/chem.pol.

Table 4.2. Details of the surface treatments on the niobium samples

---

The scanning electron-microscope (SEM) was used to examine the surfaces of the polycrystalline samples and the micrographs are shown in figure 4.4. In each case the view is looking along the axis of the cylindrical samples. Both the "as received"(a) and the spark-machined (b) samples had very uneven surfaces, the latter being the most distorted. Chemically polishing the samples (c) obviously removed a lot of the roughness but apparently brought out the swagging texture of the supplied polycrystalline rod. However, the valleys and ridges were all parallel to the sample axis and also to the applied field. The final picture (d) of the mechanically polished sample shows a fairly smooth surface with protuberances of less than a micron.

Corresponding loss measurements are given in figure 4.5; all the readings were taken at $50H_z$ and are plotted against the amplitude of the applied field H_m. Also shown is the value of H_{c1} determined from our magnetisation measurements.

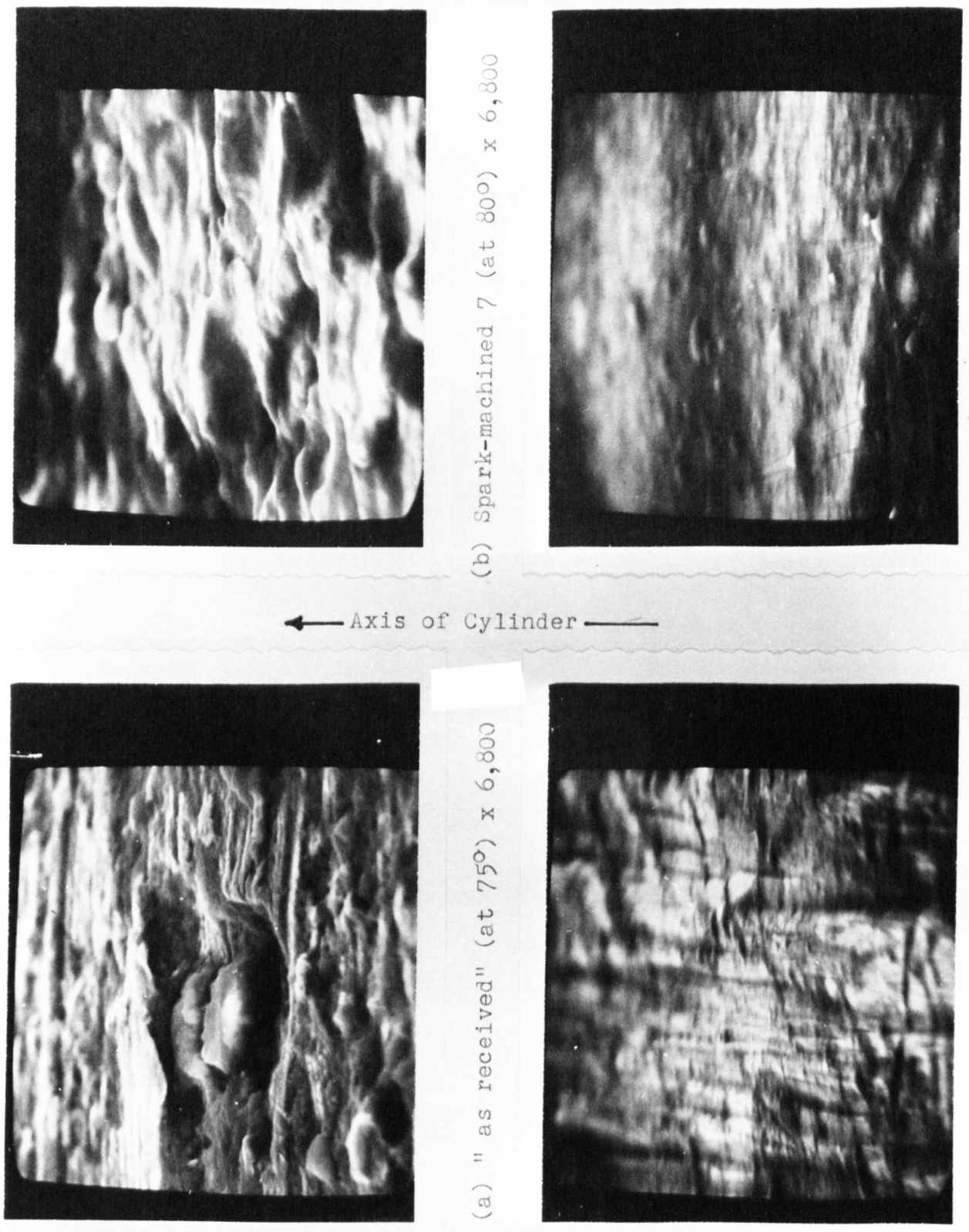

Fig.4.4 Scanning Electron Micrographs of Niobium Surfaces

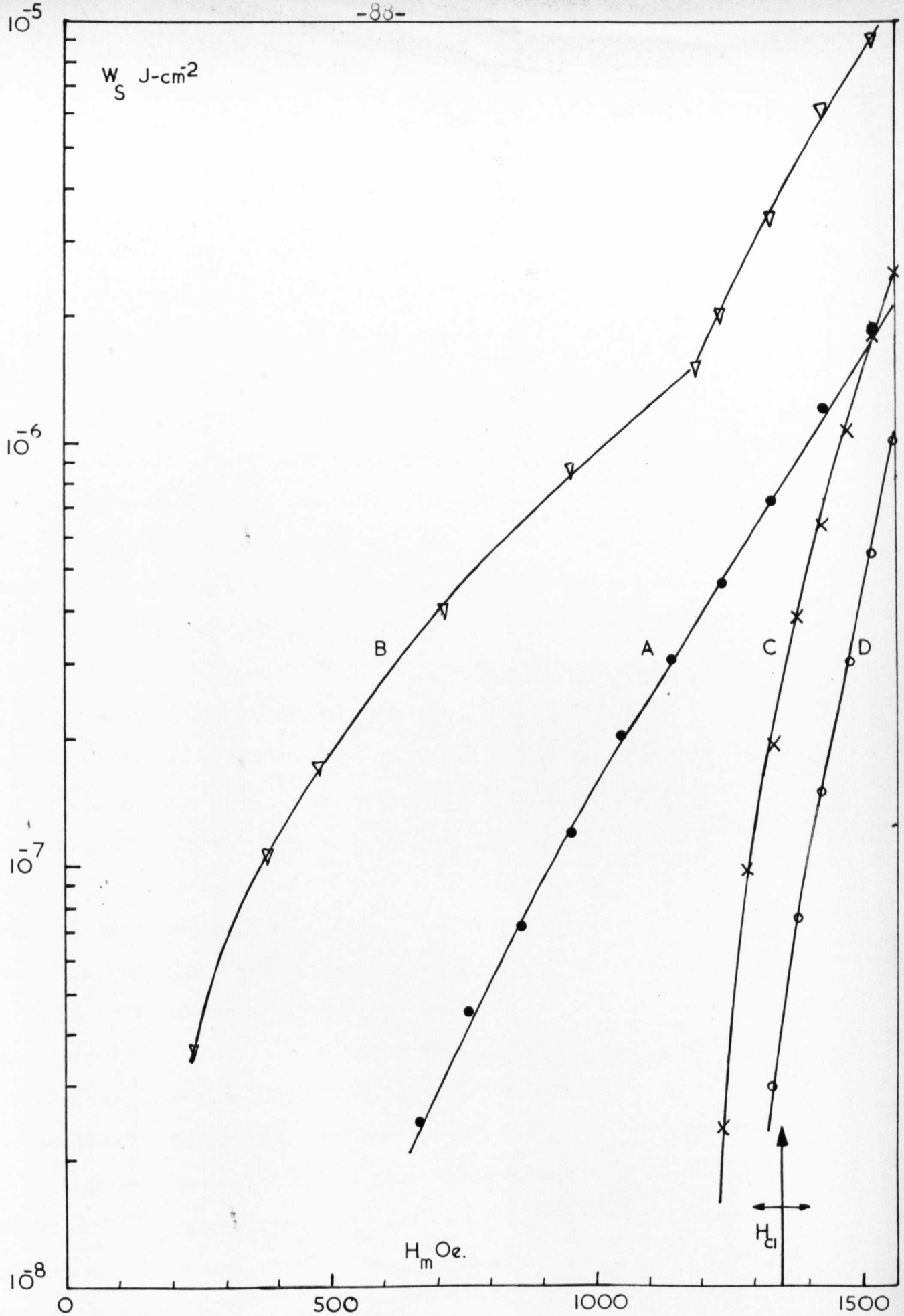

Figure 4.5 Surface dissipation in polycrystalline niobium for various surface finishes:
(A) "as received" (B) spark-machined 7
(C) chemically polished (D) mechanically polished

In such hysteretic materials it is difficult to get an exact value, but it was estimated to be 1350 ± 50 Oe.

Both the "as received"(A) and spark-machined(B) samples exhibited extensive losses in fields well below H_{c1}. The dissipation was greatly reduced by the chemical polish (C) and after a 1-micron mechanical polish (D) a detectable level was not measured until H_m exceeded H_{c1}. An identical curve was found for a 6-micron finish and when a 1-micron surface was electropolished. Each reduction in the losses shown in curves A to D corresponds to a smoother surface than the last as illustrated in the SEM pictures (a) to (d) in figure 4.4. Therefore, as with the lead samples, the low-field dissipation would seem to be due to premature penetration of the surface irregularities. Although the chemically polished surface (c) is by no means smooth, as the applied field is applied parallel to the peaks and valleys, demagnetising effects are limited.

Rough as the spark-machined surface is compared with the "as received" finish, the much larger losses in the former are probably not solely a result of the profile; indeed on a Talysurf machine the traces are remarkably alike. Even well above H_{c1}, curve B remains aboveA and this suggests that the critical current density near the surface of B is markedly less than in A. During the spark-machining process, some 0.012cm. was removed from the surface, presumably including the heavily worked layers due to the original forming of the rods (presumed to be a grinding operation). Thus in the "as received" sample, and also in the chemically and mechanically polished samples, neither of which had much of their surface removed, the dissipation is kept low by high critical current densities, even

when the surface is penetrated by the magnetic field.

In view of the importance of the metallurgical state of the surface, a set of measurements, similar to those just described, were made on single-crystal samples. The grain boundaries having been removed, the critical currents of these samples were considerably less than the previous set. Once again the level of the dissipation was reduced by successive polishings and a 1-micron finish was sufficient to eliminate measurable losses below H_{c1}.

The difference between the polycrystalline and the single crystal behaviour is illustrated in figure 4.6. Curve P is for NBC 14, a single-crystal sample which had been chemically polished, after spark-machining, and Q for the chemically polished polycrystalline sample, NBC 19 (see table 4.2). The two surfaces were of similar profile in a direction parallel to theapplied field. The greatly increased losses above H_{c1}, shown by curve P, are indicative of the much reduced critical current density in the single crystal compared with the cold worked material. However it is in the low field region where the major difference occurred. Local demagnetising factors were probably very similar for the two materials and yet measurable losses were detected at 200 Oe. for the single crystal and not until 1200 Oe. for the polycrystalline sample. Furthermore after the onset of measurable dissipation the curve P levels off until bulk penetration occurs.

We suggest the following model to account for the variation of low-field losses. Once field penetration has commenced locally at irregularities, it is expected to advance,

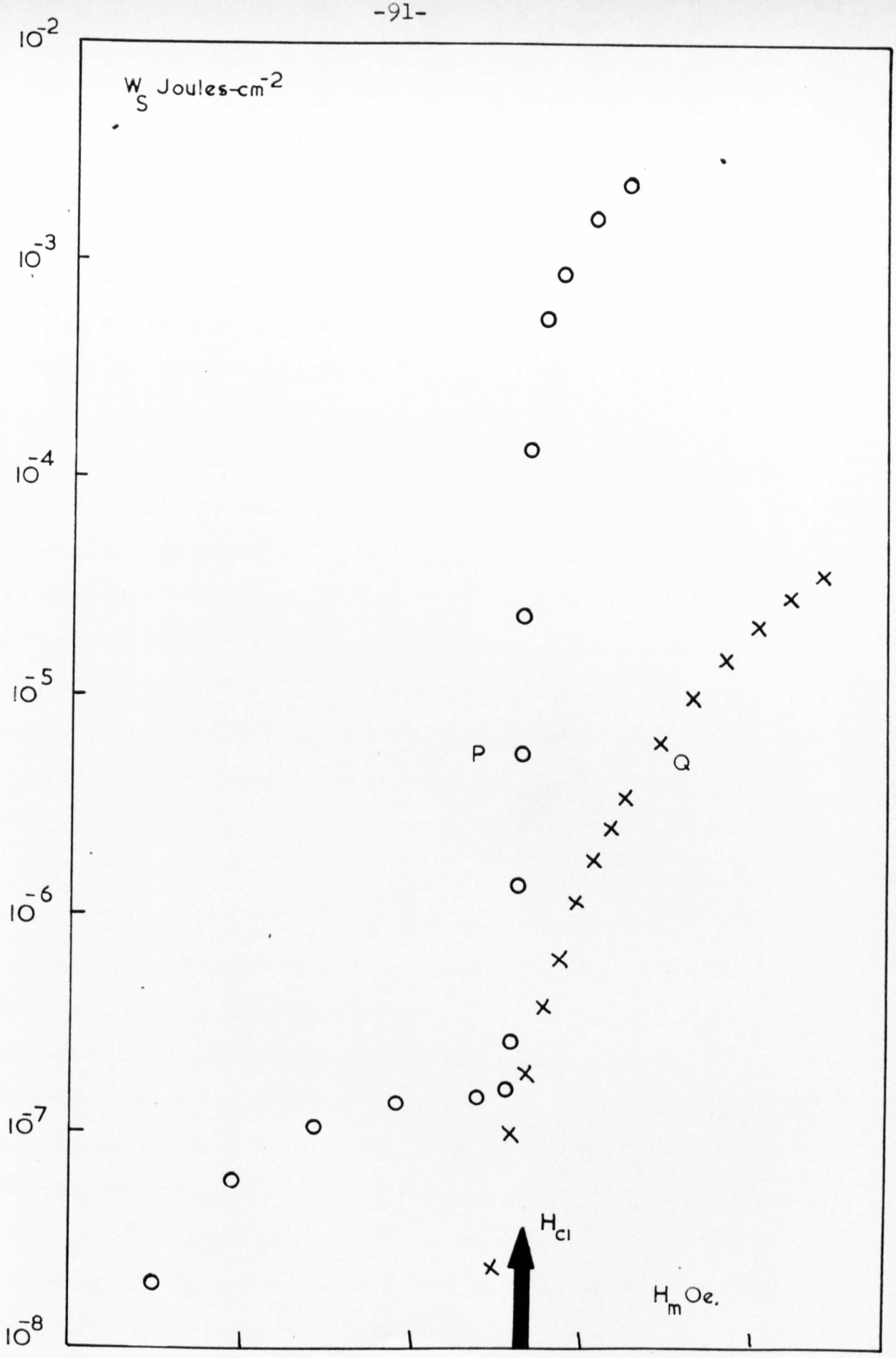

Figure 4.6 Comparison of dissipation measurements on a single crystal and a polycrystalline sample of niobium, of similar surface finish.

as the applied field is increased until all the protuberances above the mean level of the surface are complately in the mixed state. Further increase of the applied field should only result in further penetration, and thus losses, when H_m exceeds H_{c1}. The value of $H_m$at which this "surface saturation" occurs will be a function both of its critical current density and the depth of the profile.

Applying these ideas to the curves in figure 4.6, that for the single crystal (P) would indicate that "surface saturation" occurred at about 1000 Oe. while no such phenomena was noticeable below H_{c1} for the high current density, polycrystalline sample (Q). Further evidence in support of this model is that we have observed much larger losses in a single crystal with a shiny but undulating surface, than in a spark machined sample with sharp but small scale protuberances.

4.1.3. Discussion of surface losses

All the dissipation measurements, on both lead and niobium samples, support the idea of local penetration of the magnetic field at sharp peaks on the sample surface, in fields less than the appropriate critical field. The dependence of the losses in lead on $H_m/H_c(t)$, over a range of temperatures, is evidence of the formation of local areas of intermediate state, in this type I superconductor. Even a rudimentary smoothing of the surface, as shown by the SEM photographs, radically reduces the dissipation in low fields. For example, a mechanical polish to 6 microns is sufficient to reduce the losses in niobium to less than 10^{-8} Joules-cm^{-2}, until H_{c1} is exceeded.

We have proposed a model of "surface saturation" in which all the irregularities are penetrated at a value of the field determined by the metallurgical state of the surface layers. In samples with a large critical density this field is in excess of H_{c1} and no marked change in slope of the loss curve is detected when bulk penetration commences. However, the reversible single crystals show signs of saturation in low fields and the losses increase sharply when H_{c1} is exceeded.

The presence of a heavily worked surface layer due to a drawing, machining or grinding operation greatly modifies the losses both above and below H_{c1}. If the current density is approximately $10^6 A\text{-}cm^{-2}$ then such a layer need only be 0.01 cm thick to effectively shield the less hysteretic bulk of a sample, in fields up to 2,000 Oe. It is important that this point is considered when analysis of results on, say, rolled strip is attempted. We shall see later how results from a mechanically polished single crystal are radically modified in this way.

One important consequence of the results of these surface loss experiments is that if a conductor can be produced with a well polished surface the resultant losses will not be a problem in potential applications. Results we shall present later, and experiments by Easson[100], have shown that niobium strip rolled on a Sendzmir mill has such a finish and should satisfy the requirements of the designers.

4.2. Dissipation in the mixed state - high-K materials

In chapter 2 we discussed the application of the critical state model to predict the a.c. behaviour of hysteretic high-K materials. Transport current measurements on Nb-Zr wires agreed especially well with the theory (see figure 2.8). Few measurements have been reported of the dissipation in applied alternating fields when surface currents should play an important role.

When discussing the critical current techniques in section 3.3, we mentioned briefly measurement of losses made on a lead-bismith eutectic sample.[151] In these experiments, in which small modulating fields of amplitude h_m were applied in addition to a steady field H', the predictions of the simple Bean model were found to hold closely. i.e. $W_s \propto h_m$ and $W_s \propto 1/J_c(H')$. On examination of the assumptions, implicit in the use of the critical state model under alternating conditions, listed in section 2.3, it can be seen that most of them were well satisfied. Although the relationship between the current density J and the electric field E was not known in this case, the lead alloys are good thermal conductors so, for small h_m, temperature rises will have been small; no flux jumps were observed in the alternating field measurements or in the static magnetisation curve; as the sample had been aged for sometime it was of homogeneous structure. The particular assumptions of the Bean treatment were also well satisfied (see section 2.3.1) as, for small h_m, the critical current density was constant; as $H'-h_m > H_{c1}$ and $H' + h_m < H_{c2}$ the sample was always in the mixed state and the measured surface currents were very small (< 20 Oe.).

On the basis of the model, therefore, these measurements were carried out under ideal conditions. However we also performed experiments on samples of niobium-zirconium and niobium-titanium alloys in large alternating fields, which put greater demands on the theories.

4.2.1. Niobium-zirconium and Niobium-titanium

Samples of Nb25%Zr and Nb44%Ti were provided, by IMI, in the form of cold drawn rods. These were then machined to the requisite size and chemically polished before measurement. As with most of these cold-worked niobium based materials such a polish is difficult to control and a pearly finish was obtained on the specimen surfaces.

Magnetisation measurements were made on both the samples and the initial magnetisation curves are shown in figure 4.7. An attempt was made to plot complete loops but the incidence of flux-jumps made this impossible on such bulky and thus poorly-cooled samples. The curves are typical of very hysteretic type II superconductors and, as such, determination of H_{c1} was impossible, this again being hindered by the large sample volume. However, a useful parameter that was extracted from these curves, for application to theory, was the applied field at which $-4\pi M$ attained its maximum value.

The results of the dissipation measurements are shown in figure 4.8. The onset of measureable dissipation occurred at about 200 Oe. for the Nb-Ti and 400 Oe. for the Nb-Zr. Values of H_{c1} for these two materials are rarely given in the literature as, for the reasons stated above, it is difficult to determine. However, at first sight, 200 Oe. and 400 Oe.

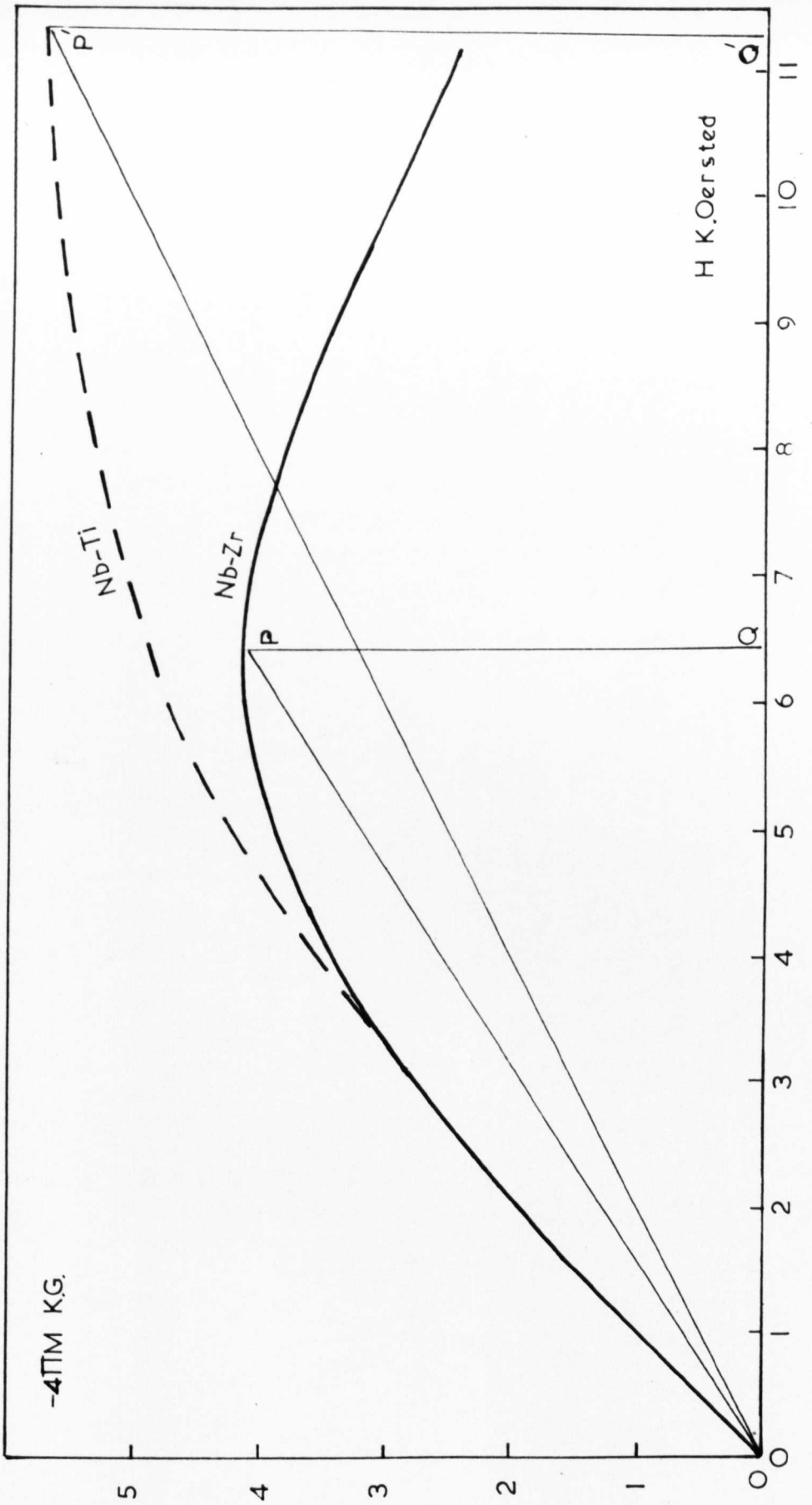

Figure 4.7 Initial magnetisation curves for the Nb-Zr and Nb-Ti samples. (The fine lines and points PP'QQ' are for determining values of H_a and γ)

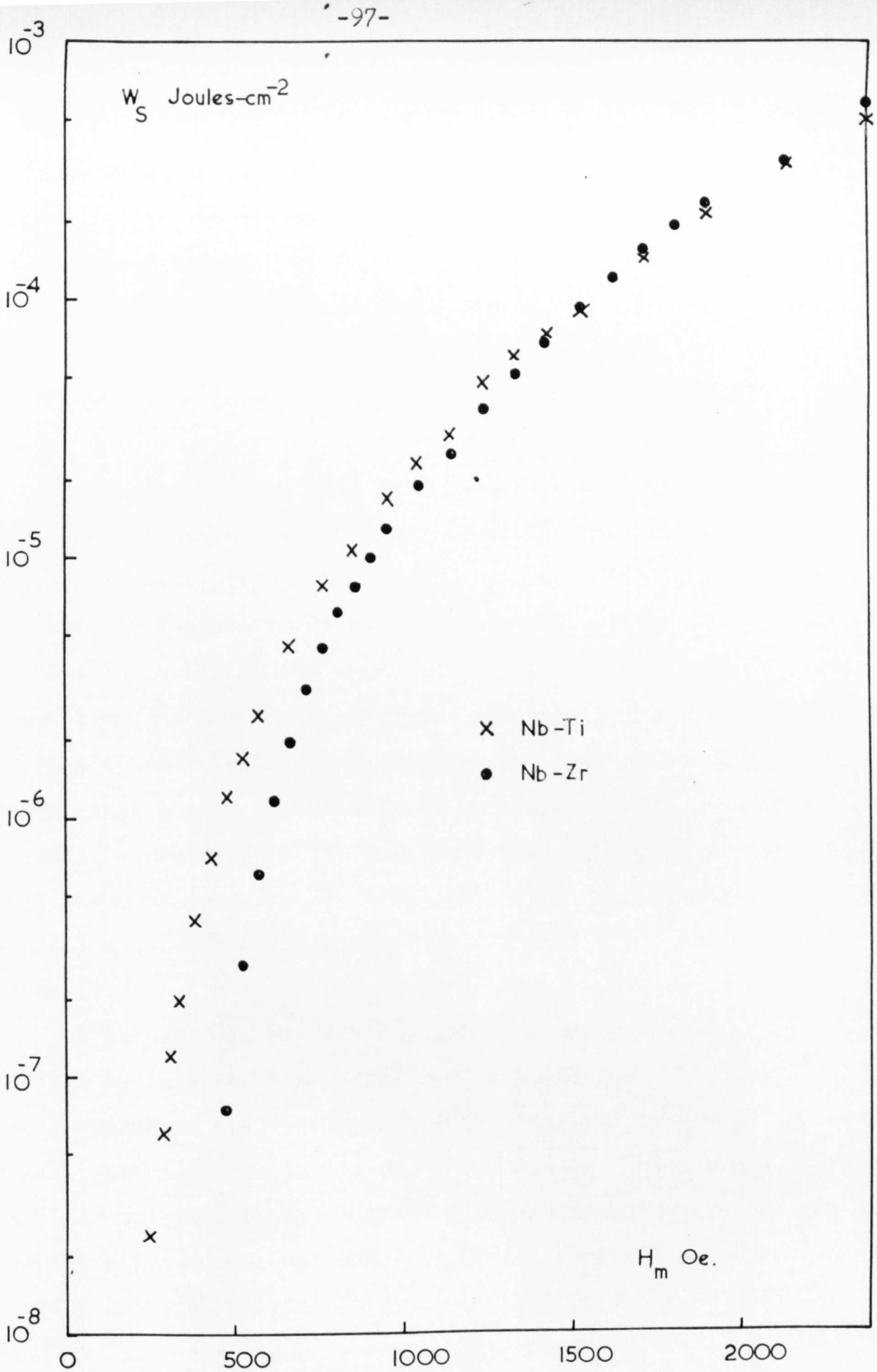

Figure 4.8 Dissipation measurements on the Nb-Zr and Nb-Ti samples.

are not unreasonable values for the respective materials . In higher fields the curves are similar but as theapplied field is increased beyond 2000 Oe.the Nb-Zr sample is the more lossy. This is consistent with the greater hysteresis shown by the Nb-Ti sample (in figure 4.7), in fields upward of this value, indicative of a larger critical current density than in the Nb-Zr.

In figure 4.9 the loss measurements have been replotted on a log-log scale and it is apparent that the dissipation obeys the power law $W_s \propto H_m^n$ in high fields. The value of n is 4.0 and 3.7 for the Nb-Zr and Nb-Ti samples respectively. The results on the Nb-Zr are therefore in agreement with the predictions of the critical state (equation 2.8), assuming the current density follows the modified Kim expression $J_c(H) = \alpha/H$. Using these ideas, a good fit was obtained, to the high-field results, with $\alpha = 2.5 \times 10^8$ Oe.A-cm^{-2} (see line A in figure 4.9). This value of α corresponds favourably with the value of $\alpha = 1.1 \times 10^8$ Oe.A-cm^{-2} obtained by Kim et al.[44] for this material.

An attempt was to have been made to apply the equation derived by Irie and Yamafuji[55], $W_v = 0.054(2-\gamma)\ H_m^{4-\gamma}/Ha^{2-\gamma}$, using values of the constants γ and H_a derived from the magnetisation curves in figure 4.7. However, the formula given in their original paper[55], for determining γ from the initial magnetisation curve, was found to be inaccurate and, at the time of writing, clarification is awaited from the authors. A partial analysis was possible however, using values of H_a determined from the magnetisation curves and a suitably chosen value of γ. As the theory predicted $W \propto H_m^{(4-\gamma)}$ ie.$n=(4-\gamma)$

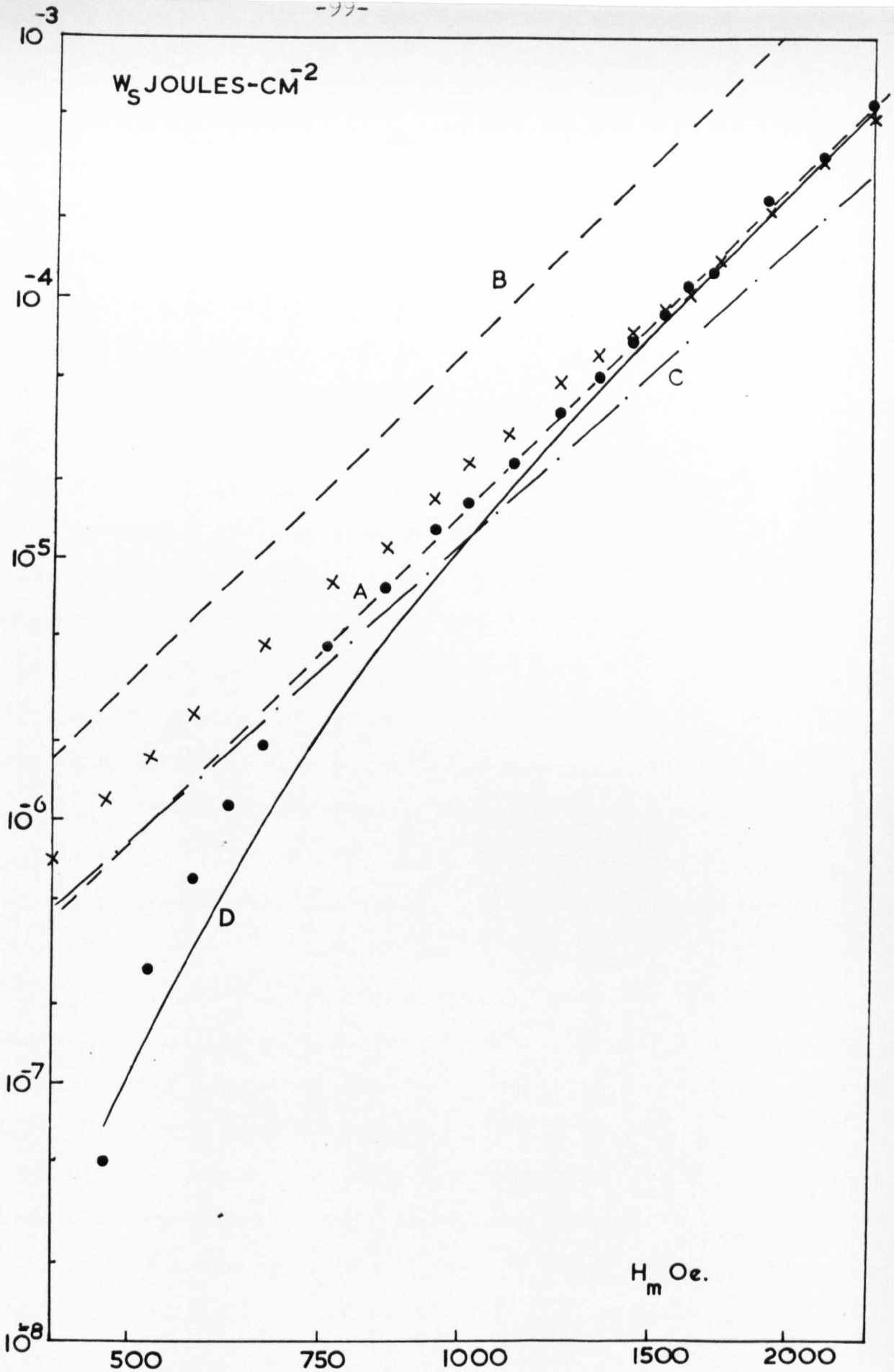

Figure 4.9 Comparison of the theoretically predicted values of dissipation with the measured values for Nb-Zr and Nb-Ti. A. Bean/Kim (Nb-Zr) B. Irie and Yamafuji(55) (Nb-Zr) C. Irie and Yamafuji(55) (Nb-Ti) D. Easson and Hlawicka(100) with modifications (Nb-Zr).

the values were taken as $\gamma = 0$ for Nb-Zr and $\gamma = 0.33$ for Nb-Ti, with H_a determined as 4.47kOe. and 15.1kOe. respectively. The resultant lines are shown in figure 4.9 for Nb-Zr(B) and Nb-Ti(C) and the agreement with experiment is not particularly good. Line B is a factor 5 too large compared with the solid circles, indicating the experimental points, and line C is a factor 2 below the crosses.

The apparent lack of success of a theory, which had reliably predicted results on Nb-Zr wires (see figure 2.8), was surprising. However, several factors may have contributed to the discrepancies. The size of the samples will have been important as H_a is size dependant and the peak values in $-4\pi M$ occurred at fields well above those used in the loss measurements. The variation of $J_c(H)$ with H, for both materials, is probably very different in the two regions. The size factor may also have been important in that the depth from the surface penetrated by the alternating field, was only a small fraction of the overall radius. The machining of the sample and the original drawing process will have resulted in structural inhomogeneities in the near-surface layers. Therefore the magnetisation curves and the loss measurements were probably on parts of the sample of effectively different average critical current density. Finally the presence of surface currents and temperature effects may have undermined the theory.

In low fields the experimental results are influences by the supposedly diamagnetic region $H_{c1} > H > -H_{c1}$. Easson's calculations[100] were used in attempt to match these low-field results on the Nb-Zr sample. Their expression for the dissipation was $W_s = 4.22 \times 10^{-9} \frac{(H_m')^2}{J_c(H)} (1.5H_{c1}+H_m')$ Joules-cm^{-2}

where $H_m' = (H_m - H_{c1})$. The problem was to select a value for H_{c1}. The point at which measurable dissipation commenced, i.e. 400 Oe., was a clue to a value, but the surface currents had to be considered. These were measured, on the NbZr sample, from the pickup-coil voltage waveforms, as described in section 3.5., and the results are summarised in figure 4.10. To a first approximation, the field interval $\Delta H(H_m)$ following the peak field H_m, during which the surface currents first reduce to zero and then reverse, is proportional to $1/H_m^2$. Ullmaier[97] has shown that the effective amplitude of the applied field is $(H_m - \frac{1}{2}\Delta H(H_m))$ and it seems likely that until this effective field exceeds H_{c1} no dissipation will be recorded. As the threshold value of H_m = 400 Oe., and $\frac{1}{2}\Delta H(400)$ = 135 Oe., on this criterion $H_{c1} \sim 265$ Oe. Yasukochi et al.[51] calculated H_{c1} = 250 Oe. from H_{c2} and thermodynamic data, so this result is credible.

Therefore we submitted $H_m' = H_m - \frac{1}{2}\Delta H(H_m) - H_{c1}$ in Easson's equation with values of Jc(H) calculated from $Jc(H) = \frac{\alpha}{H}$ and values of ΔH determined from figure 4.10. The curve D on figure 4.9 is the result with H_{c1} = 250 Oe. and $\alpha = 3.5 \times 10^8$ Oe. A-cm^{-2}. In view of the simplifying assumptions and estimates made, the agreement with the experimental points (solid circles) is good.

4.2.2. Discussion

It has been shown that the critical state model in its various forms is successful in predicting the a.c. losses in high-K superconductors, under certain conditions. With small alternating fields, in the presence of a bias field, and when

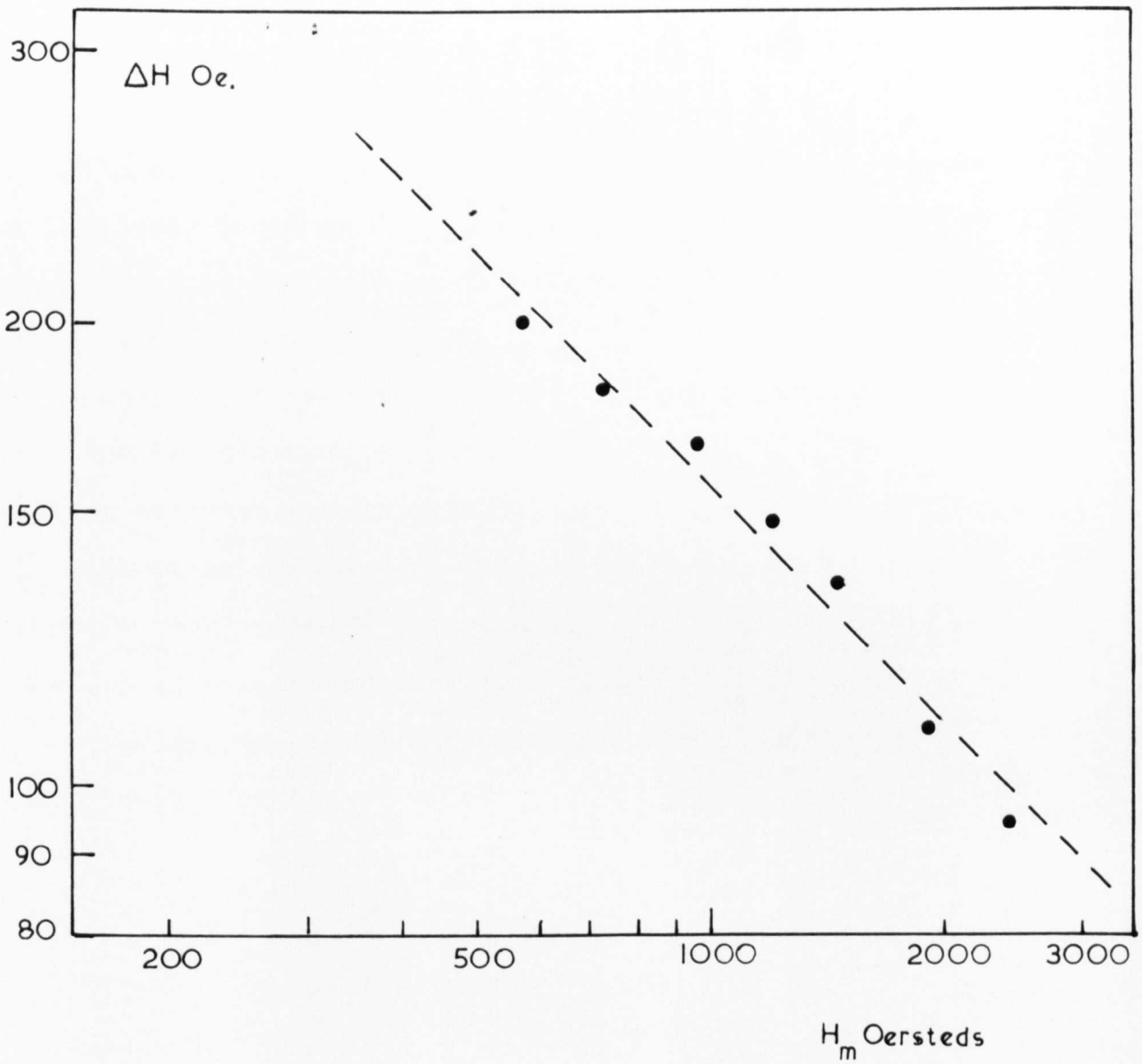

Figure 4.10 Surface current measurements on the Nb-Zr sample. The broken line represents $H \propto 1/H_m^2$

surface currents are small, the Bean simplification of the model is perfectly adequate. However, when large alternating fields are applied the more complex forms of the critical state are required. When $H_m \gg H_{c1}$ the expression $W_s \propto H_m^n$ applies with $3 < n < 4$. The Nb-Zr sample must have contained a low density of pinning centres as $n=4$ and $J_c(H) = \frac{\alpha}{H}$. A higher density of pins was present in the Nb-Ti as indicated by the lower value of n. The theory of Irie and Yamafuji[55] was applied to our results but agreement between theory and experiment was poor.

Some success was achieved in fitting Easson's[100] expression for the dissipation, suitably modified to allow for the surface currents, to experimental results near H_{c1}. However the flux distribution in a type II superconductor, when the field is reduced below H_{c1}, is still not clear. We shall consider this point in a later section.

Finally, the surface currents, in low fields, were an approximate function of $1/H_m^2$.

4.3. Dissipation in the mixed state - cylindrical niobium samples.

Of all the low-K superconducting materials, elemental niobium has been the most thoroughly studied. From a fundamental point of view, it represents an ideal type II superconductor of low-K which can be easily obtained in high-purity and single crystal form and, as such, has been the subject of many experiments. However, the properties that have lead it to be included in our experiments are its high critical temperature (9.2°K), large value of the lower critical field H_{c1}(1400 Oe.) and reasonably current carrying capacity in low fields (10^5 to 10^6 A-cm^{-2} at 2 kOe.). These are the features which are attractive to an a.c.applications engineer, especially when found in a material of which the production technology is well developed.

As mentioned in an earlier section (2.4), many of the a.c. measurements reported in the literature have been on this material. However, rarely have the results been successfully matched by theory. Apart from weaknesses in experimental techniques, two likely reasons for this failure have been the hitherto unaccounted for surface currents and the response of the material when the applied field is reduced below H_{c1}.

The experiments we have reported earlier in this chapter, have shown that for $H_m < H_{c1}$, the measured dissipation is dependent on the surface profile and can be reduced by suitable polishing. The region of uncertainty is when H_m is greater than H_{c1} but the field is reduced below H_{c1} for part of the cycle, i.e. $H < H_{c1} < H_m$. We shall discuss this, and other points, in relation to measurements on cylinders of niobium. In the next section we shall consider experiments on thin niobium strips.

4.3.1. Polycrystalline samples

The samples studied were those used in the measurement of surface losses (see section 4.1.2 for details), in particular those "as received", chemically polished and mechanically polished. The magnetisation curves for these three samples are illustrated in figure 4.11 together with magnetic data extracted from the curves. The values of H_{c1} can only be approximate as this point is difficult to identify, with such hysteretic samples.

We have already suggested that the more polished surfaces had a lower critical current density, due to the partial removal of the heavily worked outer skin, and this is probably the cause of the reduced high-field hysteresis in these two samples. On the other hand, the less zero-field trapped flux in the rough "as received" specimen is almost certainly a property of the surface profile.

Dissipation measurements, made at 50Hz on the two polished samples, are plotted in figure 4.12. (The "as received" sample is not included, as the low field dissipation masks the mixed-state losses.) The mechanically polished sample was less dissipative in high fields, which further supports the idea of a high-Jc layer partially removed by each polish. However, the lower field losseswere much less and surface currents were throught to be the cause of this differential. Therefore the pickup-coil voltage waveforms were examined to determine the value of these currents. Typical waveforms are shown in figure 4.13 for the two extreme finishes. Surface currents were calculated from the length of the horizontal part of the trace, as described in section 3.5., and the points plotted in figure 4.14(a) are the result. The field interval

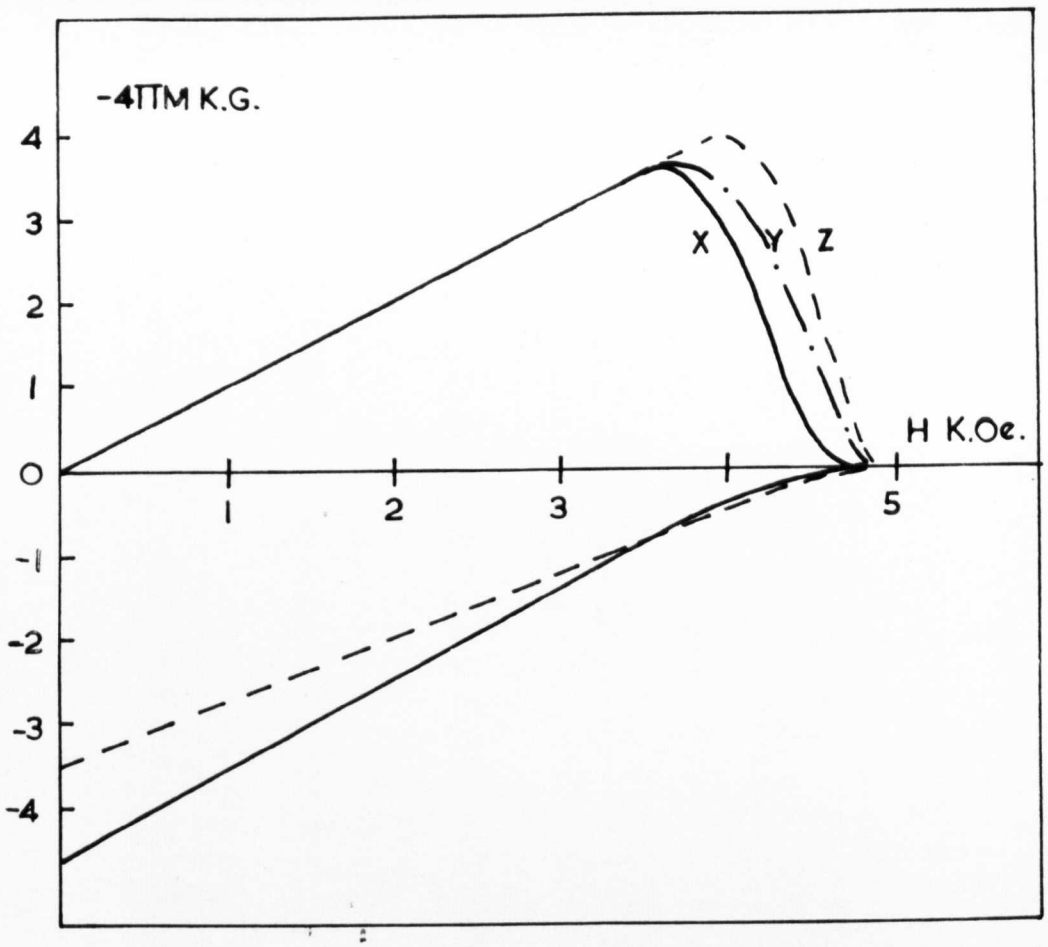

Curve	X	Y	Z
Surface Finish	Mechanical polish	Chemical polish	"as received"
H_{c1} (Oe.)	1350	1300	1300
H_{c2} (Oe.)	4850	4850	4850
Zero field trapped flux ($\%H_{c2}$)	93	93	73

Figure 4.11 Magnetisation curves, and extracted data, for polycrystalline niobium samples.

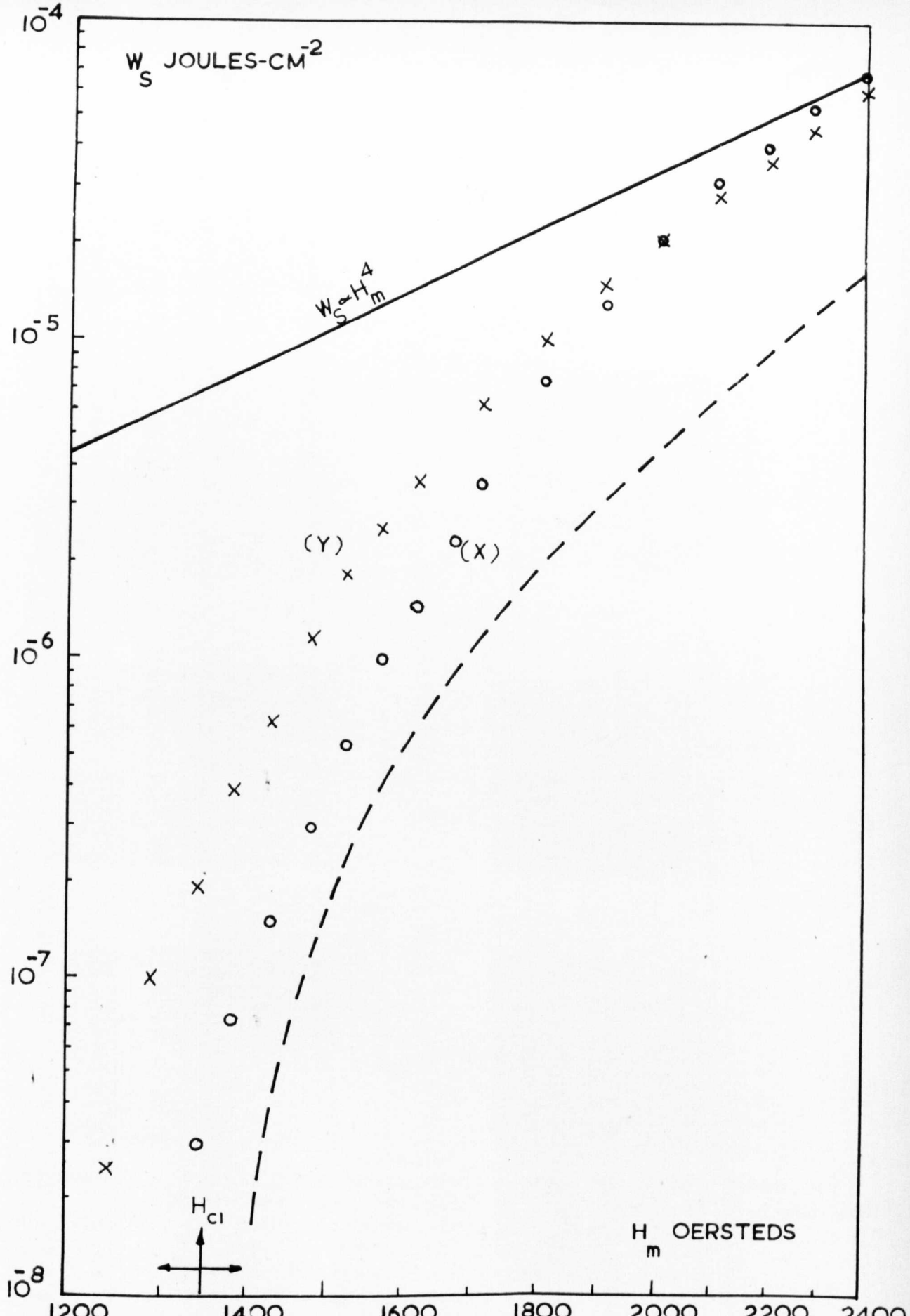

Figure 4.12. Dissipation measurements on polycrystalline niobium samples (X) mechanically polished × (Y) chemically polished ○ .

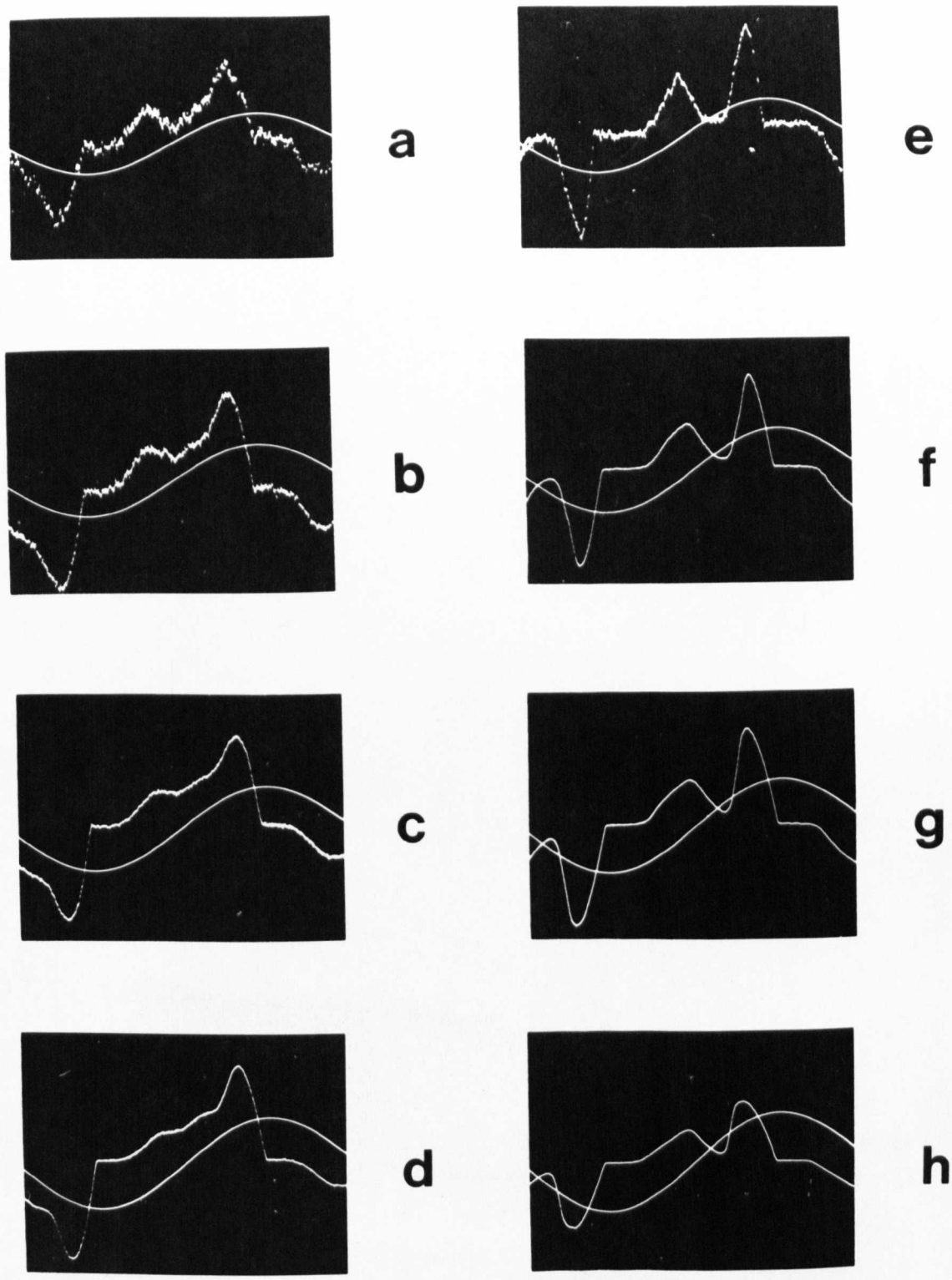

Figure 4.13 Penetration voltage waveforms for polycrystalline niobium: "as received" (a) H_m = 1430 Oe.(0.01mV/div) (b) 1665 Oe.(0.02) (c) 1904 Oe.(0.05) (d) 2140 Oe. (0.1): mechanically polished (e) 1665 Oe. (0.01) (f) 1904 Oe.(0.1) (g) 2140 Oe.(0.2) (h) 2380 Oe.(0.5).

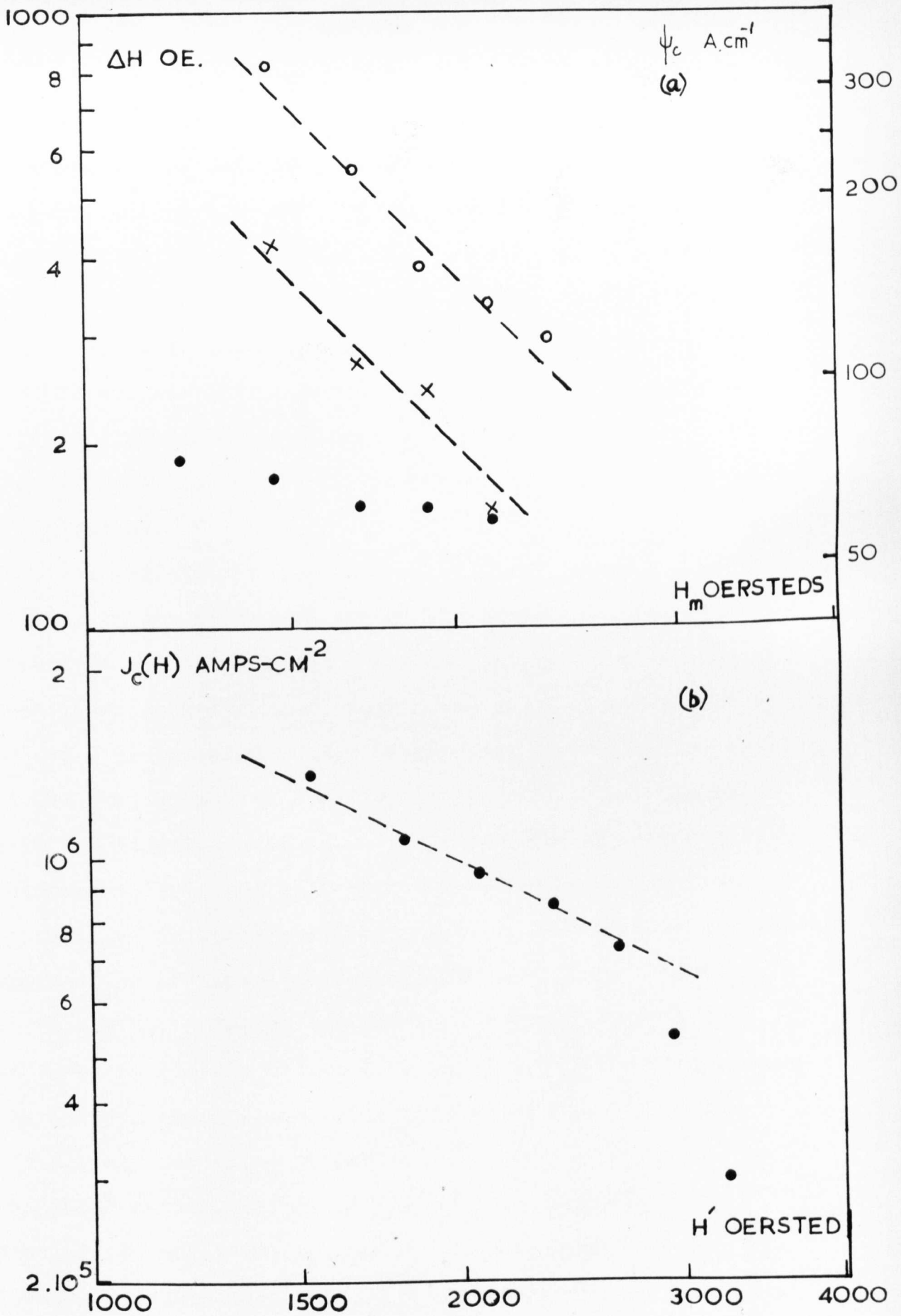

Figure 4.14 Measurements on polycrystalline niobium samples of various surface finish: (a) Surface currents: o mechanically polished, × chemically polished, ● "as received". (The broken lines have a slope of -2) (b) Critical current density: "as received". (The broken line has a slope of -1).

ΔH, for which the currents screen the bulk of the sample, is shown on the left hand axis and the equivalent surface current density, ψ_c A-cm^{-2}, on the right hand. The broken lines have gradient of -2 so $H \propto 1/H_m^2$, as an approximation, for the polished samples. Larger surface currents were observed on the smoother surfaces and ΔH was as large as 800 Oe. at Hm=1500 Oe. for that mechanically polished. Thus there was a field discontinuity across the surface of 400 Oe, and the effective amplitude of the applied field was 1500-400 = 1100 Oe., at thispoint.

The variation of ΔH between samples can therefore be used to explain the different losses observed. If indeed the effective applied field H_m' can be considered to be $(H_m-\Delta H/2)$, then the larger the value of ΔH, the smaller the losses will be for a given value of H_m. Indeed the horizontal separation of the plotted points X and Y in figure 4.12 is comparable with the difference in $\Delta H/2$ values determined from figure 4.14(a). Although H_m' is often less than the value we have put on H_{c1}, dissipation is still measured and field penetration is observed. Application of theoretical models is therefore fraught with difficulties. However the critical current density was measured to provide values of Jc(H) for substitution in the appropriate expressions. The modulating field/a.c.loss technique, described in section 3.3, was used on the "as machined" sample. Although use of this sample may have resulted in small discrepancies, it was essential that the surface currents were small for the technique to be viable. The results are shown in figure 4.14(b) and, over the low field range, the relationship $Jc = \alpha/H$ was found to apply, with

α = 1.95 x 10^9 Oe.A-cm^{-2}.

When this critical-current/field relationship was inserted into the sample critical state equation $W_s = 4.22 \times 10^{-9} (Hm)^3/Jc(H)$ J -cm^{-2} the solid line in figure 4.12 resulted. At high fields this line is a reasonable asymptote to the measured losses. As expected, when $H_m \gg H_{c1}$ and ΔH is small the predictions of the un-modified critical state model are valid.

To account for the supposedly diamagnetic region below H_{c1} the expressions $W_s = 4.22 \times 10^9 (Hm-H_{c1})^2(0.5H_{c1}+H_m)/Jc(H)$ has been proposed[100]. Using our measured values of Jc(H) and H_{c1} = 1350 Oe. the broken line in figure 4.12 was obtained. Agreement with the experiments is extremely poor, especially in high fields where the surface currents were only small. However one of the basic assumptions behind the derived expression, was that no flux entered or left the sample for $-/Hm/ < H < +/Hm/$. Examination of the waveforms in figure 4.13 reveals that $d\phi/dt$ is always non-zero in this field interval. At best, the minimum in $d\phi/dt$, shown in plates (e) to (h), only exists as the field is increased from zero to +/Hm/ and only in the best polished sample. In view of this movement of flux across the surface throughout the whole cycle, the above expression is hardly expected to be accurate.

4.3.2. Heat-treated polycrystalline samples

As the dissipation in the mixed state ispredicted to be an inverse function of the critical current density Jc(H), any change in the metallurgical state of a sample which affects $J_c(H)$, will cause the a.c.losses to vary. Heat treatment of

niobium had been shown to first increase the critical current, as the temperature of treatment was raised, and then cause it to decrease[154,155]. However previous loss measurements on heat-treated niobium strips had not matched this behaviour.[107]

To further investigate thispoint a series of our poly-crystalline rods were heat-treated and the dissipation measured. All the samples were chemically polished before and after heat treatment, in a Metals Research 2inch furnace, which we fitted with vacuum equipment. A vacuum of better than 10^{-5}torr.was maintained during the 2 hour heating cycles.

Details of the heat treatments, the magnetisation curves and extracted data are shown in figure 4.15 and the dissipation measurements, taken at 50 Hz, are in figure 4.16.

It can be seen from the magnetisation curves that the critical fields, as well as the degree of hysteresis, is changed by heat treatment. The reduction in H_{c2} in the high-temperature samples is probably due to both the modification of the dislocation structure and a reduction in the amount of dissolved gases Steigler et al[157] showed that dislocation rearrangement commenced above 760°C and Williams and Catterall [154] recorded a reduction in H_{c2} at higher temperatures. As the heat-treatment took place in a reasonable vacuum it is probable that some outgassing occurred. It is known that the presence of dissolved gasses increase K, and thus H_{c2}.[66,156] A considerable reduction in hysteresis and zero-field trapped flux was noted between 800°C and 1000°C and can be attributed to the first stages of recrystallisation.

The reduction of hysteresis is symptomatic of a decrease in the critical current density due to removal of pinning

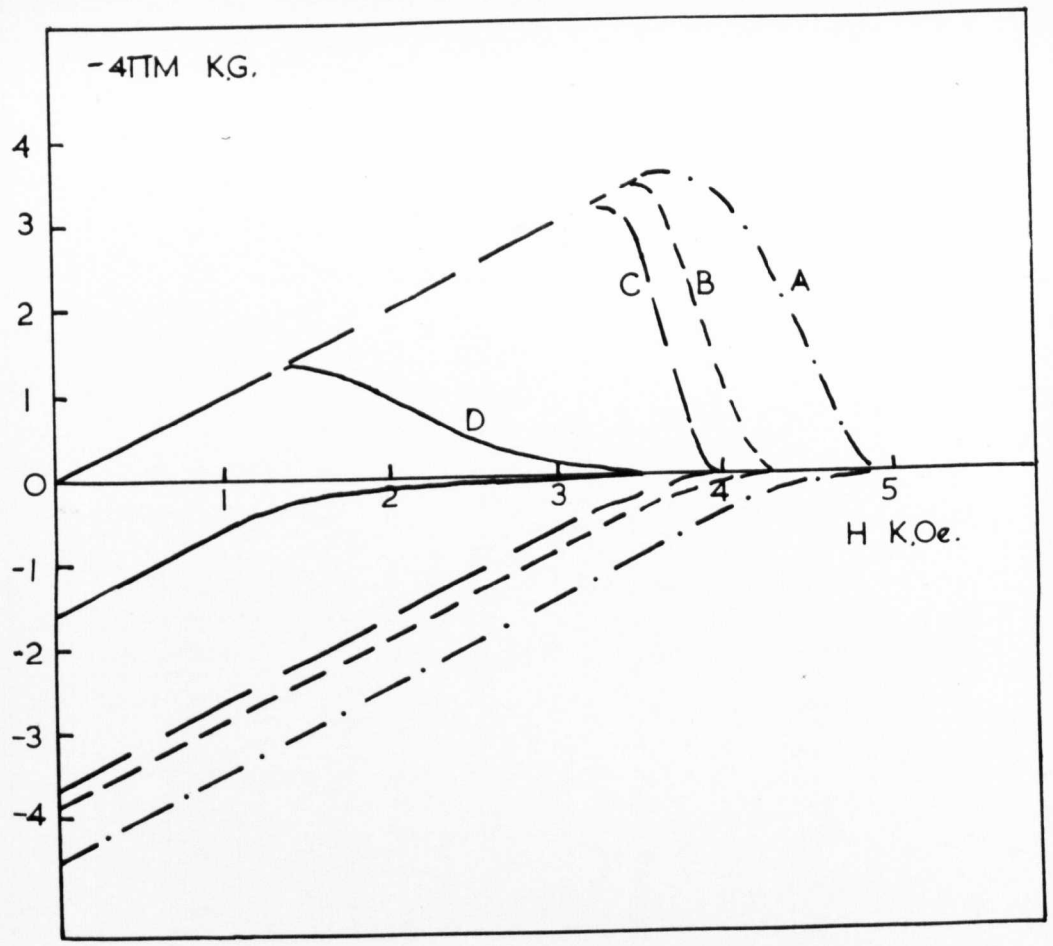

Curve	A	B	C	D
Heat treatment temperature (°C)	-	600	800	1000
H_{c1} (K Oe.)	-	1.30	1.30	1.35
H_{c2} (K Oe.)	4.87	4.42	4.05	3.58
H_{c3} (K Oe.)	8.0	7.35	-	5.98
H_{c3}/H_{c2}	1.65	1.67	-	1.67
Zero field trapped flux (%H_{c2})	92.5	88.2	91	44.7

Figure 4.15: Magnetisation curves and extracted data for the heat-treated niobium samples.

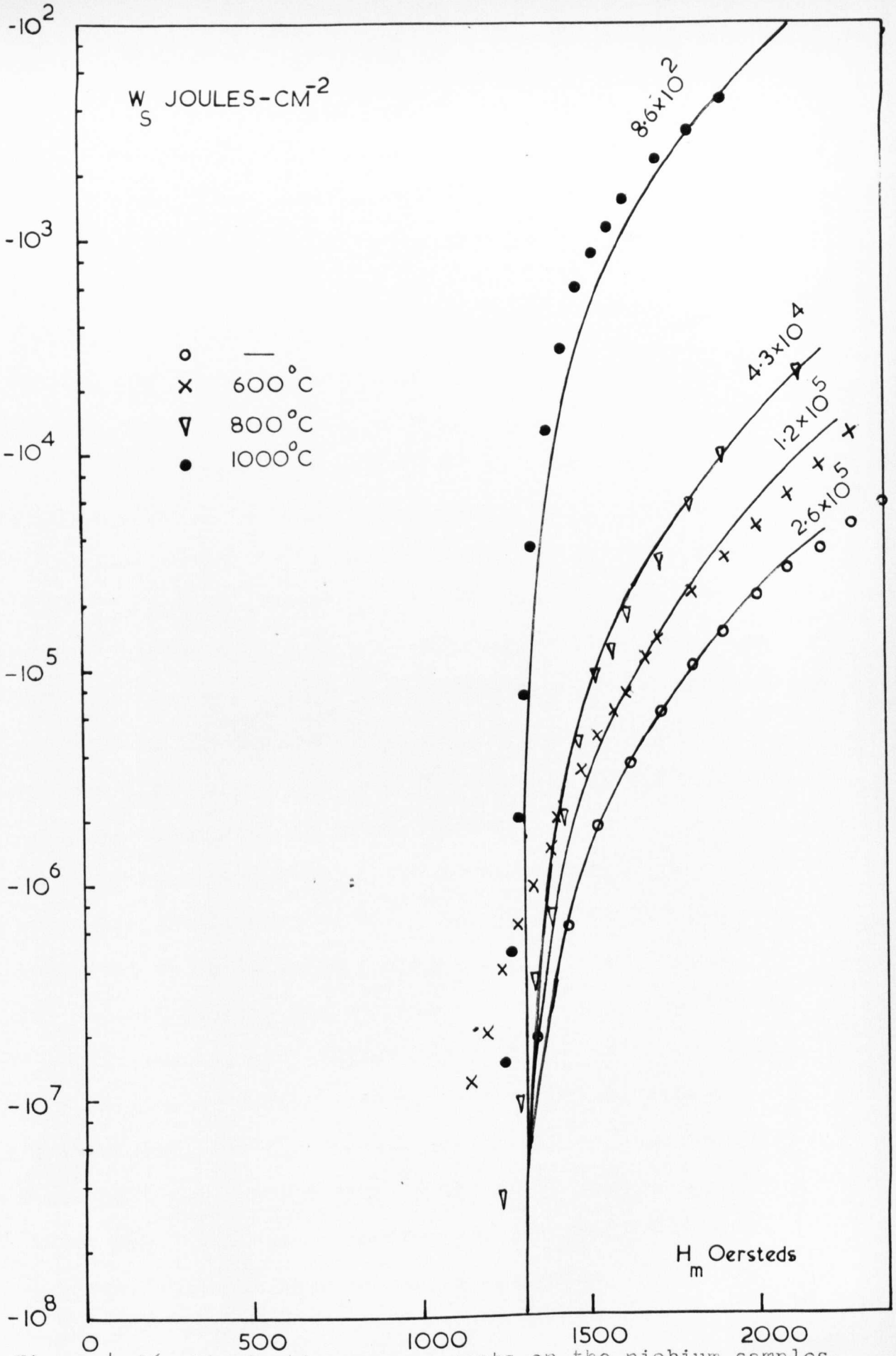

Figure 4.16 Dissipation measurements on the niobium samples, The solid lines were calculated from modified critical state (100) with H_{c1} = 1300 Oe. and J_c constant.

centres. There should therefore be a corresponding increase in the alternating field losses. This was observed, as illustrated in figure 4.16, the biggest increase being between the 800 and 1000°C samples.

A study of the voltage waveforms in these experiments showed, with the high temperature samples at least, that when the applied field was below H_{c1} during the cycle, little flux escaped from the sample. The existence of such a near-diamagnetic region, and the small surface currents, were ideal conditions for the application of the modified critical state model. With H_{c1} = 1300 Oe. and J_c assumed to be constant for each sample the solid lines in figure 4.16 were drawn. The values of J_c were chosen by matching the curves to the results at H_m = 1800 Oe. and are indicated on the diagram. The low-field discrepancies between theory and experiment are probably due to surface losses, but elsewhere the agreement is reasonable.

No evidence of apeak value for J_c was observed, but the temperature intervals were probably not sufficiently close for such an affect to be detected. From 2.6 x 10^5 A-cm^{-2} the critical current density was reduced to 8-6 x 10^2 A-cm^{-2} by a 2 hour, 1000°C anneal, striking evidence of the role of defect structure in pinning magnetic flux. It is evident from the voltage waveforms, and the success of the theory, that samples with a low critical current density are often genuinely diamagnetic below H_{c1}. This is in contrast to the samples with a high J_c where flux continues to escape, at least until the applied field is zero.

4.3.3. Single-crystal samples

As an extension to the loss measurements on heat-treated samples with a low critical current density, single crystals of niobium were studied. These were electron-beam zone-refined from the "as received" polycrystalline rod.

The lack of metallurgical defects present in the samples resulted in very low critical current densities. As soon as H_{c1} was exceeded, the losses in the "as grown" samples increased steeply, as shown earlier in figure 4.6. As this transition was very sharp, the influence of surface currents, on the field of first penetration, could be easily observed.

A careful experiment was performed, in which one sample was given a succession of surface treatments. Both magnetisation and a.c. loss curves were determined, at each stage, and these are shown in figures 4.17 and 4.18 respectively. It was (A) spark-machined, on the finest range 7, from the "as grown" crystal, then (B) mechanically polished to 1 micron and finally (C) etch-polished.

Neither curve for the spark-machined sample (A) differed from that for the "as grown" crystal, so this process would appear to have not caused any structural damage. The initial magnetisation curve was characteristic of a fairly reversible type II superconductor with $H_{c1} \sim 1300$ Oe. and $H_{c2} = 3{,}100$ Oe. Assuming H_c to be 1550 Oe. (as measured by De Sorbo[66] and Finnemore et al.[158]) this gave a value of $K = 1.4$ for this sample. Bulk losses commenced at $H_m = 1300$ Oe., consistent with the measured values of H_{c1}.

The mechanical polish (B) had a drastic effect on both the magnetisation loop and the dissipation. Detectable losses

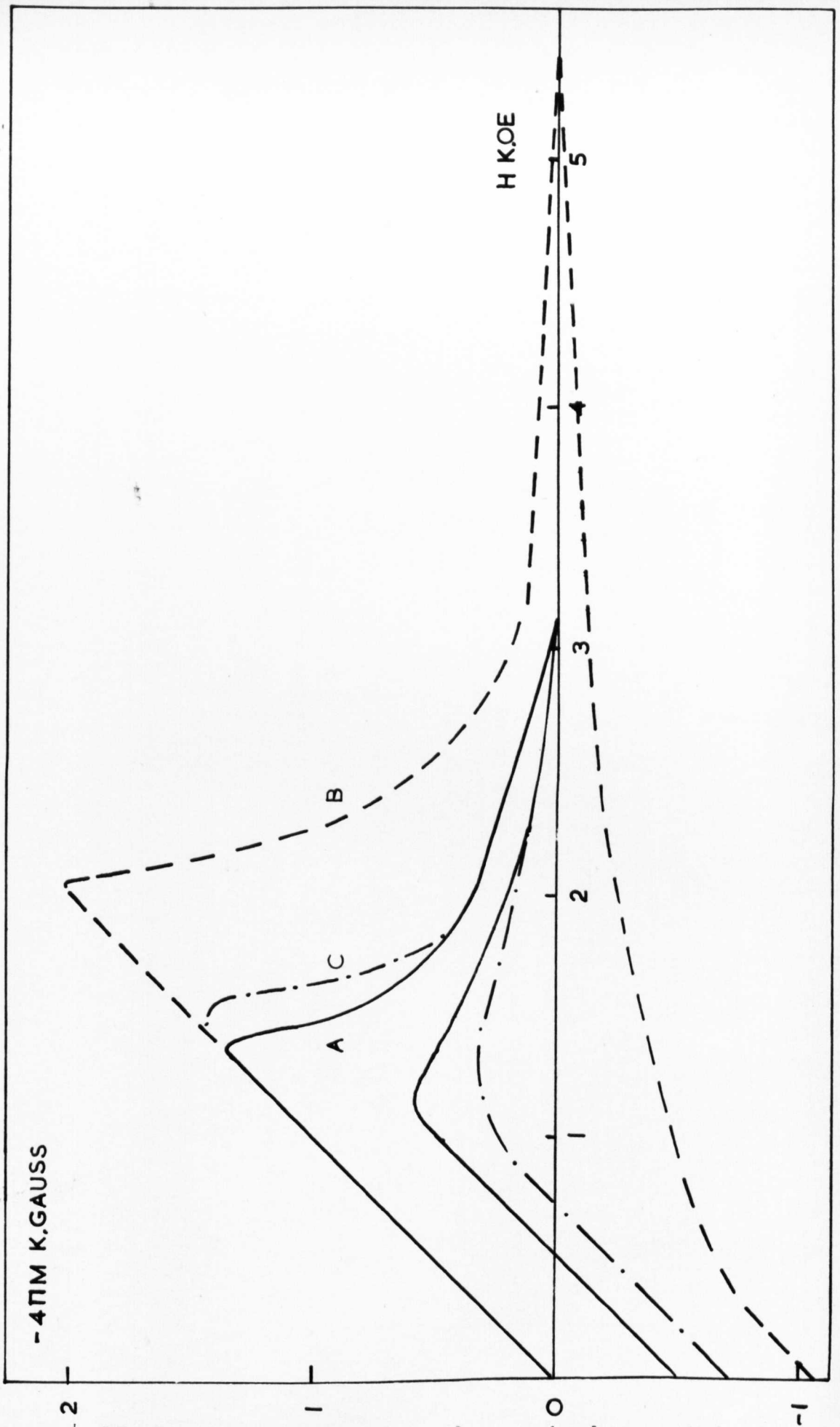

Figure 4.17 Magnetisation curves for a single crystal of niobium after various surface treatments. (A) "as grown" (B) mechanically polished (C) chemically polished.

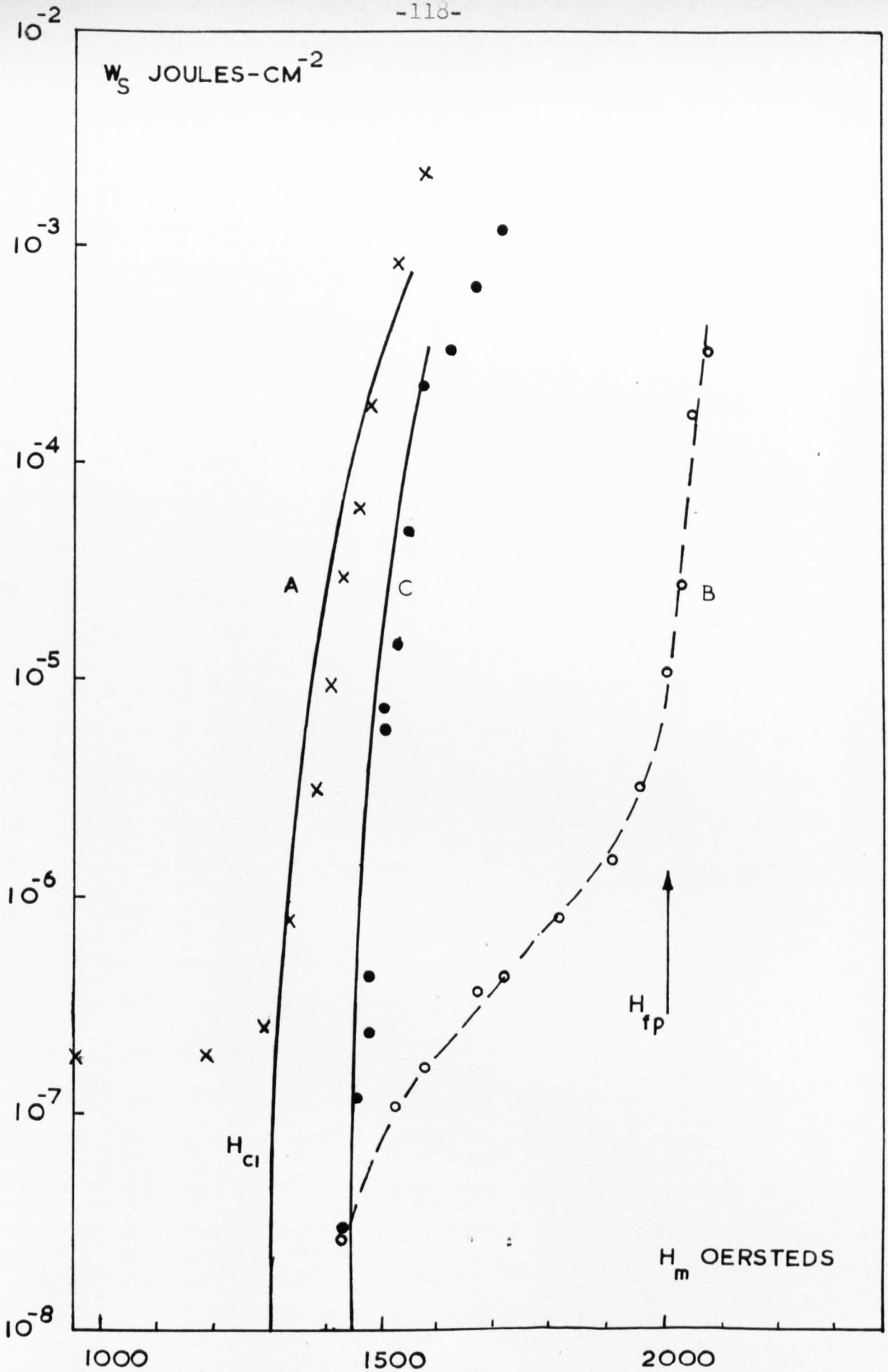

Figure 4.18 Dissipation measured on a niobium single crystal for a variety of surface finishes. (A) spark-machined 7X (B) mechanically polisned o (C) etch-polished ●. The solid lines A and C were calculated from equation 2.12.

did not occur until $H_m > 1425$ Oe. and they increased only gradually, compared with (A). Then at $H_m \sim 2000$ Oe. the curve resumed its familiar steep slope. This was also the field at which the magnetisation curve ceased to have diamagnetic slope, H_{fp}. The initial magnetisation loop exhibited considerable hysteresis and there were large sheath currents above H_{c2}.

Some 70 microns were then etched off the surface (C) leaving a highly polished finish. Much of the hysteresis was removed and when a further 30 microns were removed, in the same fashion, no change was noted in either of the curves (C) on figures 4.17 and 4.18.

It would appear, therefore, that the mechanical polish introduced cold-work into a layer less than 70 microns deep from the surface. As a result this layer had a much larger $J_c(H)$ than the bulk of the sample. We suppose that this modified the mode of field penetration upto 2000 Oe. when the bulk of the sample was penetrated. On removal of this layer the sample was, probably, once more homogeneous. However the brightly polished surface, that resulted, modified the experimental results, when compared with the original curves (A).

Once again we attributed this effect to surface currents and measured these from the voltage waveforms. Typical waveshapes are illustrated in figure 4.19 and these should be compared with those for the polycrystalline samples, in figure 4.13. The measured surface currents are shown in figure 4.20, the broken lines being drawn as an approximate mean of the results. As the values of H for the spark-machined material were insignificant and the waveshapes indicated partial diamagnetism between $-|H_{c1}|$ and $+|H_{c1}|$, the modified critical

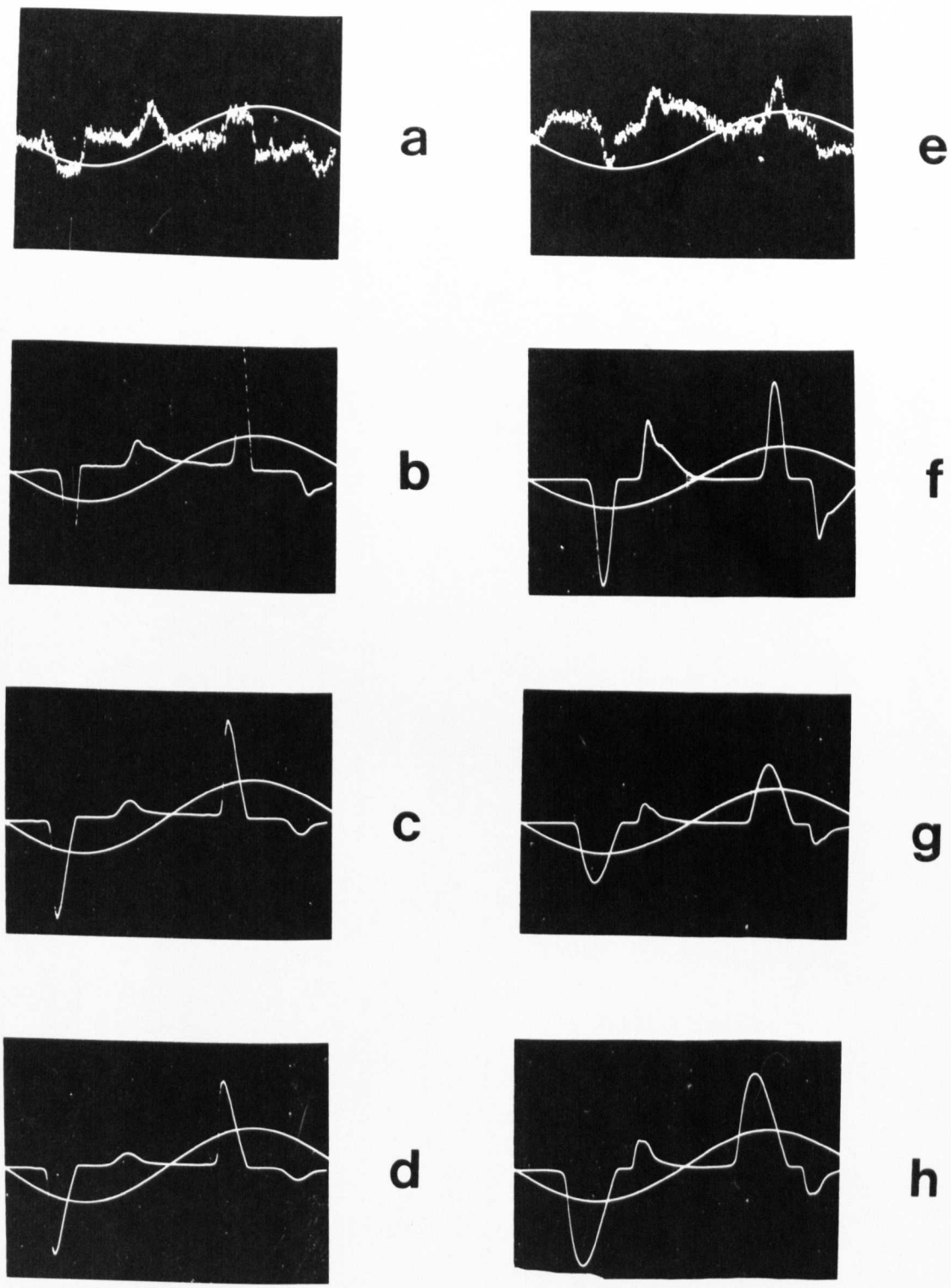

Figure 4.19 Penetration voltage waveforms for single crystal niobium: mechanically polished
(a) H_m = 1522 Oe.(0.01 mv/div) (b) 1620 Oe.(0.2)
(c) 1715 Oe.(1) (d) 1810 Oe.(2): "as grown"
(e) 1330 (0.01) (f) 1430 Oe.(1) (g) 1520 (10)
(h) 1620 (10)

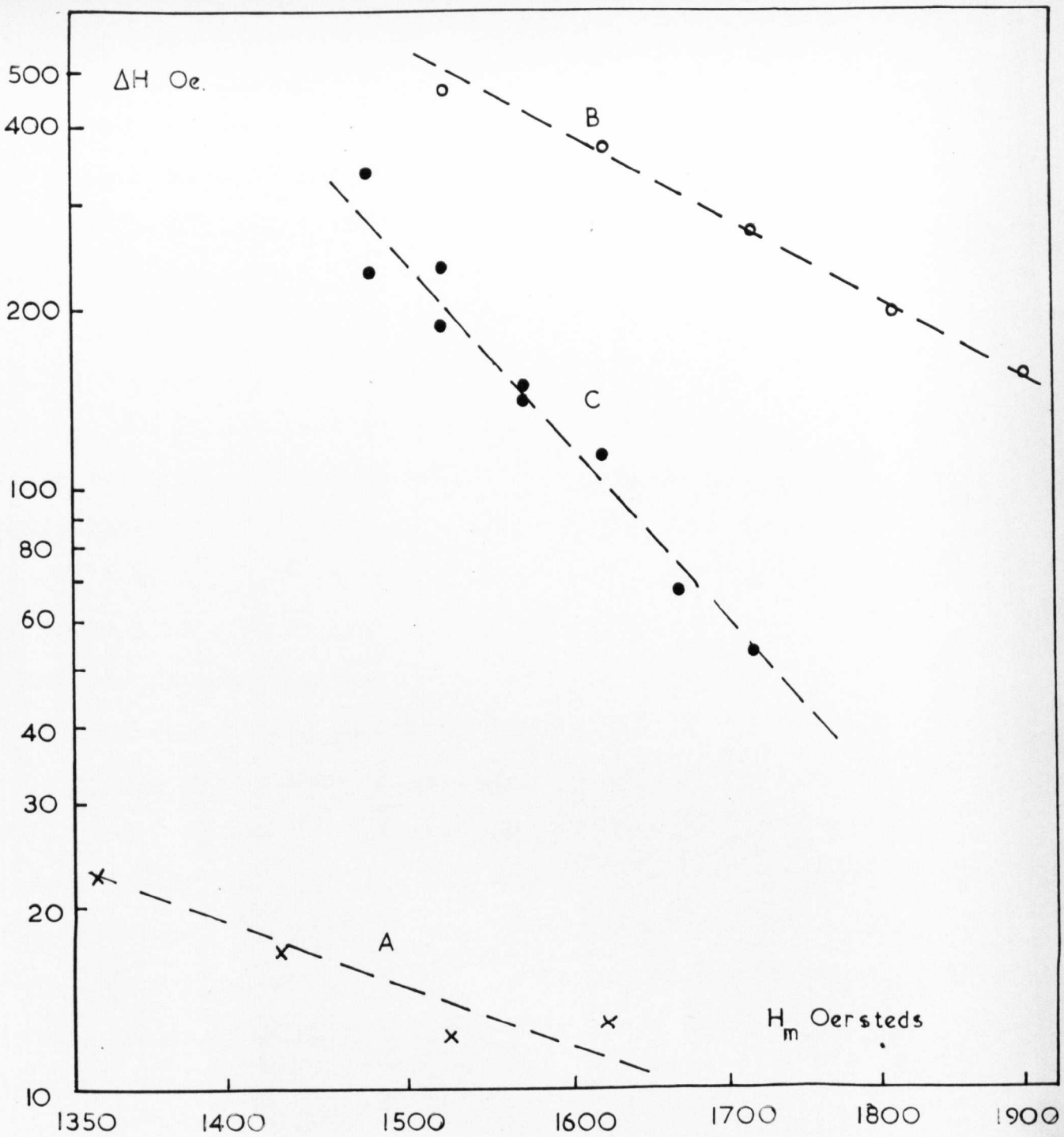

Figure 4.20 Surface currents measured on a single crystal of niobium (A) "as grown" (B) after being mechanically polished (C) after then being etch-polished.

state equations were evoked to explain the results. Three spot measurements of the critical current density were made, using the modulating field technique (see section 3.3) and the results were:

H	1350	1410	1500	Oe.
$J_c(H)$	4.2×10^3	2.4×10^3	9.6×10^2	$A\text{-}cm^{-2}$

With H_{c1} = 1300 Oersteds the empirical relation $J_c(H) = \alpha/(H-H_{c1})$ fitted these results fairly well and so equation 2.12 was applicable.

$$W_s = 4.22 \times 10^{-9} (H_m-H_{c1})^2 (1.414 H_{c1} + 1.026 (H_m-H_{c1}))/ J_c(H)$$

The solid line A on figure 4.18 is the result of such a calculation and it approximates to the measured values of the dissipation. The calculation was then repeated with H_m replaced by $(H_m - \Delta H/2)$, with values of ΔH taken from line C in figure 4.20. Solid line C in figure 4.18 emerged, and lay close to the points determined for the etch-polished sample.

Therefore, the differences in the response of the sample, to applied fields, with a rough surface and then with a bright finish, can be attributed entirely to surface currents flowing above the mixed state.

4.3.4. Discussion

In the cold-worked polycrystalline samples the high-field losses were in general agreement with the simple critical state model, with $J_c = \alpha/H$. This was only the case, however, when $H_m \gg H_{c1}$ and the surface currents were small. In low fields, and when the sample was well polished, these currents became a dominant factor. The modified critical state equations[100] were based on the assumption that the sample would be diamagnetic

in the field interval $-|H_{c1}|$ to $+|H_{c1}|$ and in the hysteretic materials this was not the case. At best, no flux moved across the sample surface between H = 0 and $+|H_{c1}|$. It was therefore not surprising that the match, between theory and experiment, was poor.

With samples of small surface currents and low critical density, such as the single crystals and the high-temperature annealed specimen, the equations which accounted for the region below H_{c1} were reasonably applicable. Values of the appropriate $J_c(H)$ were not always available but the figures, used in the equations to match the experimental points, were realistic.

The experiments on surface-treatments of one single-crystal sample showed the importance of the superconducting properties of near-surface layers. A damaged layer of less than 70 microns drastically modified both the magnetisation curve and the dissipation measurements. Similar damaged "skins" in machined, polycrystalline samples, reduced the losses in moderate fields.

Although surface currents modified the response of the samples, to the applied field, we found that the theories could be modified to account for this. By replacing H_m by$(H_m - \Delta H/2)$ in the critical state equations, the theory-experiment mismatch could be eliminated. Extending this idea, it seems reasonable that no field penetration into a sample should occur, until the applied field H is such that $(H - \Delta H(H)/2) > H_{c1}$. In this case one should regard measured values of H_{c1} with some caution until the surface currents are known. The loss curve for the spark machined sample, drawn in figure 4.5, shows a change in slope at $H_m \sim 1200$ Oe., the chemically polished sample is penetrated at

1250 and losses are not measured in the mechanically polished until 1350 Oe. It is conceivable that these differences can be accounted for in terms of the surface currents. More work is required to investigate this point.

4.4 Dissipation in the mixed state - niobium strips

In the measurements made on the cylindrical niobium specimen the complete bulk of the sample was rarely penetrated, except in the case of the more reversible single crystals. In terms of the fields defined in section 2.3.1., $H_m \ll H_p$, for most of the experiments.

Therefore, as an extension to our study, alternating field measurements were made on cold-rolled niobium strip samples of a range of thicknesses. In these experiments H_p was often exceeded and the theoretical predictions were tested over a wider range, than previously.

Apart from these points of fundamental interest, niobium strip conductors have potential application in a.c.superconducting devices. Several laboratories, including our own, had been studying such conductors, (under the sponsorship of the Ministry of Technology) but disagreed on some results taken on similar samples. Our experiments were also designed to throw some light on the points at dispute.

The strip samples were cut, from the material to be studied, into pieces 2.5 cm.square. Some 30 to 40 turns of 46 swg wire were wound flat on the strip, in the direction of rolling, and held in contact with the surface with diluted "Evostick". This relative orientation of rolling-direction and pickup-coil was

chosen to simulate the direction of roll and self-field, when the strip carried a transport current. The sample was then mounted on the perspex former (see figure 3.3) and wired into the sample holder (figure 3.4).

Dissipation measurements were made over a range of frequencies but, as no frequency dependence was observed, 50 Hz or 90 Hz were most commonly used.

4.4.1. Kawecki-Hancox strip

The major disagreement between the Ministry of Technology contractors concerned the value of the dissipation, measured in applied fields less than H_{c1}, on similar niobium strips. To settle these arguments a length of 0.005 in.strip, supplied by the Kawecki-Billiton Corporation was distributed to all the laboratories concerned, by Dr.Hancox of the Culham Laboratory. This we have identified as the Kawecki/Hancox strip. Magnetisation measurements and the variation of the surface currents with H_m are shown in figure 4.21 and the dissipation measurements are plotted in figure 4.22. Also drawn on this latter figure are results taken on the same material by two other groups. The variation between the three sets of results emphasises the remarks, made earlier, concerning the care that must be taken with experimental conditions, especially when deciding on the conductor geometry. Both the BICC and English Electric experiments were performed with transport currents in strip "sandwiches", in which edge effects are crucial. Both groups have found that the mode of sample shaping influences the results.[159,160]

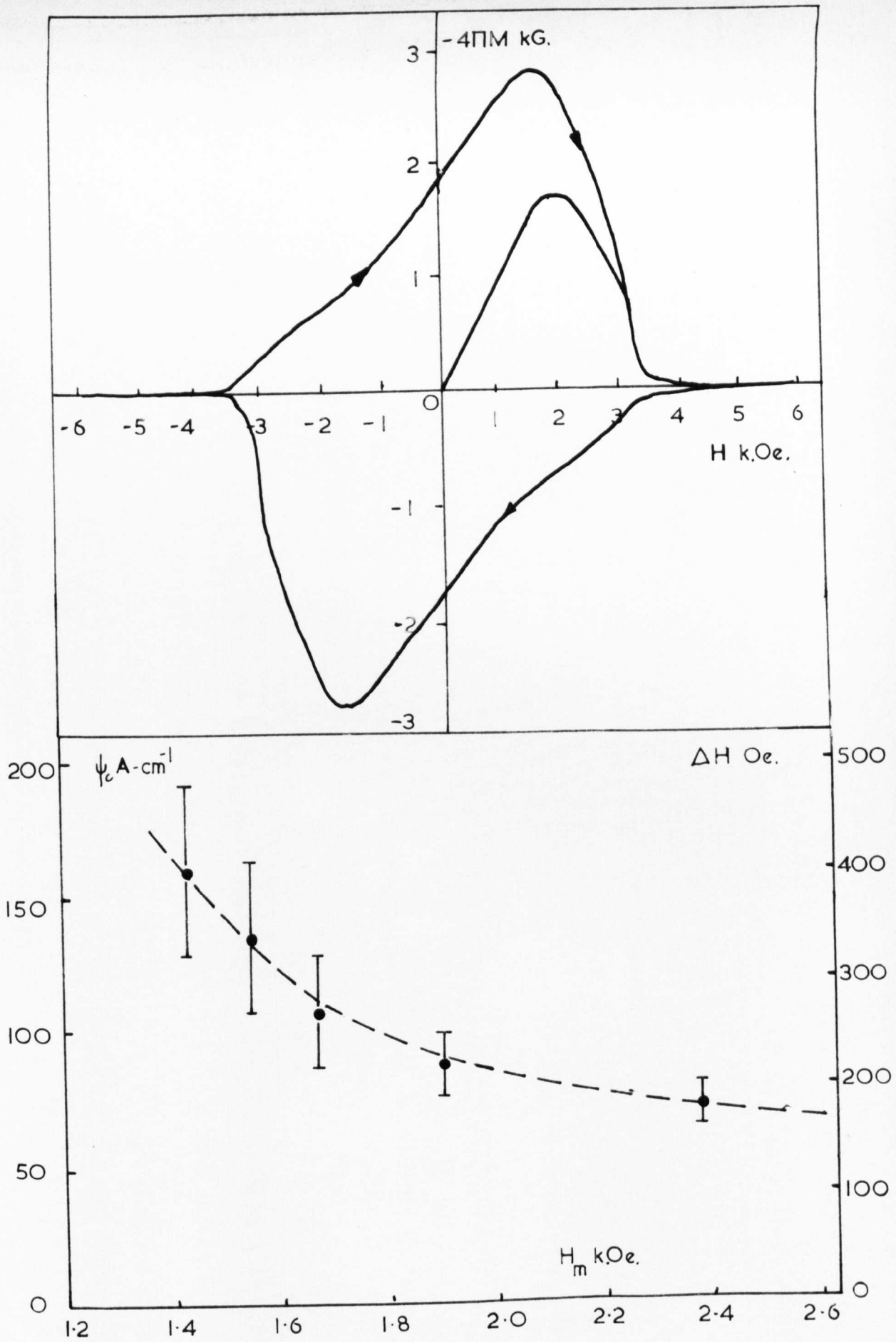

Figure 4.21. (a) The complete magnetisation curve and (b) the measured surface currents, for the Kawecki/Hancox niobium strips.

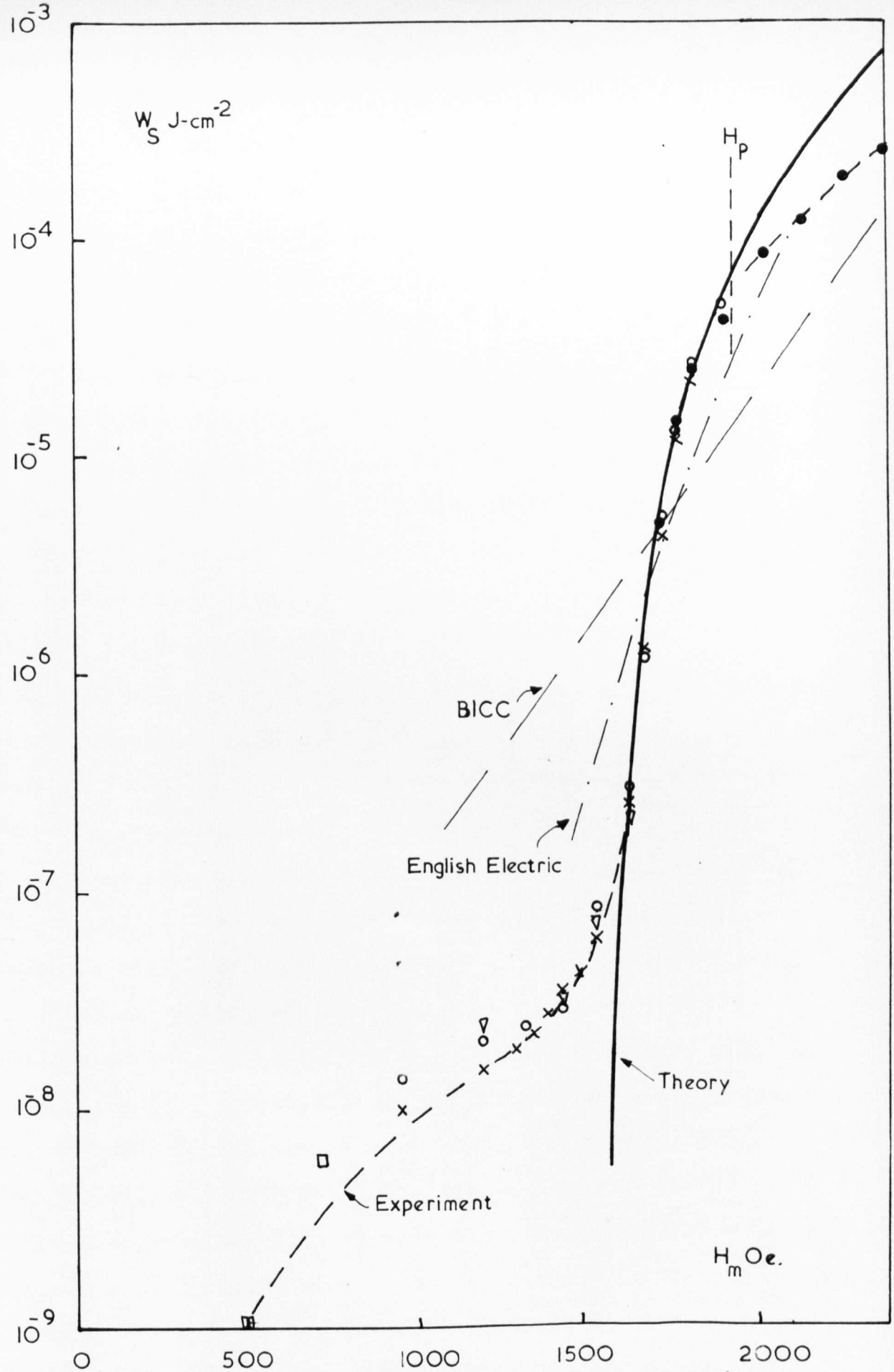

Figure 4.22 Dissipation measurements on the Kawecki/Hancox niobium strip. Readings taken at 45 Hz o, 50 Hz ●, 90 Hz ×, 180 Hz ▽, 450 Hz □.

To ensure that such effects would not undermine our experiments, pickup-coils were wound at various points along the samples, but no edge penetration was detected, except when the coils were at the extreme ends. The "as rolled" finish of the surface was reasonably bright but some uneveness was detected on the Talysurf machine and a low level of dissipation was measured in applied fields less than H_{c1}. There was some scatter in the results at this lower end but their general variation is indicated by the broken line in figure 4.22. It is interesting to note that at H_m = 1000 Oe., $Ws < 10^{-8}$ J-cm^{-2} as this is the field value often mentioned with reference to possible applications.

As H_m approached H_{c1}, the losses increased steeply as bulk penetration occurred, then increased more gradually as H_m exceeded about 2000 Oe. This levelling off coincided with a marked change in the character of the pickup-coil voltage waveform, as shown in figure 4.23. Only the part of the waveform, which corresponds to the field penetration near the peak applied field, is displayed, together with a field dependent signal. Plate (a) is typical of the voltage peaks observed in the cylindrical samples (c.f. figure 4.13) but when H_m = 2000 Oe., as in plate (b), a change in slope is detected when $H \sim 1950$ Oe. This is more exaggerated at H_m = 2280 Oe.(c) until at H_m = 2570 Oe. (d) this peak is sinusoidal in nature. In addition to the change in the form of this peak, another $d\phi/dt$ maximum appeared just in front of the one discussed. It is just apparent in plates (a) and (b) but in (c) and (d) it appears as a sharp spike. In each case it appears at $H \sim 1400$ Oe., close to the measured value of H_{c1}.

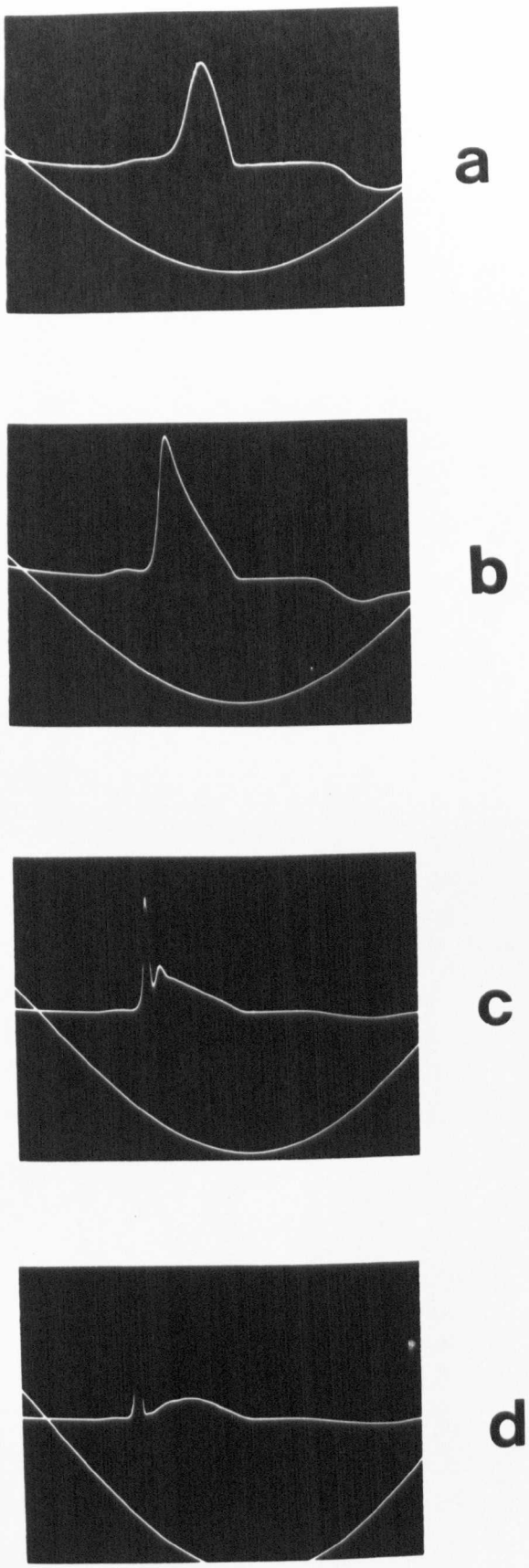

Figure 4.23 Penetration voltage waveforms for the Kawecki/Hancox niobium strip (a) H_m = 1760 Oe.(0.5 mv/div) (b) 2000 Oe.(2) (c) 2280 Oe.(10) (d) 2570 Oe.(20).

We suggest that the spiky peak corresponds to the establishment of the equilibrium, internal flux distribution, as H exceeds H_{c1}. Flux of opposite sign, trapped from the previous half cycle, must first escape and then the applied field will penetrate to establish the critical state in the material. Both these flux movements are expected to be sudden and will lead to a voltage pulse of the same sign.

The change in slope in the main peak we associate with complete penetration of the strip. When this occurs, at $H_m = H_p$ (H^* in some papers[47,100]), it can be shown, on the basis of the Bean model, that $d\phi/dt \propto dH/dt = 2\pi f H_m \cos 2\pi ft$. The waveshape in figure 4.23(d) has this form and the latter half of the peak in (b) and (c) also suggest a sinusoidal variation. On this basis we have estimated that H_p = 1995Oe. and, assuming J_c to be independant of H, this leads to $J_c = 2.3 \times 10^5$ A-cm^{-2}. It is interesting to note that the maximum in the magnetisation curve also occurred at 2000 Oe.

Before attempting to apply the critical state calculations to the strip, we compared the dissipation measurements with hysteresis loops, plotted with the vibration magnetometer. The applied field was swept slowly round a complete cycle, from $-H_m$ to H_m then back to $-H_m$, and the area enclosed in the resultant hysteresis loop was measured with a planimeter. Results of two such measurements are shown as points on figure 4.24, compared with the a.c.loss measurements, shown as a solid line. The errors involved in the magnetometer measurements were large, especially at low levels of dissipation, but within the estimate of these errors, the results of the two experiments are in fair agreement. The outcome of this lack of variation in the

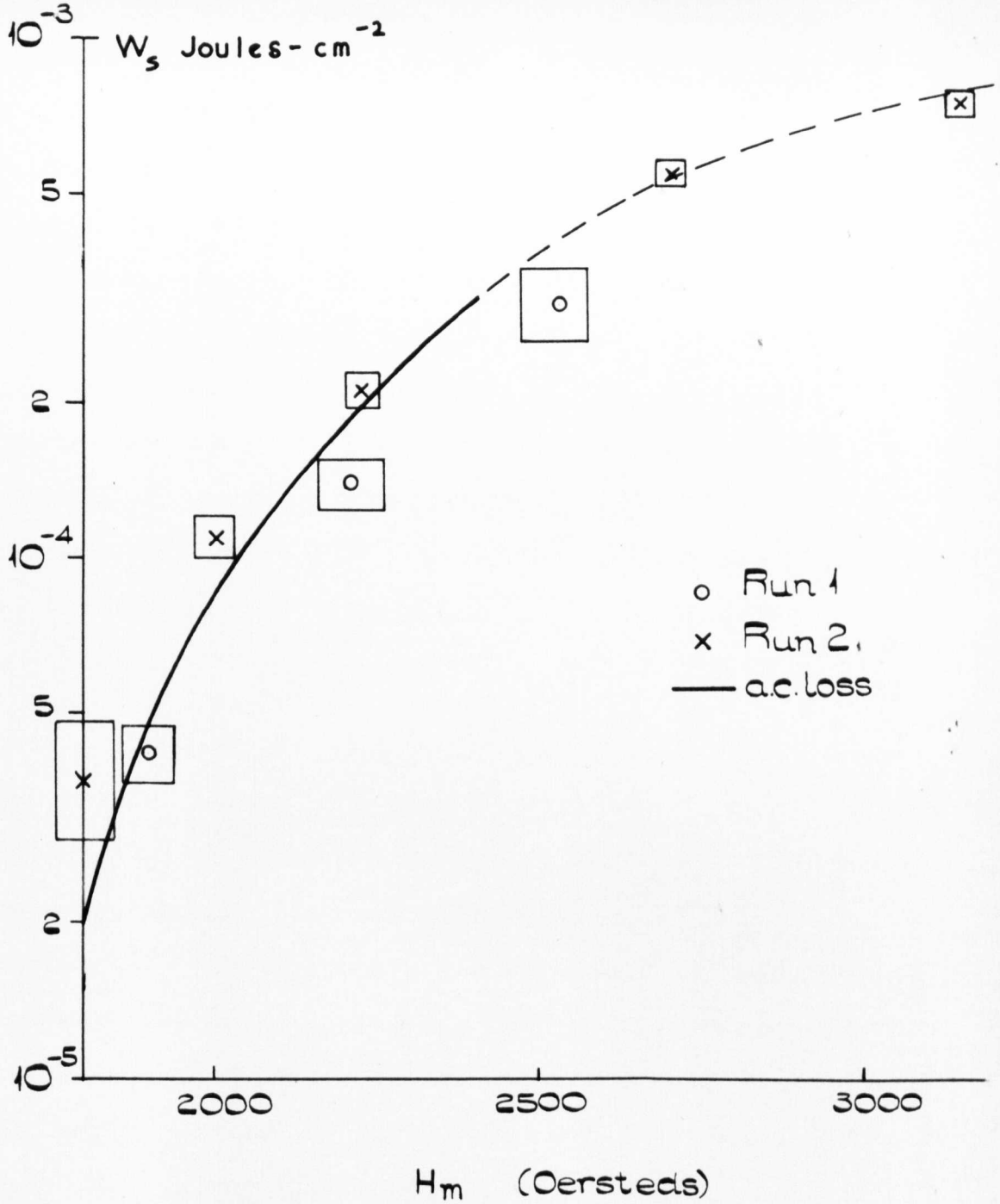

Figure 4.24. Comparison of the dissipation in the Kawecki/Hancox niobium strip, measured (a) from the magnetisation loops and (b) by the alternating field technique.

dissipation per cycle, with frequency, between 0.002 and 450 Hz, is that the critical state ideas can be applied without fear of time dependant and temperature effects.

We have seen, in earlier sections, that the modified critical state equations proposed by Easson and Hlawiczka[100] (equations 2.11 and 2.12) are sometimes adequate to predict the dissipation, in fields close to H_{c1}, if $(H_m - H_{c1} - \Delta H/2)$ is substituted for H_m'. The success of the application of this theory depends on the form of $J_c(H)$ chosen. In the case of this strip sample neither a constant J_c or $J_c(H) \propto 1/H$ fitted the results. Equation 2.12 was derived on the assumption that $J_c = \alpha/H'$ and

$$W_s = 4.22 \times 10^{-9} (H_m')^2 (1.414 H_{c1} + 1.026 H_m') / J_c(H)_{J\text{-}cm^{-2}}$$

Substitution of H_{c1} = 1400 Oe., ΔH values from figure 4.21 and $\alpha = 1.2 \times 10^7$ Oe. A-cm^{-2} produced the solid line in figure 4.22. The value of was calculated from H_p, as determined in the waveform measurements, also assuming $J_c(H) = \alpha/H'$.

As expected, in low fields, the agreement between theory and experiment was poor, as surface losses affected the results. However, as soon as bulk penetration occurred, a good match was obtained, until H_m exceeded 2000 Oe. Above this value $H_m > H_p$ so the theory was not applicable.

4.4.2. Strips of varying thickness

The two important parameters of a strip conductor are its critical current density $J_c(H)$ and the penetration field H_p, which depends on $J_c(H)$ and the thickness d. As both d and $J_c(H)$ are influenced by rolling, we investigated the a.c. properties of a series of niobium strips of varying thickness. Four samples

were measured, each one rolled from the previous thickness, without any intermediate anneals. They ranged from 2.5×10^{-2} cm to 2.5×10^{-3}cm and were all measured in the "as rolled" condition.

Magnetisation curves and the critical fields are given on figure 4.25 and the measured critical currents are plotted in figure 4.26. The magnetic data indicates that the successive rollings increased the value of K, as H_{c2} was increased and H_{c1} was decreased. Microhardness tests made at the BICC research laboratories(161), and included in figure 4.25, showed that the dislocation density was similarly increased by rolling. Therefore the dislocation distribution must have been such that it effectively reduced the electron mean free path and increased K as a result. Approximate values, calculated from $H_{c2} = \sqrt{2}K\, H_c$, with H_c = 1550 Oe., are included in the table on figure 4.25. It is interesting to note that three of the magnetisation curves are coincident in low fields, despite having different thicknesses and K-values. However, the critical current densities, illustrated in figure 4.26, are roughly in inverse proportion to the dimensions of the strip, and the cancelling of these two factors results in similar curves for the different samples.

Apart from reducing the mean free path, the new dislocation networks introduced by rolling appear to have resulted in an increase in the number of pinning centres. The critical current density was increased by a factor 20 between the 250μm and 25μm strips. It has been suggested(62,63) that both an increase in the density of dislocation tangle and the decrease of the scale of the cell structure of these networks, result in greater pinning. Without electron-microscope studies on

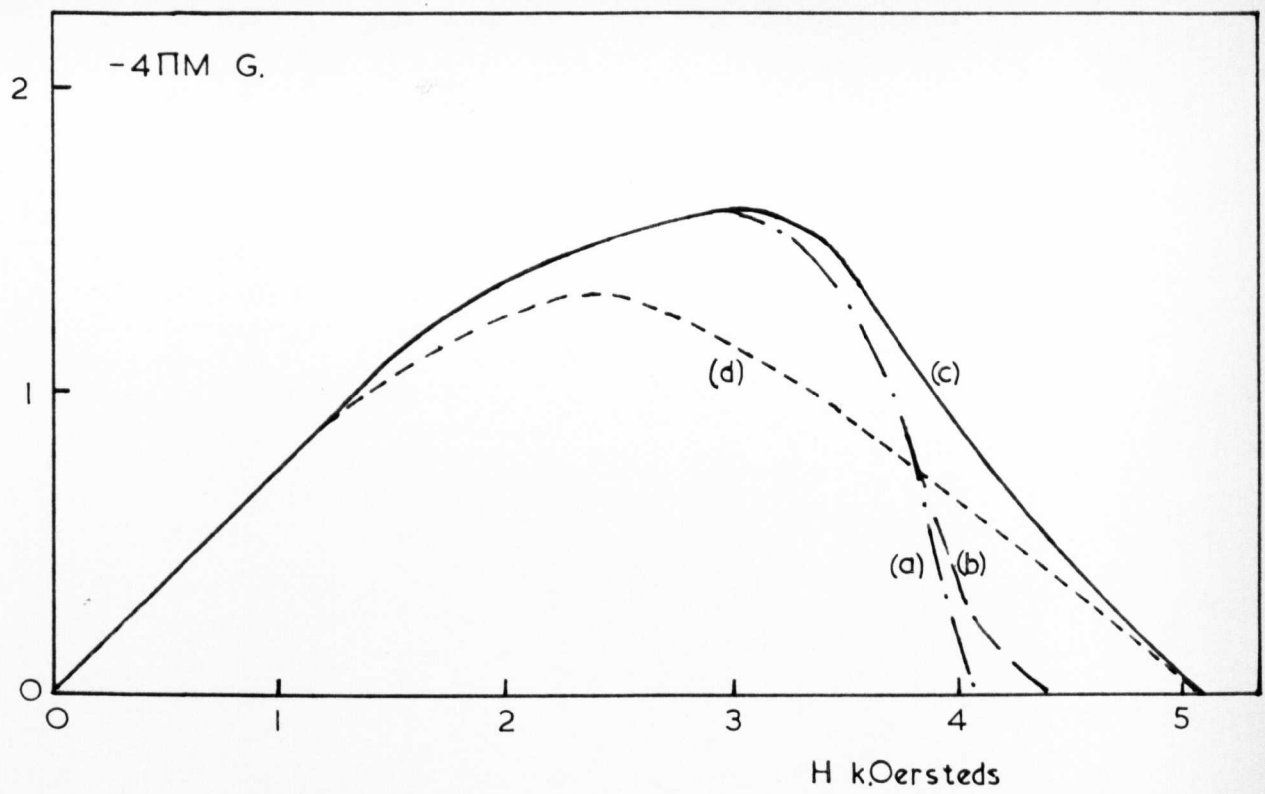

Curve	(a)	(b)	(c)	(d)
Nominal thickness (mil)	10	6.3	3	1
Thickness d (cm)	2.5×10^{-2}	1.6×10^{-2}	7.6×10^{-3}	2.5×10^{-3}
H_{c1}(Oe)(±250e)	1350	1350	1300	1300
H_{c2}(Oe)	4,140	4,400	5,040	5,050
K (Calculated)	1.9	2.0	2.3	2.3
Hardness (HV/10)	149	165	180	>189
H_p(Oe)	1630	1655	1570	<H_{c1} or >2800
α-calculated (OeA-cm-2)	8.5×10^{7}	1.36×10^{8}	2.6×10^{8}	$<5\times10^{8}$ $>2.5\times10^{9}$
α-measured (Oe A-cm^{-2})	3.8×10^{7}	1.46×10^{8}	4.45×10^{8}	1.78×10^{9}

Figure 4.25 Magnetisation curves and other date relevant to the niobium strips of various thicknesses.

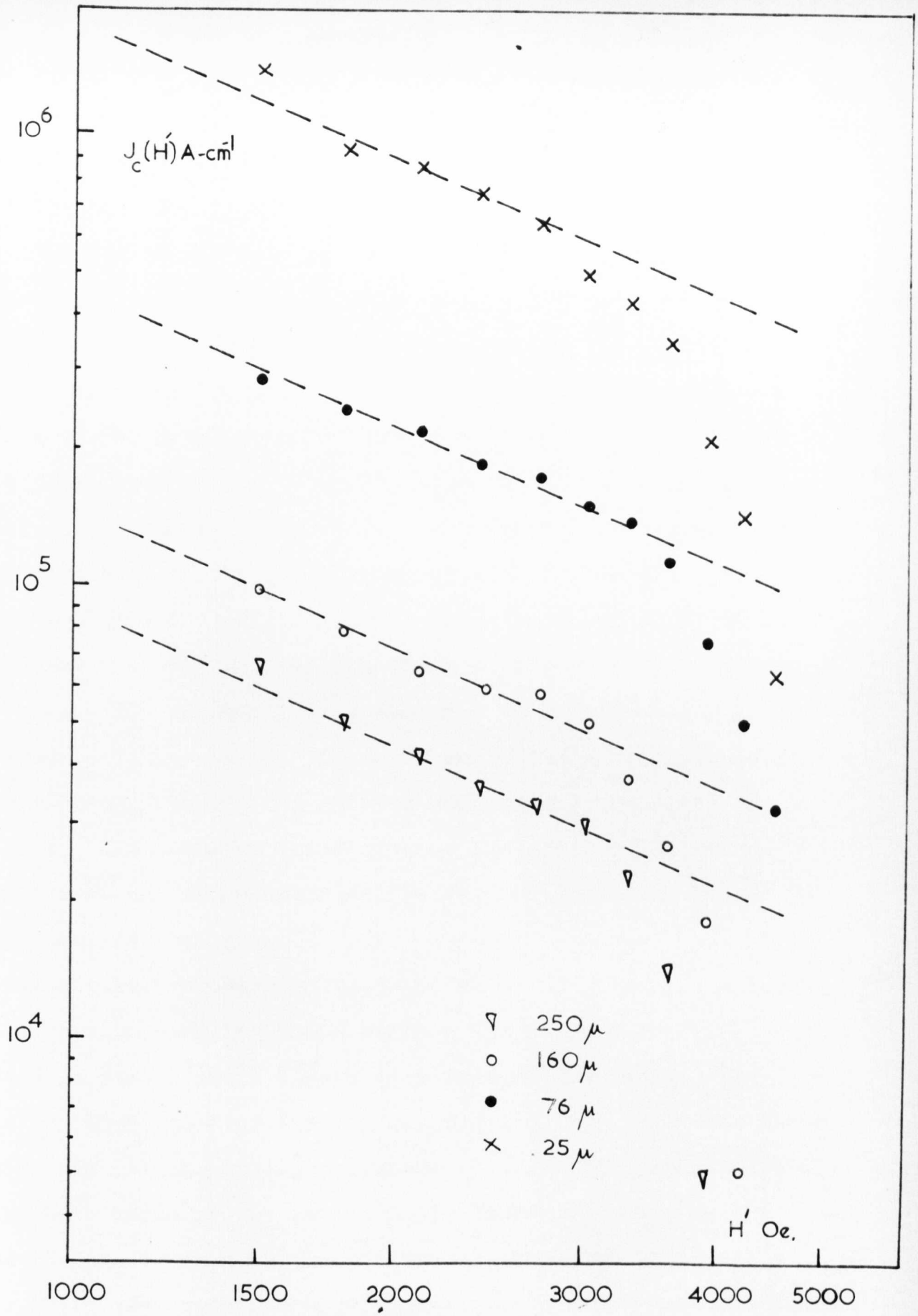

Figure 4.26 Critical current measurements on the niobium strips of varying thickness. (The broken lines have slope -1)

the strips, it is difficult to draw any detailed conclusions.

The broken lines on figure 4.26 are of slope -1 and indicate that $J_c(H) = \alpha/H$. Values of α taken from the curves are listed in the table on figure 4.25.

Examples of the voltage waveforms produced during the measurement of the dissipation are shown in figure 4.27(a) - (h). Once again, for the two thicker strips illustrated (a) - (d), the waveshape is modified as the applied field exceeds a certain value, which we have identified with H_p. This effect was not detected in the thinnest strip (e) - (h) so we believe either $H_p < H_{c1}$ or $H_p > 2,800$ Oe., the highest field used. The sinusoidal form of the penetration peak in figure 4.27 (h) is evidence of the former condition. From the value of H_p we have calculated the critical current density of the strips, assuming $J_c = \alpha/H$. The calculated and measured values of α can be compared in figure 4.25. The two results for the thicker strips agree closely, but for the thinner samples a discrepancy is apparent. The measured value of α for the 1 mil strip is bracketed by the two calculated figures, based on the two assumptions regarding H_p.

Dissipation measurements, taken at 50 Hz, are point-plotted in figure 4.28. Although the surface finish of the strips was reasonably smooth, small losses were measured below H_{c1}, but these are excluded from the diagram for clarity. With the three thicker samples the losses increased steeply as H_m exceeded the appropriate value of H_{c1} but as H_m is increased above H_p the losses level off to a curve dictated by the strip thickness d and $J_c(H)$. The curve for the 1 mil strip is shallow at all field values, in sympathy with our belief that $H_p < H_{c1}$.

Equation 2.11 has been used to match the results, i.e.

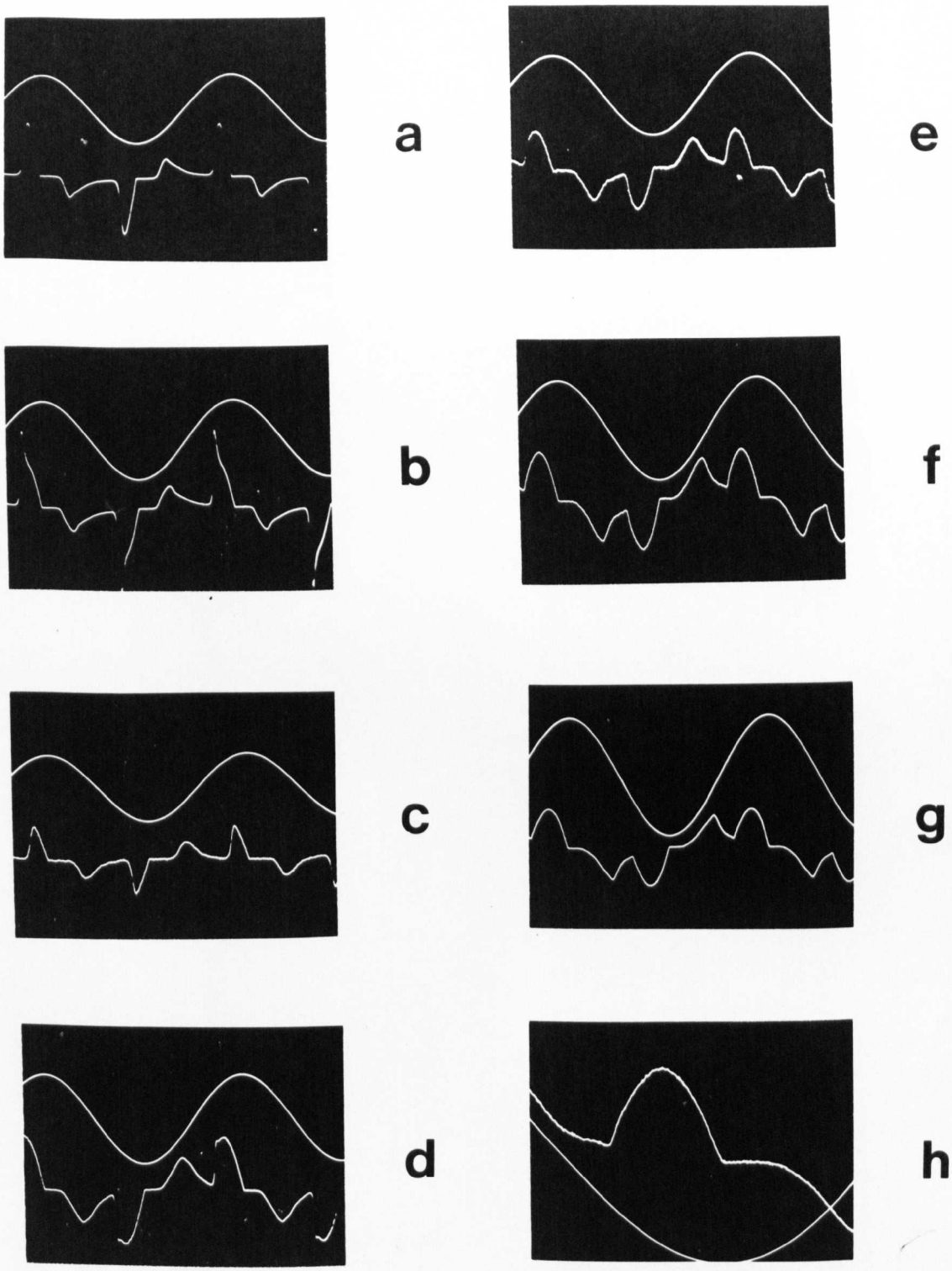

Figure 4.27 Penetration voltage waveforms for the niobium strips: 250 micron (a) H_m = 1620 Oe. (b) 1850 Oe.: 75 micron (c) 1525 Oe. (d) 2140 Oe.: 25 micron (e) 1905 Oe. (f) 2380 Oe. (g) 2860 Oe. (h) 2380 Oe.

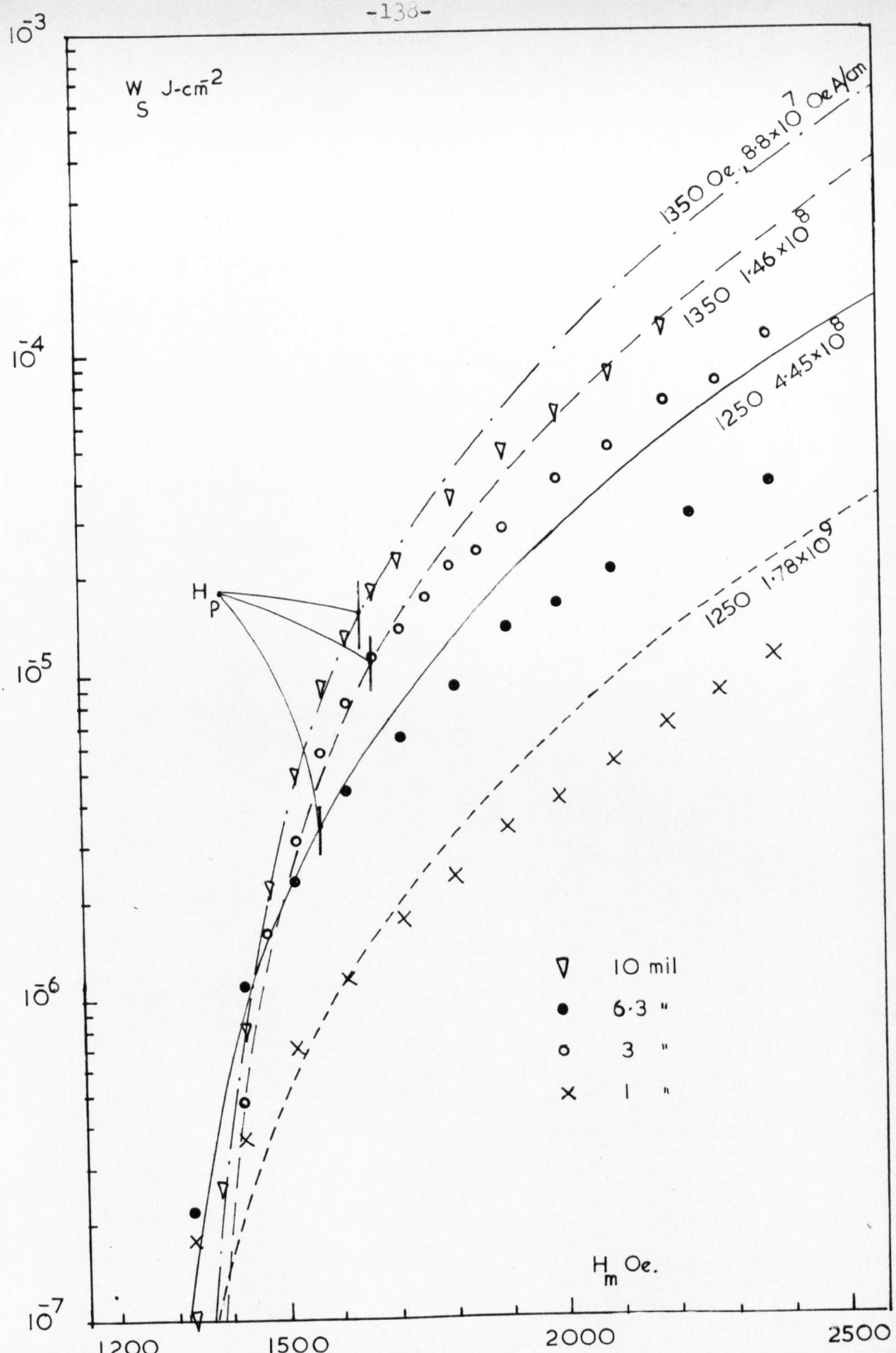

Figure 4.28 Dissipation in niobium strips over a range of thicknesses. The points represent the measured values, the lines were drawn from the theory.

$W_s = 4.22 \times 10^{-9} (H_m - H_{c1})^2 (\frac{1}{2}H_{c1} + H_m)/J_c(H)$ J - cm^{-2} with $J_c = \alpha/H$. The lines in figure 4.28 were drawn with the measured values of α and H_{c1} listed in figure 4.25. Agreement between the predictions and the experimental points is extremely good for $H_m < H_p$ especially as, for simplicity, surface currents were not allowed for. As expected, once $H_m > H_p$ the measured results are lower than the theoretical line. On the basis of the simple Bean model of the critical state, it can be shown that when $Hm >> Hp$, $Ws = \frac{1}{2}H_m J_c\ d^2 \times 10^{-8}$ J-cm^{-2}, or, if $J_c(H) = \alpha/H$, $Ws = \frac{1}{2}\alpha d^2 \times 10^{-8}$ J- cm^{-2}. Therefore the dissipation is expected to increase linearly with the applied field, or eventually to approach a saturation level. As $H_m > H_p$ for all the measurements, and the value of α is approximate, the match for the 1 mil strip is not significant.

4.4.3. Discussion of strip measurements.

We are satisfied that the chosen experimental configuration has eliminated all errors due to spurious field and current distributions at the edges of the sample. Such factors undoubtedly account for the variation between the results of several groups, on similar material.

It would appear that, if niobium is cold-rolled on a rolling mill of performance similar to the Sendzmir mill, through which our sample passed, the resultant strips are ideal for a.c. applications. A bright, smooth surface can be attained and, as such, exhibits only a low level of a.c.losses in fields below H_{c1}. In all the measurements we have made on rolled strips W_s has never exceeded 10^{-8} J - cm^{-2} at H_m = 1000 Oe.

The pickup-coil voltage waveforms have been usefully interpreted to yield values of H_p, and, subsequently, J_c or α. In addition, the pattern of flux distribution has been studied. Despite the evidence of the waveforms, that the samples were hardly ever diamagnetic below H_{c1}, the modified critical state equations, which are based on such assumptions, were used with some success. A detailed comparison of the theory with the results on the Kawecki-Hancox sample have shown that H_m can often be replaced by $(H_m - \Delta H/2)$.

Thickness effects, in the series of rolled strips, have manifested themselves as changes in K, $J_c(H)$ and the losses above H_p. Measured values of α in $J_c(H) \sim \alpha/H$ have led to predictions of the dissipation which have closely matched the observed levels. It should be noted that such a good fit was obtained only when the <u>measured</u> values of H_{c1} were substituted. We emphasize that values extracted from other papers, for this structure-sensitive constant, may lead to unsatisfactory results.

In conclusion, the modified critical state model is extremely useful for matching experimental results, if certain points are observed. Large surface currents must be allowed for, the value of H_{c1} must be checked, the form of the critical current density variation known and the limiting value of H_m (i.e. H_p) not exceeded.

4.5. Surface currents in the mixed state

In section 2.2.2. we discussed the existence of currents flowing in near-surface layers, when the bulk of the sample was in the mixed state. The alternating field techniques we developed were well suited to the study of these currents and we have described the various approaches used in section 3.5.

While describing the loss measurements some values of the surface currents have been given and their effect accounted for in the theoretical equations. In this section we intend to collate these results and report further experiments designed to investigate the nature of these currents.

The roughness of the surface of samples has been one of the factors known to affect the surface currents. However, some authors have found the currents increase on roughening,[76,88] others that they decrease.[89,90] Our experiments on surface-treated niobium samples have favoured the first school of thought. In figure 4.14a the values of ΔH(Oe.), the shielding effect of the currents on field reversal, and the equivalent surface current density ψ_c (A-cm^{-1}), were plotted for three grades of surface finish. The mechanically polished sample carried by far the greatest currents, $\sim$300 A-cm^{-1} at H_m = 1500 Oe., compared with the as received sample, $\psi_c \sim 70$ A-cm^{-1} at 1500 Oe. A similar increase in the surface currents, with polishing of the sample, was detected in single-crystal samples (see figure 4.20).

Unfortunately the mechanically polished and etch-polished surfaces were not measured on the same crystal. However, it would appear that the former surface was capable of supporting a larger current than the latter, although the finishes were of comparable quality. This effect may have been due to the

structural damage in the near-surface layers that we believe to have been caused by the mechanical polish. The relative values of ψ_c at 1500 Oe. for polycrystalline and single crystal surfaces, 300 A-cm^{-1} and 200 A-cm^{-1} respectively, support the idea that the bulk properties of the sample are important. Even more striking is the difference in the ψ_c vs.H relationship. The empirical relation $\psi_c = \beta / H^m$ fits the results approximately. For both the polished, heavily-worked, polycrystalline samples m=2, for the single-crystal with the worked surface m=5.4 and for the undamaged crystal m=11.2.

This marked variation in the slope of the surface-current/field curves, with the defect structure of the near-surface layers, is similar to the way in which the critical current density is affected. In figure 4.29 we have plotted the measured values of $\Delta H(\psi c)$ and $J_c(H)$ for the etch-polished single crystal and a mechanically polished polycrystalline sample, of niobium. There is a noticeable correlation between the two quantities for a given sample and a marked change between samples. Little significance can be attached to the relative values of the currents but the variation with applied field is a genuine trend. The results in figure 4.29 were taken over a limited field range, but the correlation between ψ c and J_c was observed in higher fields, with the niobium strips. Measurements on the two extreme thicknesses are shown in figure 4.30. For both samples the two properties, ΔH and $J_c(H)$, vary in a like manner with the applied field H. Once again, little importance can be attached to the absolute values, as the surface finishes were not exactly alike, but the shape of the curves can be assumed to be typical of the material properties.

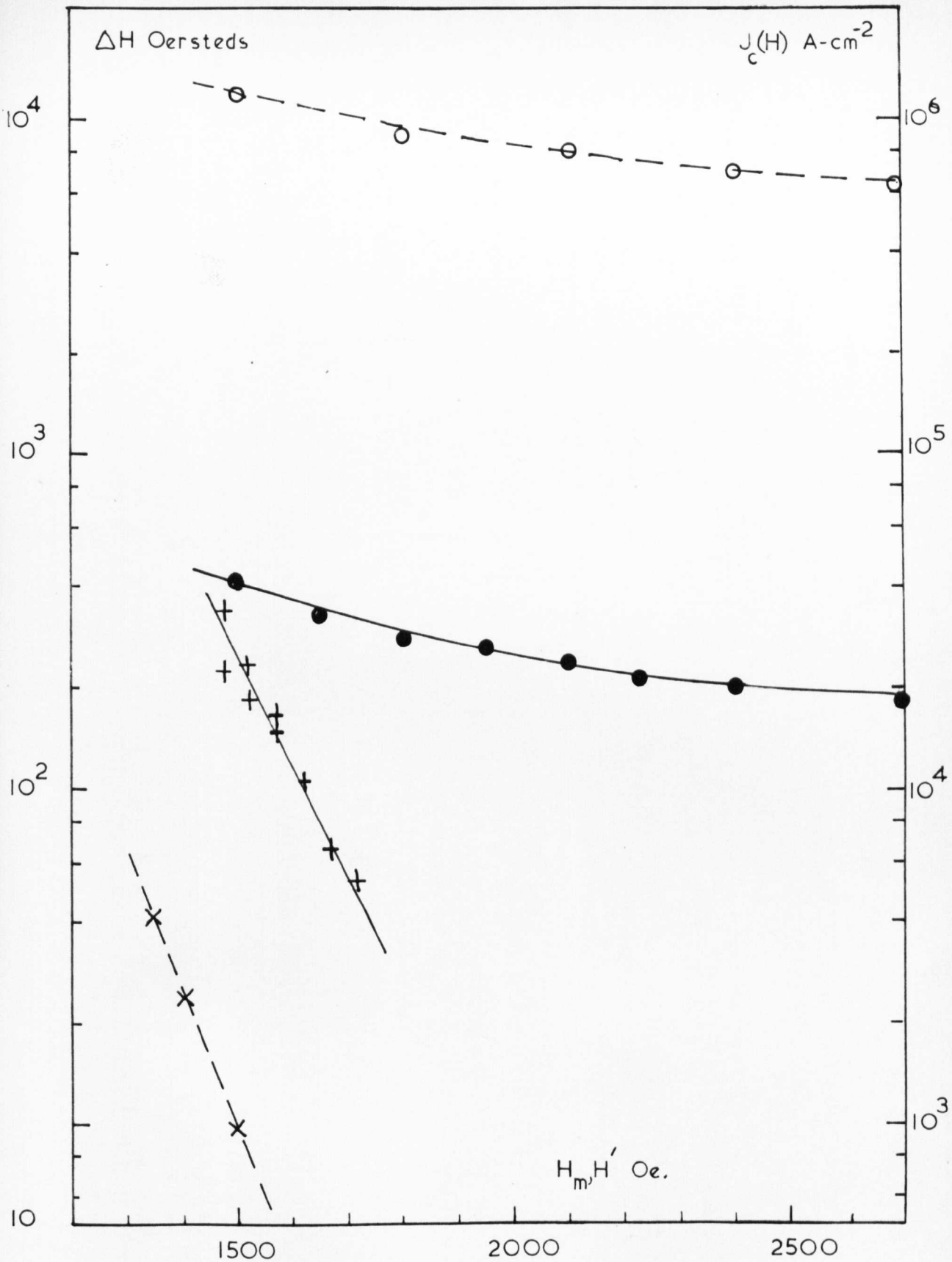

Figure 4.29 Comparison of the surface currents (solid lines) and the critical current densities (broken Lines) of polycrystalline (circles) and single crystal (crosses) niobium.

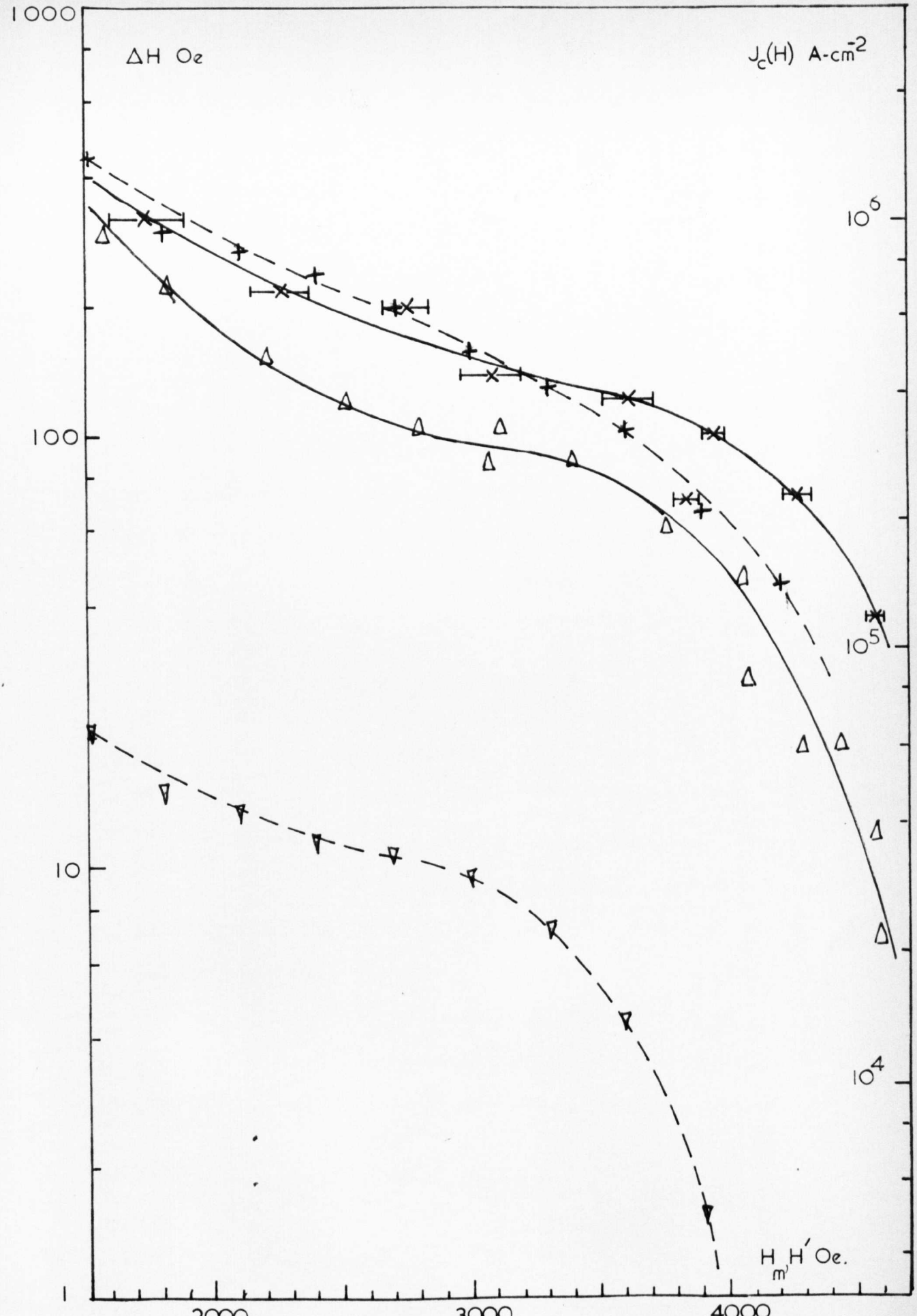

Figure 4.30 Comparison of surface currents (solid lines) and critical current density (broken lines) for rolled niobium strips. 10 mil (triangles) and 1 mil (crosses).

The discovery, that the metallurgical state of the surface drastically modified the surface currents, threw some doubt on the real effect of the surface profile. However, measurements of magnetic hysteresis, in mercury-thallium alloys, confirmed our previous conjectures[162]. The alloys used were liquid at room temperature and they were poured into glass moulds and frozen in liquid nitrogen. By varying the internal surface finish of the moulds different sample surfaces were prepared. The magnetisation curves showed that the hysteresis was reduced by roughening the surface with fine carborundum powder. As no other property could have been possibly altered, other than the number and size of the asperities on the sample surface, it was concluded that the surface currents were radically decreased by the roughness.

4.5.1. Discussion of surface currents.

Campbell[71] has recently considered the origin of the mixed-state surface currents, in terms of the pinning of fluxoids at surfaces. In effect, he expanded on the "image force" ideas of Bean and Livingstone, in terms of the small change in vortex density across the surface. He calculated that the contribution of the currents to the hysteresis was $\Delta M = 2\phi_0^{\frac{1}{2}} M(\text{rev}) / \lambda B^{\frac{1}{2}}$ where $M(\text{rev})$ was the equilibrium magnetisation and B the internal flux density. This is equivalent to a surface current density of:

$$\psi_c = 20 M(\text{rev})/\lambda^2 \left(\frac{\phi_0}{B}\right)^{\frac{1}{2}} \quad \text{A-cm}^{-1} \qquad 4.1$$

Equation 4.1 predicts $\psi_c \propto M(\text{rev}) / B^{\frac{1}{2}}$ and a similar expression can be obtained for $J_c(H)$ [71], based on the assumption that

bulk pinning is at precipitate/matrix boundaries. Thus in two phase alloys a correlation between J_c and ψ_c is expected, and indeed has been observed.[163] Such interphase boundaries are not expected to exist in niobium but it has been suggested[62] that the dislocation cell walls might fulfill a similar function. These ideas could be used to explain the similar variation of ψ_c to that of J_c, on one given sample. However, it is difficult to account for the marked change in ψ_c - H relationship between samples. Of the terms on the right-hand side of equation 4.1, only B is likely to vary with a change, in the metallurgical variables, that does not radically alter K. B is the flux density just inside the sample boundary and for a reversible material can be determined from the ideal magnetisation curve. However, it is difficult to say what value should be attached to B for a hysteretic superconductor, and how it will vary with H.

One possible explanation of the observed behaviour is that the currents were not true surface currents but flowed in a near-surface critical state. To fit the observed waveforms these would have to be in an exceptionally thin, highly hysteretic, "skin" and the experiments on an etch-polished single crystal suggest this is unlikely. We were unable to measure the depth of the penetration of the currents but this can be done with a.c. susceptibility and harmonic analysis techniques.[82,91]

The "surface barrier" model is sympathetic with the observed reduction in ψ_c by roughness. Sharp excerances will provide points of easy entry for the flux although some pinning is expected at the flatter portions of the surface.

5.0. Conclusions

(a) Sensitive equipment has been built and developed, to make accurate measurements of the power losses in superconductors, in applied alternating fields. Down to a level of 10^{-8} J-cm^{-2}, the values of the losses obtained are believed to be free of serious discrepancies, due to the method of measurement, end effects, temperature variations or other factors. The ultimate level of sensitivity was achieved at 10^{-9} J-cm^{-2}. Results can be taken speedily and the losses calculated in a straightforward manner.

Variable temperature facilities have been assembled and measurements can be made over a range of operating frequencies, up to 1000 Hz. Cylindrical and strip geometry can be studied with equal facility, the only preparation required being the winding of the small pickup-coil.

The use of short cylinders for most of the experiments enabled us to prepare various surface finishes and to control the metallurgical variables throughout the sample. This geometry was also easy to analyse mathematically.

Electrical techniques of the kind used here have many advantages over other approaches. In particular, results are obtained directly and the field penetration can be determined at any point in the cycle or the losses measured over a long period of time. Considerable care must be taken with the compensation of stray voltages but these can be successfully eliminated.

(b) Several vital, ancilliary apparata have also been assembled. A vibration magnetometer, capable of plotting out a complete

magnetisation loop automatically, and sensitive to 1 Gauss, has been built. Both the critical current density and the surface currents can be measured by apparatus based on the loss-measuring equipment.

(c) The low-field losses in niobium and lead have been explained on the basis of flux penetration at surface asperities. The existence of local areas of intermediate state, in lead, has been established and similar patches of mixed state, in niobium, postulated. We have shown how the metallurgical state of the surface layers also influences these losses and developed a model of "surface saturation". Mechanical polishing to a 6-micron finish is quite sufficient to greatly reduce the losses, below the sensitivity of our equipment, until H_{c1} is exceeded.

(d) Experiments on hysteretic, high-K superconductors have shown that the critical state model can be applied, with some success, to match the experimental results. The use of the generalised theory of Irie and Yamafuji, has led to qualitative agreement with the results but a poor numerical fit. The results on the Nb-Zr sample were matched in high fields, by the simple Bean model, with $J_c \propto 1/H$. Attempts to apply Easson's expressions, incorporating the effect of H_{c1}, and modified to allow for the surface currents, gave a reasonable fit to experiment.

(e) With niobium samples, the applied fields are usually less than $2H_{c1}$ so the Bean model and similar studies cannot be utilised to explain the experimental results. Derivation of a successful model, to allow for the region below H_{c1}, is dependant on choice of field distribution in the bulk of the superconductor. The expressions produced by Easson[100] assume

that the effective applied field $H_m' = (H_m - H_{c1})$, and that no flux crosses the sample surface for $H < H_{c1}$. We have found this to be true only of the more reversible samples and even then, flux escapes until H = 0. As a result measurements on samples of cold-worked polycrystalline niobium cannot be fitted to these equations. Massive surface currents, on the polished samples, further undermine the theory.

As $J_c(H)$ was reduced, by heat-treatment, the assumptions outlined above appear more valid and rough agreement with experiment was obtained. When the experiments were extended to single crystals the influence of a very thin damaged layer of material near the sample surface was illustrated. More striking however was the effect of the surface currents on the losses. The shielding effect of these currents exceeded 400 Oe., near H_{c1}. However, the theory was successfully modified by assuming that $H_m' = (H_m - H_{c1} - \Delta H/2)$.

(f) Dissipation measurements on a niobium strip, distributed for comparison with other authors' results, demonstrated the influence that edge effects can have in this type of experiment. Our experiment was proved free of such complications. Small losses were measured in the "as rolled" surface but in this, and similar measurements, $W_s < 10^{-8}$ J-cm^{-2} at H_m = 1000 Oe.

In this work the full depth of the strip was often penetrated and the pickup-coil voltage waveforms have been successfully interpreted to yield values of H_p, the field of complete penetration. As a series of strips were successively rolled, the measured critical current density increased from sample to sample. Over the values of H_m used, $J_c(H)$ was found to be well represented by α/H and the measured values of α agreed well with

those calculated from H_p, at least for the thicker strips.

With the Kawecki/Hancox strip, for which $H_p > 2000$ Oe., the Easson equations could be applied over a reasonable range of H_m. With $H_m' = (H_m - H_{c1} - \Delta H/2)$, and values of H_{c1} and ΔH substituted from our own experiments, remarkably good agreement was observed between experiment and theory. In all the strip measurements there was a noticeable separation between predictions and results as H_m exceeded a field close to H_p.

(g) Surface currents have been found to be reduced by roughness on the sample surface. This effect has been determined, free of the influence of bulk properties. It is important to remember, however, that while this is true in our field-induced measurements, surface transport currents may not be similarly affected.

The correlation between the surface currents and the critical current density has been examined on the basis of the "surface barrier" ideas. While these ideas can explain results on any given sample some uncertainty exists concerning the overall variation of ΔH, between samples of different bulk hysteresis.

Significant surface currents have been observed on every type II superconductor studied in the course of this work.

(h) Some general remarks can be made with regard to future possible lines of investigation.

It is now apparent that, from the practical point of view, dissipation can be reduced below acceptable levels in fields below H_{c1}, if sufficient care is taken with the surface preparation. Although further research in this field is perhaps not required, should it be deemed necessary, we suggest that the use of the scanning electron microscope is a powerful tool.

There is still a deal of uncertainty as to the flux distribution in a sample when the applied field is reduced below H_{c1}. It is felt that careful magnetisation measurements and waveshape studies would provide more useful information on this region.

Surface currents in the mixed state are certainly in need of further investigation, especially as to the basic nature of the currents. When very large, as in some of our polished niobium samples, they can have a profound effect on the a.c. losses.

Appendix A

Calculation of the critical current of a conductor

It is convenient to do this calculation in terms of the critical current per unit surface area of the conductor j_c. The results can then be applied in terms of the half dimension d, where d is the radius of a cylindrical conductor or the half thickness of a strip.

(a) Bean limit. J_c assumed independent of H

$$j_c = dJ_c$$

(b) Kim limit. Assuming $J_c(H) = \alpha/(H + H_o)$

where α and H_o are constants for a given sample, in two dimensions.

$$dH/dx = 4\pi/10 \times J_c(H)$$

Therefore $dH/dx = -A/(H_o + H(x))$ where $A = 4\pi\alpha/10$

giving $H''(H_o + H''/2) = Ad$

where H" is the surface field at which $j = j_c$

In the limit $H >> H_o$ this reduces to

$$H'' \propto \sqrt{d}$$

or $$j_c \propto \sqrt{d}$$

Thus the critical value of the surface field, or current/unit surface of a conductor, is proportional to the square root of the appropriate dimension.

Appendix B

Publications by the author

Parts of this thesis are to be submitted for publication in the near future and two papers will be read at the conference on "The a.c.properties of superconductors" to be held at the University of Warwick in August, 1968. A short contribution has recently been published in phys.stat.solidi (July 1968).

Some half dozen reports were written on the a.c.properties of niobium strips, while the author was employed by BICC. For the rest of his published work, reference is made to references 107, 108, 138, 142 and 151.

No reprints are submitted, as the salient features of the above papers are included in the text of the thesis.

References.

1. E.A.Lynton, "Superconductivity" 2nd.ed. Methuen (1964).
2. P.G.de Gennes, "Superconductivity of Metals and Alloys" Benjamin (1966).
3. J.D.Livingstone and H.W.Schadler, Prog.Mater.Sci. 12(3),183 (1964) .
4. D.Dew-Hughes, Mater.Sci.Eng. 1,2 (1966).
5. J.A.Catterall, Metallur.Rev.11,25 (1966).
6. A.A.Abrikosov, Usp.Fiz.Nauk. 87,125 (1965) trans.in Sov. Phys.Uspk.8, 5 (1966).
7. J.Lowell, Cryogenics 5 (4), 185 (1965).
8. B.B.Goodman, Rep.Prog.Phys. 29(2),445 (1966).
9. Y.B.Kim, Physics Today, p.21 (Sept.1964).
10. J.Bardeen, Physics Today, p.19 (Jan 1963).
11. W.F.Druyvesteyn, Phillips Res.Rep.Suppl.No.2 (1966).
12. G.A.Saunders, Contemporary Physics, 17,(3),192 (1966).
13. H.Kammerlingh Onnes, Leiden Commun.Suppl.34(b),55 (1913).
14. D.J.Quinn and W.B.Ittner, J.Appl.Phys.33,748 (1962).
15. B.W.Roberts, Prog.Cryogenics, 4, (1964).
16. B.T.Matthias, T.H.Geballe, L.D.Longinotti, E.Corenzwit, E.W.Hull, R.H.Willens and J.P.Maita, Science 156,645(1967).
17. W.Meissner and R.Ochsenfeld, Naturwiss.,21,787 (1933).
18. C.J.Gorter, Arch.Mus.Teyler. 7,378 (1933).
19. W.H.Keesom, 4e Congr.Phys.Solvay, p.288 (1924).
20. C.J.Gorter and H.B.G.Casimir, Physica 1,306 (1934).
21. E.Saur, IPPS meeting, NPL Teddington (March 1968).
22. C.J.Gorter and H.B.G.Casimir, Phys.Z. 35, 963 (1934).
23. J.Bardeen, L.N.Cooper and J.R.Schriffer, Phys.Rev. 108 1175 (1957).
24. J.G.Daunt and K.Mendlessohn, Proc.Roy.Soc, A185,225 (1946).

25. B.B.Goodman, Proc.Phys.Soc.A66, 217 (1953).

26. W.S.Corak, B.B.Goodman, C.B.Satterthwaite, and A.Wexler, Phys.Rev.102, 656 (1956).

27. B.Serin, C.A.Reynolds and L.B.Nebsitt, Phys.Rev.80,761, (1950).

28. H.Fröhlich, Phys.Rev.79, 845 (1950).

29. J.Bardeen, Phys.Rev. 80, 567 (1950).

30. F.and H.London, Proc.Roy.Soc. A149, 71 (1935).

31. D.Schoenberg, Proc.Roy.Soc. A175, 49 (1940).

32. A.B.Pippard, Proc.Roy.Soc. A216, 547, (1953). Physica, 19, 765, (1953).

33. V.L.Ginzburg and L.D.Landau, J.Exp.Theor.Phys.20, 1064 (1950) in Russian.

34. D.St.James and P.G.de Gennes, Phys.Letts.7,306 (1963).

35. e.g.C.F.Hempstead, Y.B.Kim, Phys.Rev.Letts.12,145 (1963). W.J.Tomasch and A.S.Joseph, Phys.Rev.Letts.12,148 (1963).

36. p.203 of ref.3.

37. A.A.Abrikosov, Sov.Phys. J.E.T.P.,5,1174 (1957).

38. C.Caroli, P.G.deGennes and J.Matricon, Phys.Letts.9,307 (1964).

39. B.S.Deaver Jr. and W.M.Fairbank, Phys.Rev.Letts.7,43,(1964).

40. J.Matricon, Phys.Letts. 9, 289 (1964).

41. D.Cribier, B.Jacrot,L.Madhav Rao and B.Farnoux. Phys.Letts. 9,106,(1964).

42. B.B.Goodman, Phys.Rev.Letts. 6, 597 (1961). Compt.Rend. 258, 5 (1962).

43. P.W.Anderson, Phys.Rev.Letts. 9,(7),309 (1962).

44. Y.B.Kim, C.F.Hempstead and A.R.Strnad, Phys.Rev.129,528 (1963).

45. Y.B.Kim, C.F.Hempstead and A.R.Strnad, Phys.Rev.Letts. 9(7), 306 (1962).

46. C.P.Bean, Phys.Rev.Letts. 8,250 (1962).

47. C.P.Bean, Rev.Mod.Phys. 36 (1 pt 1) 31 (1964).

48. K.Mendlessohn, Proc.Roy.Soc. A152, 34 (1935).

49. W.A.Fietz, M.R.Beasley, J.Silcox and W.W.Webb Phys.Rev. 136,A335(1964).

50. J.Silcox and R.W.Rollins, App.Phys.Letts.2(12),231(1962) Rev.Mod.Phys.36(1pt1),52 (1964).

51. K.Kasukochi,T.Ogasawara and N.Ushio, Jour.Phys.Soc.Japan, 19(9),1649(1964).

52. A.M.Campbell, Ph.D.Thesis, Cambridge,(1965).

53. J.Friedel,P.G.de Gennes and J.Matricon, Appl.Phys.Letts. 2,119(1963).

54. A.M.Campbell,J.E.Evetts and D.Dew-Hughes, Phil.Mag.10,333 (1964).

55. F.Irie and K.Yamafuji, Phys.Letts.24A(1),30(1967) J.Phys.Soc.Japan,23(2),255(1967).

56. I.M.Green and P.Hlawiczka,Proc.I.E.E.114(9),1329(1967).

57. D.G.Schweitzer and M.Garber,Phys.Rev.160,(2),348(1967).

58. J.J.Hauser and E.Buehler,Phys.Rev.125,142(1962).

59. J.A.Catterall,I.Williams and J.F.Duke,Brit.Jour.App.Phys. 15,1369(1964).

60. J.W.Heaton and A.C.Rose-Innes,Cryogenics,4,85(1964).

61. A.V.Narlikar and D.Dew-Hughes, phys.stat.solidi,6,383(1964).

62. A.V.Narlikar and D.Dew-Hughes, Jour.of Mater.Sci.1,317(1966).

63. G.J.van Gurp, Phillips Res.Reports,22,10(1967).

64. W.W.Webb, Phys.Rev.Letts.11,191(1963).

65. I.Williams and J.A.Catterall, to be published.

66. W.De Sorbo, Phys.Rev.132,107(1963), ibid.135,A1190(1964). ibid,134,A1119(1964).

67. J.D.Livingstone, Acta.Met.11,1371(1963);J.Appl.Phys.341, 3028(1963);Rev.Mod.Phys.36(1ptl),54(1964).

68. J.Sutton and C.Baker,Phys.Letts.21(6),601(1966).

69. S.A.Levy,Y.B.Kim and R.W.Kraft,Jour.App.Phys.37(10),3659 (1966).

70. J.J.Hanak and R.Enstrom,R.C.A.Progress Reports No.3,54(1964).

71. A.M.Campbell,J.E.Evetts and D.Dew-Hughes, to be published in Phil.Mag.

72. C.P.Bean and J.D.Livingstone, Phys.Rev.Letts.12,219(1964).

73. A.A.Abrikosov, Sov.Phys.JETP.20,480 (1966).

74. J.G.Park, Phys.Rev.Letts.15,352 (1965).

75. K.Yamafuji, Phys.Letts.21(1),11 (1966).

76. R.Bellau, Phys.Letts.21(1),13 (1966).
Solid State Commun.5,533 (1967).

77. P.S.Swartz and H.R.Hart Jr. Phys.Rev.137(3A),A818 (1965).

78. B.Bertman, D.G.Schweitzer and F.A.Lipschultz, Phys.Letts. 21(3),260 (1965).

79. M.Strongin, A.Paskin, D.G.Schweitzer, O.F.Kammerer and P.P.Craig, Phys.Rev.Letts.12,442 (1964).

80. H.J.Fink, Phys.Letts.19,364 (1965).

81. D.P.Jones and J.G.Park, Phys.Letts.20(2),111 (1966).

82. G.R.Love, J.Appl.Phys.37,3361 (1966).

83. B.Bertman and D.G.Schweitzer, Phys.Letts.21(4),361 (1966).

84. A.S.Joseph and W.J.Tomasch, Phys.Rev.Letts.12,219 (1964).

85. R.W.DeBlois and W.DeSorbo, Phys.Rev.Letts.12,499 (1964).

86. P.G.DeGennes, Solid State Commun.3,127 (1965).

87. H.J.Fink, Phys.Letts.20(4),356 (1966).

88. H.R.Hart Jr. and P.S.Swartz, Phys.Rev.156,403 (1967).

89. H.J.Fink (unpublished).

90. H.A.Ullmaier and W.F.Gauster, Jour.Appl.Phys.37,4519 (1966).

91. A.M.Campbell, private communication.

92. H.R.Hart Jr., G.E.Report on contract No.AF-33(657)-11722, 1,3 (1963).

93. H.London, Phys.Letts.6,162 (1963).

94. R.Hancox, Proc IEE.113,1221 (1966).

95. H.Voigt, Phys.Letts.20(3),262 (1966).

96. C.P.Bean,G.E.Report on contract No.AF-33(657)-11722,3,3 (1964).

97. H.A.Ullmaier, Phys.Letts.21(5),507 (1966).

98. H.A.Ullmaier, phys.stat.solidi,17,631 (1966).

99. H.J.Fink, Phys.Rev.Letts.16(11),447 (1966).

100. R.M.Easson and P.Hlawiczka, Report on a Ministry of Technology contract on a.c.losses. (June 1967).

101. M.F.Fagan, Westinghouse Engineer, 21(4),103 (1961).

102. R.McFee, Elect.Engr.81,122 (1962).

103. C.H.Jones and H.L.Schenck, Adv.in Cryo.Eng. 8,579 (1963).

104. T.Pech,J.P.Duflot and G.Fournet,Phys.Letts.16,201 (1965).

105. R.G.Rhodes, E.C.Rogers and R.J.A.Seebold, Cryogenics 4, 206 (1964).

106. R.J.Slaughter,E.C.Rogers,and R.Grigsby, Phys.Letts. 23(3), 214 (1966).

107. E.C.Rogers and R.M.F.Linford, Paper presented at the European Symposium on Electrical Conduction at Low Temperatures (London 1965).

108. R.M.F.Linford, Paper presented to IPPS meeting on Calorimetry (Leeds 1965).

109. M.L.Claude and M.A.Mailfert, Phys.Letts.24A(3),150 (1967).

110. B.F.Figgins and T.A.Shepherd, Nature 202,890 (1964).

111. H.R.Hart and P.S.Swartz, Bull.Am.Phys.Soc.9(3),252 (1964).

112. T.A.Buchold and P.J.Molenda, Cryogenics 2(6),344 (1962).

113. C.Grenier and B.Elschner, Phillips Res.Reps.20,235 (1965).

114. Y.A.Rocher and J.Septfonds, Cryogenics 7,96 (1967).

115. W.R.Wisseman,L.A.Boatner and P.J.Low, Jour.App.Phys.35(9) 2649 (1964).

116. R.M.Easson and P.Hlawiczka, Brit.Jour.Appl.Phys.18,1237 (1967).

117. T.A.Buchold, Cryogenics 3,141 (1963).

118. T.A.Buchold, and P.J.Molenda, G.E.Report on contract No. AF-33(657) - 11722 1,47 (1963).

119. T.A.Buchold and P.J.Moldena, ibid 3,17 (1964).

120. T.A.Buchold and R.L.Rhodenizer ibid 2,29 (1964).

121. T.Pech and G.Fournet, Cryogenics 7,26 (1967).

122. T.Pech and G.Fournet, Paper presented to Cryogenic Engineering Conference (Houston 1967).

123. K.Hidaka,H.Miyata,K.Shinada,S.Ihara and T.Sekine, Bulletin of the Electrotechinal Laboratory, Tanashi-machi, Japan, 28(8),1 (1964).

124. G.Bogner and W.Heinzel, Solid State Electronics,7,93 (1964).

125. C.Damman,E.Santamaria,J.Maldy and L.Donadieu, Phys.Letts. 24A(11), 574 (1967).

126. W.Heinzel,Phys.Letts.20(3),260 (1966).

127. R.A.Kamper and P.F.Chester,Proc.L.T.8.(Butterworth) 1963.

128. R.A.Kamper, Phys.Rev.Letts.2,290 (1961).

129. P.F.Chester, Proc.IEE, 111(2),411 (1964).

130. J.L.Zar, Rev.Sci.Inst.34(7),801 (1963).

131. J.L.Zar, Jour.App.Phys,35(5), 1610 (1964).

132. R.M.Easson and P.Hlawiczka, Phys.stat.solidi,32,K129 (1967).

133. R.J.Slaughter, private communication.

134. H.F.Taylor, Phys.Rev.165(2),517 (1968).

135. V.V.Sychev, V.B.Zenkevish,V.V.Andrianov and V.A.Al'tov - Sov.Phys.Dokaldy, 9(11),978 (1965).

136. M.P.Thomas, C.R.Acad.Sc.Paris,Series 8, 5(58),633 (1964).

137. E.C.Rogers, Phys.Letts.5(5),317 (1963).

138. R.M.F.Linford, ibid.17(1),18 (1965).

139. R.M.F.Linford, unpublished.

140.

141. A.Mailfert,G.Fournet and J.Huret, Phys.Letts.7(4),227 (1963).

142. R.M.F.Linford,B.I.C.C.Research Organisation report No. P/T 476 (1965).

143. E.C.Rogers, Phys.Letts.5(5),317 (1963).

144. R.M.Easson and P.Hlawiczka, Electronics Letts.2,123 (1966). Phys.Letts.20,465 (1966). ibid.25A(1),53 (1967).

145. T.W.Grasmehr and L.A.Finzi IEEE TransMag.2(3)334 (1966).

146. L.A.Finzi and T.W.Grasmehr ibid.3(3)277 (1967).

147. A.F.Brown and H.Kroenberger, Jour.Sci.Inst.24,151 (1947).

148. H.O.Lorch - private communication.

149. C.P.Bean,R.L.Fleischer,P.S.Swartz and H.R.Hart, Jour.Appl. Phys.37,2218 (1966).

150. R.M.Easson and P.Hlawiczka, Report on a Ministry of Technology contract on a.c.losses (September 1967).

151. R.M.F.Linford, Report on a Ministry of Technology contract on a.c.losses (June 1967).

152. J.E.Evetts, A.M.Campbell and D.Dew-Hughes, Phil.Mag. 10, 339 (1964).

153. S.Foner, Rev.Sci.Inst. 30(7), 548 (1959).

154. I.Williams and J.A.Catterall, Brit.Jour.Appl.Phys.

155. C.S.Tedmon, R.M.Rose and J.Wulff, Jour.Appl.Phys. 36(3), 829 (1965).

156. C.S.Tedmon, R.M.Rose and J.Wulff, Jour.Appl.Phys. 36(1), 164 (1965).

157. J.O.Steigler, C.K.H.Dubose, R.E.Reed Jr. and C.J.McHargue Acta.Met. 11, 851 (1963).

158. D.K.Finnemore, T.F.Stromberg and C.A.Swenson, Phys.Rev. 149(1), 231 (1966).

159. R.J.Slaughter. Letter to the Ministry of Technology a.c. losses contractors. (June 1968).

160. H.O.Lorch. Letter to the Ministry of Technology a.c.losses contractors. (January 1968).

161. R.J.Slaughter. Report on a Ministry of Technology contract on a.c.losses in superconductors. No.EV/T 38 (August 1967).

162. J.E.Goodfellow and R.M.F.Linford - unpublished results.

163. A.M.Campbell - private communication.

150. R.M.Easson and P.Hlawiczka, Report on a Ministry of Technology contract on a.c.losses (September 1967).

151. R.M.F.Linford, Report on a Ministry of Technology contract on a.c.losses (June 1967).

152. J.E.Evetts, A.M.Campbell and D.Dew-Hughes, Phil.Mag. 10, 339 (1964).

153. S.Foner, Rev.Sci.Inst. 30(7), 548 (1959).

154. I.Williams and J.A.Catterall, Brit.Jour.Appl.Phys.

155. C.S.Tedmon, R.M.Rose and J.Wulff, Jour.Appl.Phys. 36(3), 829 (1965).

156. C.S.Tedmon, R.M.Rose and J.Wulff, Jour.Appl.Phys. 36(1), 164 (1965).

157. J.O.Steigler, C.K.H.Dubose, R.E.Reed Jr. and C.J.McHargue Acta.Met. 11, 851 (1963).

158. D.K.Finnemore, T.F.Stromberg and C.A.Swenson, Phys.Rev. 149(1), 231 (1966).

159. R.J.Slaughter. Letter to the Ministry of Technology a.c. losses contractors. (June 1968).

160. H.O.Lorch. Letter to the Ministry of Technology a.c.losses contractors. (January 1968).

161. R.J.Slaughter. Report on a Ministry of Technology contract on a.c.losses in superconductors. No.EV/T 38 (August 1967).

162. J.E.Goodfellow and R.M.F.Linford - unpublished results.

163. A.M.Campbell - private communication.